

RES

THE SCHOOL
for RENEWABLE ENERGY SCIENCE

Hydraulic Hammer Drilling Technology to Replace Air Hammer Drilling in Deep BHE Design

The design of the drilling and completions for a building renovation at
the Technische Universität Darmstadt

Michael John Thompson



UNIVERSITY OF ICELAND



University
of Akureyri



TECHNISCHE
UNIVERSITÄT
DARMSTADT

Hydraulic Hammer Drilling Technology to Replace Air Hammer Drilling in Deep BHE Design

Design of the drilling and completions for a building renovation at the
Technische Universität Darmstadt

Michael John Thompson

A 30 ECTS credit units Master's thesis

Supervisors

Prof. Dr. Ingo Sass

Dipl. Ing. Sebastian Homuth

A Master's thesis done at
RES | The School for Renewable Energy Science
in affiliation with
University of Iceland &
University of Akureyri &
Technische Universität Darmstadt

Akureyri, February 2010

Hydraulic Hammer Drilling Technology to Replace Air Hammer Drilling in Deep
BHE Design

Design of the drilling and completions for a building renovation at the Technische
Universität Darmstadt

A 30 ECTS credit units Master's thesis

© Michael Thompson, 2011

RES | The School for Renewable Energy Science

Solborg at Nordurslod

IS600 Akureyri, Iceland

Telephone + 354 464 0100

www.res.is

Printed in February 18th, 2011

at Stell Printing in Akureyri, Iceland

ABSTRACT

The following thesis addresses a few of the issues surrounding the geothermal energy sector of the renewables movement; how to drill deeper in order to utilize important geothermal potential? And, what to do with that potential once the depths have been reached? In order to arrive at this answer, a project originating at TU Darmstadt was taken as the main topic of interest for the analysis. The project is the design of drilling and completions for a deep borehole geothermal heat exchanger in the renovation of a building on campus. A combination of one dimensional heat transfer, FEM software analysis and literature studies on the existing drilling technology is used to guide these answers. The study and calculations show that hydraulic hammer drilling technology makes it possible to cheaply and effectively drill to depths of 800+ meters. Also a steel coaxial design of the heat exchangers allows for the transfer of nearly 150 W/m of thermal energy from a reservoir charged to 90°C. The collapse resistance of PVC and PE pipe limits the use of these materials for heat exchanger application. This study gives evidence that further research into hydraulic hammer drilling and borehole thermal energy storage could provide a promising future in the integration of cheap and effective alternate energy sources.

PREFACE

The following thesis was written in cooperation with TU Darmstadt in order to provide a working model and preliminary design for a borehole heat exchanger drilling and completions technique. The end goal of the research and analysis contained in this thesis is twofold. First of all the thesis was written to inform the reader of the availability of hydraulic percussion drilling technology; namely hydraulic drilling. Hydraulic drilling technology is moving towards replacing rotary drilling in many applications and is, in this student's perspective, the next major advancement in the drilling industry. My goal with this paper is that engineers and geoscientists alike will view its contents as a stepping block into further advancements and understanding of geothermal deep drilling. Secondly, the thesis is a preliminary design scenario for deep borehole heat exchangers. The information and calculations included in the thermodynamic analysis show one instance where basic thermodynamic equations can be applied. The design of such BHE systems needs to be streamlined for integration into industry, and thus the BHE spreadsheet was created in conjunction with the BHE thermodynamic design.

I would like to take this opportunity to single out a few important sources. Consultation with industry experts from Germany, Iceland, and Canada has shown me that the will to improve the geothermal and drilling industry is an important effort shared internationally.

I spent 3 days at the Geothermal Research Center (GZB) in Bochum, Germany, and in that time learnt more than would have been possible in any number of weeks reading textbooks and articles. Without this exposure my understanding of the drilling process would not be where it is today.

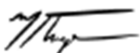
Mr. Keith Corb dedicated a large amount of his personal time to discussing practical questions I had during the writing of my thesis. He was also able to supply me with valuable contacts within the Canadian drilling and completions industry. I am extremely grateful for his help during this period.

I would also like to extend thanks to the professors and administrators who have made the RES program as successful as it could be. The downfall of RES has not given light to the amount of talent and knowledge shared during this past year. RES may be gone but the student body will continue to prosper for years to come.

Finally, to Dr. Sass and his working group at TU Darmstadt. Their partnership and contacts within Germany have been the major contributing effort to my thesis. For this reason I choose to send my greatest thanks and regards to this group. I have no doubt that the talent and knowledge contained in this group is world leading. Thank you for everything.

There were so many others who will not be mentioned but had a significant influence on the information presented in this thesis, to them I also say thank you.

Sincerely,



Michael John Thompson

TABLE OF CONTENTS

1	Project Details	1
1.1	Proposed Design	1
1.2	Proposed Drilling	3
1.3	Proposed Completion	4
1.4	Direct vs. Indirect Geothermal Systems	5
2	Site geology	7
2.1	“Red Bed”	7
2.2	Granodiorite	8
2.3	Hydrogeological Conditions	8
2.4	Geothermal Conditions	9
3	Percussion Drilling Technology	11
3.1	Air Hammer Drilling	11
3.1.1	Components of a typical DTH Hammer	11
3.1.2	Benefits of Air Hammer Drilling	12
3.1.3	Drawbacks of Air Hammer Drilling	17
3.2	Hydraulic Hammer Drilling	19
3.2.1	Present Hydraulic Hammer Technology	19
3.2.2	Advantages over Air Hammer Drilling	21
3.3	Drilling Theory: Air vs Hydraulic Hammer	24
3.3.1	Mud Flow Rate and Density Calculations	24
3.4	The Comparison	27
3.5	Drilling Design	31
3.6	Environmental Impact / Risk Identification	34
4	Completions Theory – Coaxial vs Double U-Tube	35
4.1	BHE Materials Design	35
4.2	BHE Fluid Flow Design	38
4.3	BHE Grouting Design	45
4.4	Borehole Heat Exchanger Length Design	46
4.5	Introduction to the Thermo Tab of the BHE Spreadsheet	49
4.6	BHE FEFLOW Modeling	55
4.7	BHE Model Comparison	61

5	Drilling Program	65
5.1	Scope.....	65
5.2	Well Information	67
5.3	Well Site Preparation and Rig Move.....	67
5.4	ERP: Emergency Response Plan.....	68
5.5	Area Study and Risk Identification	68
5.6	Drilling Operations	70
6	Completions Program.....	75
6.1	Scope.....	75
6.2	Well Information	77
6.3	Well site preparation and rig move	77
6.4	ERP: Emergency Response Plan.....	78
6.5	Area Study and Risk Identification	79
6.6	Completions Operations	79
7	Conclusions.....	81
	References	83
	Appendix A	A1

LIST OF FIGURES

Figure 1-1: Idealized Project Charging Perspective.	1
Figure 1-2: Idealized Project Extraction Perspective.....	2
Figure 1-3: Solar insolation vs thermal gradient.	3
Figure 1-4: Side by side comparison of common BHE Designs.....	4
Figure 1-5: Visual representation of Energy Flow	5
Figure 1-6: Energy flow in the TU Darmstadt project	6
Figure 2-1: Visual representation of the horst and graben fracture system	7
Figure 2-2: Ground water contours in the Darmstadt area.....	9
Figure 3-1: Typical DTH Percussion Hammer	12
Figure 3-2: Tri-cone Toller Bit.....	13
Figure 3-3: Typical design of a DTH hammer drill bit.....	14
Figure 3-4: Diagram of the stress loading seen in the typical impact of a percussion bit ...	14
Figure 3-5: Drill bit crater mechanism.....	15
Figure 3-6: Tri-cone roller bit wear and damage visualization	16
Figure 3-7: DTH hammer drill bit broken carbide tooth..	17
Figure 3-8: Hydraulic hammer at the GZB Geothermal Research Center.....	20
Figure 3-9: Hole deviation, Air vs Hydraulic Hammer	23
Figure 3-10: Diameter and thickness of cuttings.....	29
Figure 3-11: Borehole stick diagram correlating to drilling design	33
Figure 4-1: Inspection classifications chart.....	38
Figure 4-2: Conceptual model of the BHE.....	40
Figure 4-3: Radial thermal resistance model.....	42
Figure 4-4: Theory resistance model	42
Figure 4-5: Radial BHE model and respective resistance network	44
Figure 4-6: Figure Showing variables for Table 4.1.....	48
Figure 4-7: Input spreadsheet for thermodynamic calculations of charging phase.....	50
Figure 4-8: Temperature distribution input parameters	51
Figure 4-9: BHE thermodynamics spreadsheet output for charging phase.....	51
Figure 4-10: Horizontal temperature field at varying depths.....	52
Figure 4-11: Reservoir temperature gradient approximation after charging.....	53
Figure 4-12: Input spreadsheet for thermodynamic calculations of extracting phase	54

Figure 4-13: BHE thermodynamics spreadsheet output for extraction phase.....	54
Figure 4-14: Super element dimensions in mesh design.....	56
Figure 4-15: 2D mesh view	57
Figure 4-16: Nodal design of mesh.....	58
Figure 4-17: Spaced out nodes around the FEFLOW BHE.....	59
Figure 4-18: BHE input screen auto filled inputs.....	60
Figure 4-19: User input parameters for the BHE	61
Figure 4-20: Chart of FEFLOW and spreadsheet data comparison	64
Figure 5-1:Drilling design sick diagram	74
Figure 6-1: Completions stick diagram.....	81

LIST OF TABLES

Table 2-1: Measured properties of the thermal reservoir.....	10
Table 3-1: Properties of the granodiorite formation	29
Table 3-2: Output data for water	30
Table 3-3: Output data for air	31
Table 4-1: Temperature dist.	48
Table 4-2: FEFLOW temperature distribution	62
Table 4-3: Spreadsheet temperature distribution.....	63
Table 5-1: Scope Change Summary Sheet.....	66
Table 6-1: Record summary of scope changes.....	76

1 PROJECT DETAILS

This thesis was written to compliment a renovation to be undertaken by Technische Universität Darmstadt (TU Darmstadt). The project will involve a more than 40 year old university building which is to be redesigned in an environmentally friendly and energy efficient way. The introduction of a geothermal space heating system and an energy efficient envelope will help to facilitate sustainable energy sources for the next period of its life.

1.1 Proposed Design

The project was originally slated to include two or three deep borehole heat exchangers (BHE) and to be operated without the need for a heat pump. The system will use the waste heat from a nearby power station to thermally charge the rock underneath the campus. In the summer months the waste water will be pumped into the ground and will exchange energy via the BHE into the formation. This process will act as an open cycle system and the waste water will join its original path after the exchange process. The well flow path will start with flow down the tubing of BHE. This hot water will flow up the annulus of the BHE and exchange heat with the borehole walls. The schematic diagram below shows how the process is visualized in the scope of the project.

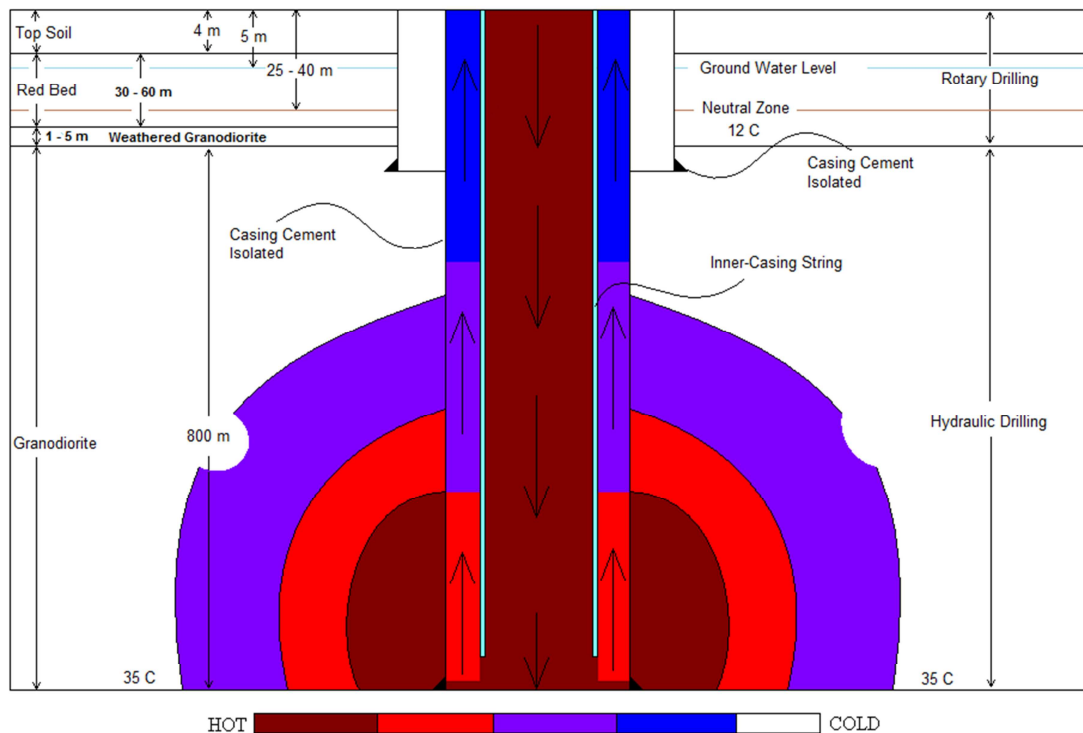


Figure 1-1: Idealized Project Charging Perspective. Figure is not to scale and does not represent calculated values. It is solely for the conceptual understanding of the project.

In order to use this stored energy the system will enter a new fluid loop. The building water circulation system will act as a closed loop heat exchanger similar to that used in shallow geothermal applications. The difference is the need for a heat pump will not be necessary as the ground will be charged to a proposed temperature of up to 90 degrees Celsius. The aim of the heat exchanger design is to reach a borehole outlet temperature of 65 – 75 degrees Celsius for circulation in the buildings heating system. A building water supply will be pumped down hole via the tubing and will exchange heat with the wellbore via the annulus. The returning water flow will need to be approximately 55 degrees Celsius in order to supply the building with useable heat. An estimated heating load of 300 kW is the target heat extraction of the BHE system. The diagram below shows the proposed flow path in the wellbore for the heat extraction loop.

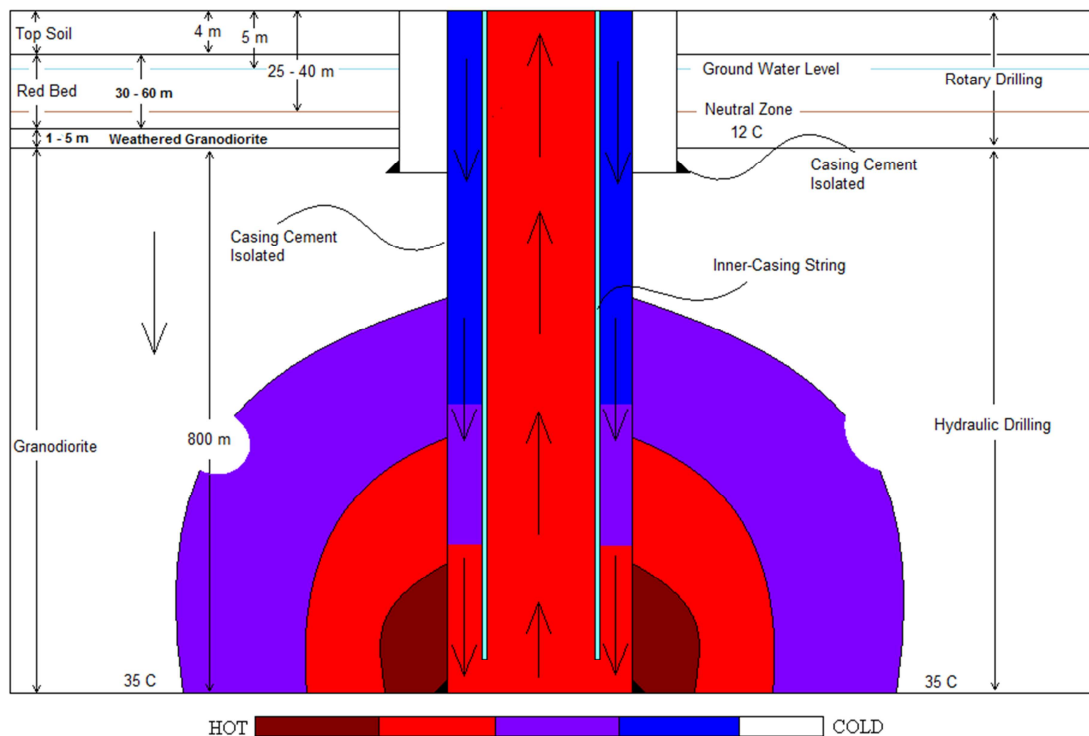


Figure 1-2: Idealized Project Extraction Perspective. Figure is not to scale and does not represent calculated values. It is solely for the conceptual understanding of the project.

The idea of using BHE's for the purpose of storing energy is not a new one. Back in 1991 Hellstrom wrote about this idea saying, "A device where heat can be stored for some period of time may improve the economy of the energy's supply system. The basic idea is to charge the store when cheap energy...is available and to discharge when the stored heat can replace more expensive sources" (Hellstrom, 1991). Hellstroms book covers in detail the design of an underground thermal storage.

1.2 Proposed Drilling

The drilling of the TU Darmstadt BHE project has been suggested as a hydraulic percussion drilling operation. Plans are to drill two to three bore holes as deep wellbore heat exchangers. Each wellbore would have a projected depth of approximately 500 m to 1000 m below surface. The reasons for going so deep with the wellbores include a small surface footprint, higher bottom hole temperatures and available technology.

The typical plan on a project such as this would not include deep wellbore heat exchangers. The plan would normally be to install a multiple BHE array which would be drilled with an air hammer and completed to a depth of around 200 m. At the Institute of Applied Geoscience (TU Darmstadt) the wellbores will be placed in a parking lot next to the building. Because of space availability, an extensive array of wellbores is not as welcome as the smaller footprint of a few deeper wells. For this reason the project was chosen to have two to three deep wellbores instead of a multiple wellbore array.

Normally the shallow wellbores will be placed at a true vertical depth (TVD) of around 200 m. At this depth the insitu temperature will be quite close to the seasonal average. This is because it lies below the neutral zone which is approximately 40 m TVD at the TU Darmstadt well site. The neutral zone is where the temperature flux from the solar insolation reaches a heat transfer rate equal to the earth's natural gradient, see figure 1.3 below. The figure shows this zone in relation to solar insolation and natural earth thermal gradient. The insitu heat flow in the Darmstadt area is approximately 0.03 W/m^2 (Gu, 2010). The temperature at the neutral zone under the TU Darmstadt campus is around 12 degrees Celsius (Gu, 2010); this is the yearly average temperature for the area.

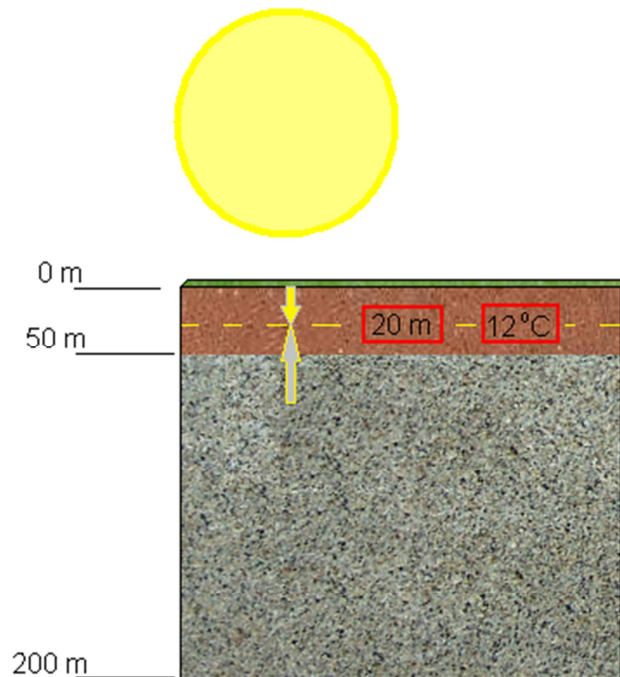


Figure 1-3: Solar insolation vs heat flow. Values are to demonstrate the neutral zone and are not measured or calculated.

The multiple reasons for going with a deeper borehole then becomes clear when calculating the likely temperature at the proposed depths. The temperature should be approximately 40°C at a depth of 1000 m and 27°C at a depth of 500 m. The project aims at warming the rock to a temperature of close to 90°C. The deeper the well, the less energy is needed to be transferred into the rock.

Finally, the technology needed to drill deeper wells is commercially available. Companies are starting to recognize the benefits of drilling with the hydraulic hammer as opposed to an air hammer system. It allows the drill to reach depths not possible with air hammers and also create a generally cleaner and straighter wellbore. The benefits of this technology have allowed for the design of the TU Darmstadt deep BHE system. Hydraulic hammer drilling will be covered in detail later in this publication; benefits will include hole stability, smaller power requirement, and more efficient cuttings transport.

1.3 Proposed Completion

Each borehole has a number of options for installed equipment in order to exchange heat with the prospective reservoir. The option originally considered in the proposed completion is a coaxial heat exchanger. Different from the usual design of a double U shaped heat exchanger, the coaxial heat exchanger has a central flow path surrounded by an annular flow path. The figure below shows the schematic of both types of heat exchangers side by side.

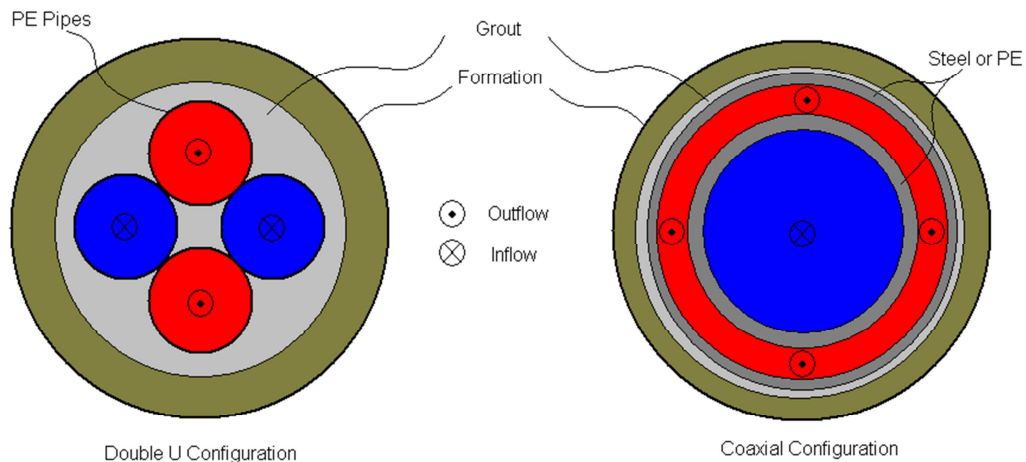


Figure 1-4: Side by side comparison of common BHE Designs

The reason to go with the coaxial heat exchanger lies in the depth of the proposed wellbores. At 500 m – 1000 m there is a risk that the PE/PVC pipe, used in the construction of U pipe heat exchangers, will fail under the conditions to be expected in the TU Darmstadt BHE Project. This failure will happen under hydrostatic loading or temperature limits of the material. Later in this publication, the feasibility of using thermoplastic pipe will be calculated. A pipe failure would cause flow to be pinched off down hole and render the BHE useless for heat transfer. To avoid this problem a steel pipe construction will also be considered for its suitability. Due to the apparent difficulties of manufacturing and installing a steel double U pipe, the coaxial design was chosen.

1.4 Direct vs. Indirect Geothermal Systems

There exists two different ways to utilize geothermal energy, direct and indirect geothermal use. Neither one is better than the other, each has its own advantages and disadvantages. Direct geothermal use is when water or heat is taken from the ground and used directly in a system. This system could be anything from district heating to turbine power generation. Indirect geothermal is a process named for the use of water or heat indirectly with the considered system. Usually these systems are heating systems but with advances in binary type power cycles the ability to generate power in an indirect utilization system is becoming a reality. In order to understand the process of heat conversion and the difference to geothermal direct or indirect utilization, it is first beneficial to review the concept of exergy.

Exergy

Total energy is split into two different portions; energy which can be converted to work and energy which cannot. Exergy is that energy which can be converted to useful work. This means that the exergy extracted from an indirect utilization system can be used to turn a turbine and produce electricity. There are often losses in the amount of exergy obtained and, because energy is only split into exergy and anergy, the remaining losses account for the anergy of the system. Please see the diagram below for a visual representation of energy flow typical to geothermal systems.

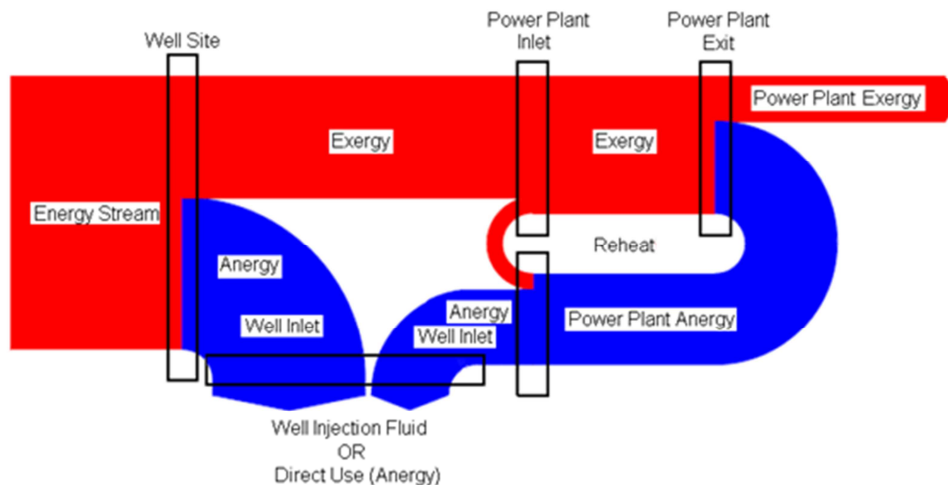


Figure 1-5: Visual representation of Energy Flow(modified from Valdimarsson, 2010)

Geothermal Utilization

The system to be used in the TU Darmstadt BHE project is an indirect geothermal system but is different than previously discussed. Heat energy will enter the formation via hot waste water from an electricity generation plant. The water will exchange heat (not mass) with the formation rock which will act as a storage medium for the heat. It should be noted that this process is an open process and not all of the anergy can be transferred to the rock. Some of the anergy will exit the wellbore and join its initial path as waste heat. When the anergy is needed, a separate loop will act to extract it from the rock and transfer it to the surface for use in a building heating system. The heat flow diagram can be seen in figure 1.6.

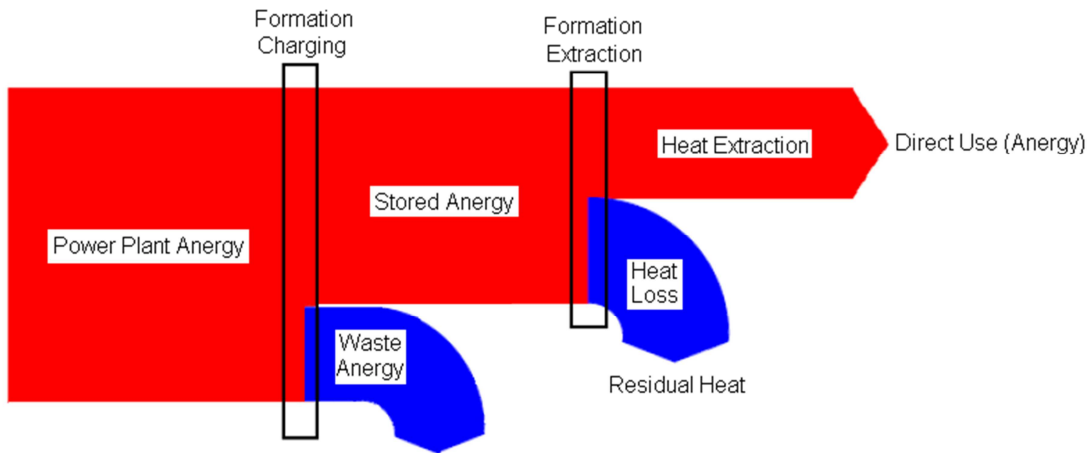


Figure 1-6: Anergy flow in the TU Darmstadt project (modified from Valdimarsson, 2010)

The energy flow depicted above is all anergy because it will never change forms. It enters this stream from the direct use stream seen in figure 1.5 and stays as heat throughout the utilization process until its direct use end life.

The reason the heat is not used directly is mainly because of its temperature and the geological setting of TU Darmstadt. Darmstadt lies on an area of thicker continental crust which means that the earth's mantle heat is far removed from its surface. The distance to this global heat source also explains the small heat flow/temperature gradient seen in the region. Because reachable bottom hole temperatures are so low, there is not enough energy provided by the earth to produce temperatures high enough for electricity production. Furthermore, the building is connected to an electrical grid and therefore does not have the need to produce its own power. It does need to be heated, and so the anergy stream is finally used as indirect geothermal energy.

2 SITE GEOLOGY

The Darmstadt area lies on the eastern fault of the Rhine Graben. The Rhine Graben is a major rift zone between the borders of Germany and France. The eastern fault divides Darmstadt into two different geological areas in a NS trending direction. The institute building lies on an area belonging to the Odenwald and Sprendlinger Horst. The lithology of the Odenwald and Sprendlinger Horst consists of four distinguishable layers. The top three layers will be insulated from the BHE and so their thermal and water transport properties will not be considered in this thesis. The final layer, the consolidated granodiorite, will be the target thermal reservoir for the BHE project. The following diagram, from Yixi Gu's thesis "*Design Calculations for Optimizing of an Existing Multifunction-Building with Borehole Heat Exchangers*", is a good visual representation of the fault structure and layering of each formation underneath the institute.

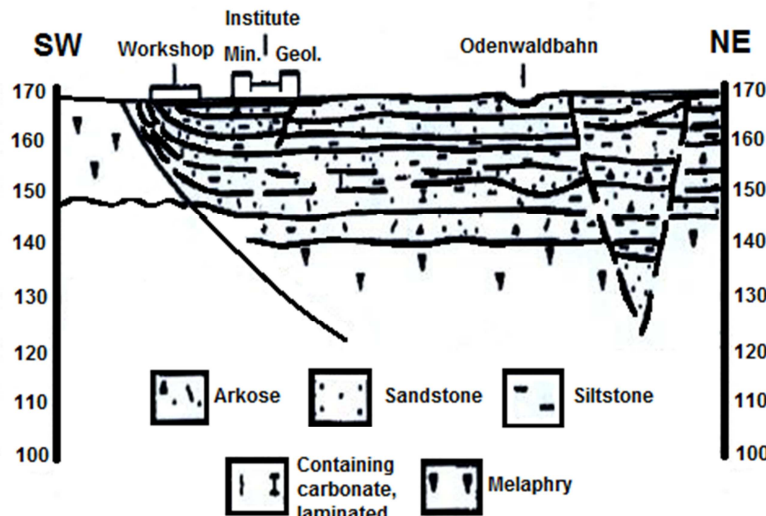


Figure 2-1: Visual representation of the horst and graben fracture system which structures the geology underneath the geosciences building at TU Darmstadt (Gu, 2010)

2.1 “Red Bed”

Two of the four mentioned distinguishable layers lie within the Red Bed rock formation underneath the top soil of the geosciences building on campus. The Red Bed layer gets its name from the reddish colour of the sand and silt stones of which it is comprised. The layers of sand and silt stone are stratified throughout the formation. Within this stratified formation there is a chance to encounter sporadic zones of what is referred to as melaphyre; this is a local nomenclature for a type of rock in the area. The melaphyre is a partly altered basalt and andesite layer which is characterized by large grained crystals of feldspar or quartz. In other words, it resembles granite with a smaller crystalline structure and the existence of large vesicles containing mineral deposits.

The thermal and hydrogeological properties of the Red Bed can be ignored when designing the heat extraction portion of the completions design. This is because the zone is believed to be no more than 40 m in thickness and will lie very close to the neutral zone. To avoid potential flow problems caused by freezing and thawing of this area, this zone will be thermally insulated against the top of the BHE. The thermal insulation also acts to avoid microbiological changes and chemical changes in the ground water aquifer that could be caused by higher ground temperatures. Additionally, to avoid chemical contamination of the ground water this zone will need to be sealed off from the rest of the deep wellbore.

2.2 Granodiorite

The granodiorite is the targeted heat reservoir in the TU Darmstadt BHE project. It is an intrusive rock similar to granite but darker in colour and containing a greater concentration of plagioclase, a mineral within the feldspar family. The granodiorite formation contains the remaining two distinguishable layers of which are expected to be drilled. First of all there is a zone of weathered granodiorite. This rock may contain some of the ground water flow and will have a visible fracture system mainly filled in with deposited minerals. The depth of the weathered zone begins after the Red Bed layer and continues for approximately 5 m – 10 m. After this weathered granodiorite, the consolidated and nearly impermeable granodiorite formation is believed to exist.

The un-weathered granodiorite will remain relatively homogeneous and un-fractured for the proposed project depth (approximately 1000 m). However, there is a fracture system which can be seen in drill core samples taken from outcrops in the area. The fractures occur in intervals of 1 m – 5 m with apertures of a few centimetres. These fractures will contain some amount of water and thus the granodiorite is not expected to be completely dry. However, the small porosity and permeability of the rock will not allow for ground water flow. As the drilled depth increases into the formation, the fractures will occur in smaller frequency and with smaller size. The importance of the fracture system is not considered in the heat transfer but must be reflected in the potential existence of loss of circulation zones while drilling.

2.3 Hydrogeological Conditions

The hydrogeology begins with the ground water table underneath the geoscience building of TU Darmstadt. The thesis titled “*The urban influence of ground water emissions in Darmstadt*” (translated from German to English) provides a good collection of information on the hydrogeological conditions seen under the geoscience building. The author Beier (2007) states that “The ground water surface is 240 m above sea level in the SE to below 90 m above sea level in the SW” (translated from German to English). The following diagram (Figure 2.2) was used in the mentioned thesis to show the ground water contours existing in the Darmstadt area. Using Figure 2.2, comprised of data from 2002, the following assumptions have been made. The ground water table should lie at a depth of approximately 160 m a.s.l (above sea level) while the elevation at the parking lot of the institute building is at an elevation of 166 m a.s.l. This translates to a ground water level of between 2.5 m and 5 m below surface (Gu, 2010). Measurements taken at the institution in 2009 validate these assumptions. The measured depth of the ground water table at that time was 4 m TVD (Gu, 2010).

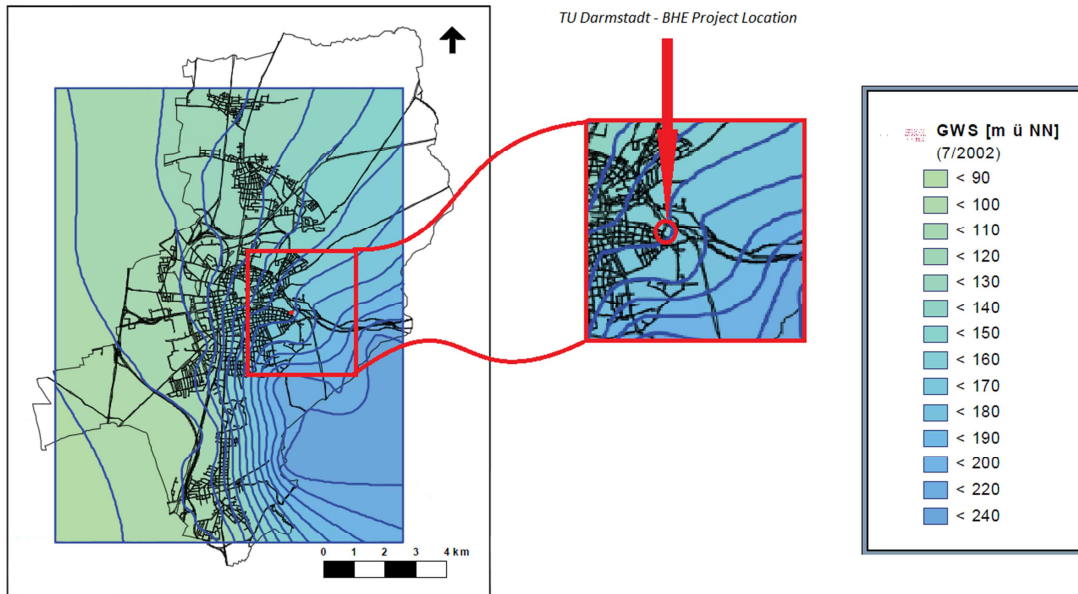


Figure 2-2: Ground water contours in the Darmstadt area (modified from Beier, 2007)

Hydraulic conductivity to be expected in the upper layers of the underground could vary between 10^{-5} m/s – 10^{-7} m/s (Beier, 2007). This equates to a relatively slow ground water velocity compared to other values estimated around Darmstadt. The hydraulic conductivities do show that there is a risk of contamination to potential potable water sources in the area of Darmstadt. There is some evidence of water source wells located in the SW region of Darmstadt city limits. These wells could be used to tap into the water table and for this reason the natural flow of water towards these wells cannot be contaminated. According to figure 2.2, the ground water level at the institute building lies above the ground water levels in the south west area of the city. Therefore if the areas are hydraulically connected water flow will tend to move in a SW direction. Since the planned BHE will lie upstream of potential water source wells in the SW, and the map in figure 2.2 shows potential water flow towards the SW, care must be taken during the drilling and operation of the BHE not to contaminate the ground water table.

2.4 Geothermal Conditions

In terms of geothermal conditions, the Darmstadt area does not have much for direct geothermal potential. As well, the temperatures underground are not hot enough to support the generation of power unless boreholes are extended past 2500 m (Baer, 2010). Even at depths of 2500 m temperatures reach a maximum of about 125 degrees Celsius (Baer, 2010). The geothermal potential comes in the various forms of indirect utilization; like the planned BHE project at TU Darmstadt. It has already been mentioned that the BHE will interact with the granodiorite to store heat during the summer and utilize this heat during the winter, but how exactly this happens has yet to be discussed.

There are three general heat transfer mechanisms available when transferring heat; conduction, convection and radiation. Conduction is the heat transferred between neighboring masses due to a difference in temperature of the pieces of material. Convection is heat transfer aided by forced or free movement of fluid particles. Radiation is the transfer of heat by the emission of radiation energy from a hot surface; thermal radiation does not require a medium for heat transfer. The BHE will react with the

granodiorite thermal reservoir which contains only one of the three modes of heat transfer. Because the granodiorite is homogeneous and non-porous, convective heat transfer will not be considered. As well, thermal radiation can be ignored because of the depth of our heat reservoir. The granodiorite lies below the neutral zone and by definition thermal radiation from the sun is absorbed by the ground long before it reaches the prospective thermal reservoir. The remaining mode of heat transfer is conduction.

Conductive heat transfer depends on the properties of the medium in order to transfer heat. Thermal conductivity and volume specific heat capacity both play a major role in determining how much heat is conducted and at what rate it flows. In order to determine the thermal conductivity, the Thermal Conductivity Scanner was used to apply an optical scanning technique. This work was done in the thermal lab at TU Darmstadt. Several outcrop samples of the granodiorite were scanned into the computer and thermal conductivity/diffusivity data compiled. The exact measurement results are outlined in table 2.1.

Table 2-1: Measured properties of the thermal reservoir

Sample		Mean Thermal Properties		Minimum Thermal Properties		Maximum Thermal Properties		
Name	Description	Thermal Conductivity [W/mK]	Thermal Diffusivity [m ² /s]	Thermal Conductivity [W/mK]	Thermal Diffusivity [m ² /s]	Thermal Conductivity [W/mK]	Thermal Diffusivity [m ² /s]	Percent deviation [%]
Granodiorite	Weathered	1.89	0.546	1.766	0.471	2.008	0.644	4.215
	Consolidated	2.461	0.683	2.237	0.527	2.591	0.823	2.926
	Vesicular	2.624	0.719	2.468	0.509	3.116	1.189	5.017

The machine measured and displayed values to three decimal places. However, when talking about the average properties of the granodiorite accuracy can only be assumed to one decimal place. It can be seen that the average thermal conductivity of the consolidated granodiorite is around 2.5 W/mK while the thermal diffusivity is around 0.7 m²/s. In contrast, granite rock samples taken from a similar outcrop nearby show thermal conductivities of approximately 2.9 W/mK. The samples for granite were measured at the same time as the granodiorite samples for a reason. This reason is because there is a small chance that due to the fracture system running underneath the geosciences building, granite will be encountered instead of granodiorite. However since the thermal conductivity of the granodiorite is smaller than the thermal conductivity of the granite, it is reasonable to assume granodiorite in the design of the BHE. This assumption is based on a conservative estimate as the granodiorite represents a worst case scenario calculation.

In order to calculate the volume specific heat capacity, the thermal conductivity need only be divided by the thermal diffusivity. When this is done the volume specific heat capacity for the granodiorite can be estimated between 4.24 J/m³K and 3.14 J/m³K. These properties not only govern the rate at which the thermal reservoir will accept the heat, but also the current temperature gradient existing insitu (3°C/100 m TVD).

3 PERCUSSION DRILLING TECHNOLOGY

Presently in the geothermal industry the percussion-drilling world is separated into two different categories. There are top hammer drills (drifters) and down the hole hammer drills (DTHH drills). DTHH drills have become more widely used in borehole drilling applications than their drifter counterparts. For this reason the DTHH drills are the focus of this publication and the basis for drilling and completion design. Percussion drilling is a technique where a 'standard' rotary drill is combined with the action of a down the hole (DTH) hammer drill. This allows the driller to utilize the best of both worlds. First of all, the percussion drill at the bottom of the drill string applies stronger forces than just the string weight alone (seen in rotary drilling). The reason for this is a mixture of the types of stresses being applied and the presence of impact loading.

There are two methods of DTH percussion drilling available to the geothermal industry today; pneumatic and hydraulic. Pneumatic, or air hammer drilling, has been around for many years and was developed as an alternative to rotary drilling in shallow hole applications. There are several advantages to air hammer drilling compared to pure rotary drilling; these will be covered in this chapter. However, pneumatic percussion drilling does have its disadvantages. The hydraulic hammer drill was created in an attempt to solve these disadvantages and is the primary method of interest for the TU Darmstadt BHE project.

The following chapter is dedicated to comparing the different drilling techniques by discussing the pros and cons of each. Then, with some basic drilling theory, the potential limitations of pneumatic and hydraulic drilling methods will be applied to their use in the TU Darmstadt BHE project.

3.1 Air Hammer Drilling

Air hammer drilling is a process used widely in the geothermal and water well industry for drilling shallow (10 m – 200 m) wells. The shallow wells drilled with pneumatic hammers are used for different types of applications ranging from the installation of energy piles, to borehole heat exchangers, to water source wells. This technology is generally cheaper and easier to implement than rotary drilling for shallow applications because of a few important factors. There are certain benefits and drawbacks associated with pneumatic drilling. They include rate of penetration, ease of implementation, hole stability and dust.

3.1.1 Components of a typical DTH Hammer

There are a few common elements to all hammers even though specific designs can vary. A valve system must exist to direct air above and below the piston, there is a piston, there are usually springs in order to aid in the actuating of the piston assembly, there is a rod attached to the piston, a striking peen, an anvil, and finally the drill bit. These components can be seen in the diagram below.

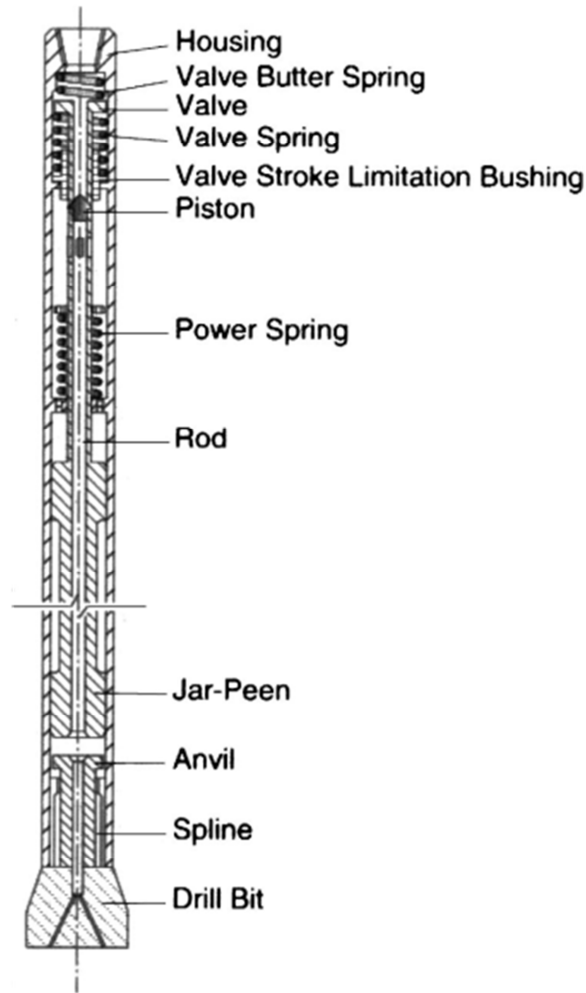


Figure 3-1: Typical DTH Percussion Hammer (Melamed et al. 1997)

3.1.2 Benefits of Air Hammer Drilling

Because of the value of resource being drilled, water and geothermal drilling often have less funding as would an equal depth oil and gas well. The drilling company must keep costs quite low for this reason. When looking at the air hammer, the benefits are directly correlated to their cost saving measures. Air as a drilling fluid, rate of penetration (ROP) increases and decreased weight on bit are all cost saving measures implemented to replace more expensive rotary drilling applications.

Rate of Penetration

One reason why air hammer drilling is more economical than rotary drilling in shallow applications is the increased ROP. The rate of penetration is one of the largest cost saving measures. The air hammer drill, in some instances, can drill up to five times faster than a rotary drill in a similar environment (Bar-Cohen et al, 2009). The reasons for this are mainly due to the frequency of the hammer impacts and the high loads applied to the rock during impact. Frequencies can be in the range of 40 Hz and thus rock breaking mechanics will happen forty times for every second.

In normal rotary drilling the only action on the drill string is rotation; the driller applies weight to the bit and simply rotates the string. This action, coupled with the use of a tri-cone bit, allows the drill to crush and shear the rock away from the bottom of the hole. A tri-cone bit is also referred to as a roller bit because the cones rotate at the bottom of the drill bit. A picture of a tri-cone bit can be seen below in figure 3.2.

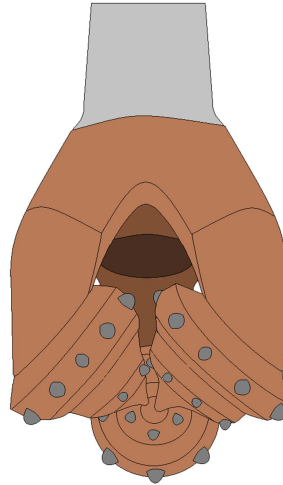


Figure 3-2: Tri-cone Toller Bit

This concept works well to begin with, but as the drill bit continues to be used the process becomes less efficient. Rock particles or bit wear can hinder the rotational motion of the tri-cone bit and if it does not rotate drilling becomes quite hard. Instead of crushing the rock the bit scrapes across the top of the rock face and drilling ROP is sacrificed. Sometimes the driller will choose to use a polycrystalline diamond compact (PDC) insert drag bit instead of a tri-cone bit. In this case the bit has no moving parts and has been designed to handle the increased torsion and wear applied when shearing the rock face. The fault of these types of bits is their cost and the top drive power required to use them efficiently.

In percussion drilling the problem with tri-cone roller bits is avoided completely and this is why the ROP is often much higher. The rock fracture mechanics in a hammer bit are a combination of both impact loading and string rotation. There is no need to have rotating cones on the bottom of the bit because it is reciprocated up and down between impacts. This allows the hammer bit to avoid damaging shear loading so a stationary bit can be used. An illustration of a typical percussion hammer bit is seen in figure 3.3. The bits are made of steel impregnated with much harder button or cone inserts.

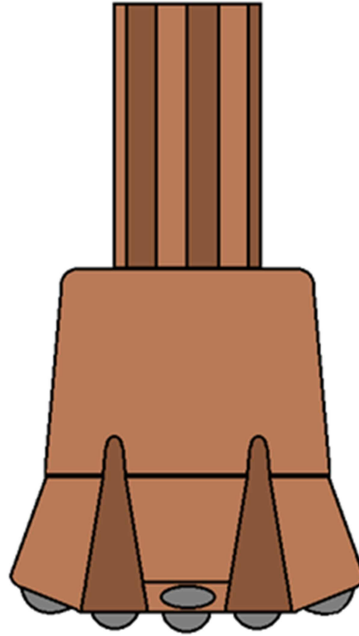


Figure 3-3: Typical design of a DTH hammer drill bit.

The mechanics involved in impact loading is the reason for such high impact energy. Unlike rotary bits, the hammer bit applies all three of the dimensional stresses to the rock at the same time; compression, tension, and shear loading. Directly underneath the bit a zone of compression is formed and on either side of the compression zone the rock is being pulled downwards. The downward movement of the rock material applies a tension force on the rock. As well, due to the rock under the bit being forced downwards, a shear stress exists between the effected compression zone and the stationary rock on either side. These stress mechanisms all act to create a complicated web of micro fractures directly underneath the bit inserts (figure 3.4). The blue area in figure 3.4 represents the compression effected zone, the green area represents the zones of tension, and red areas the zones of shearing.

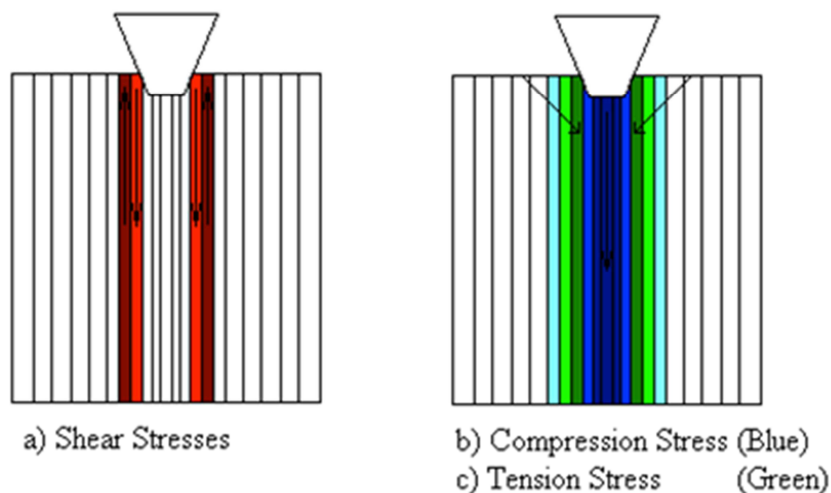


Figure 3-4: Diagram of the stress loading seen in the typical impact of a percussion bit

Once the stress loading reaches the rocks breaking strength the material is fractured enough to allow it to separate from the rock face. The stress that has not gone into fracturing the rock is used to eject the material out of the formed crater. Often, residual energy still remains in the percussion action of the hammer. At this instant a second impact occurs ejecting more material out of the formed crater. The figure below models this process.

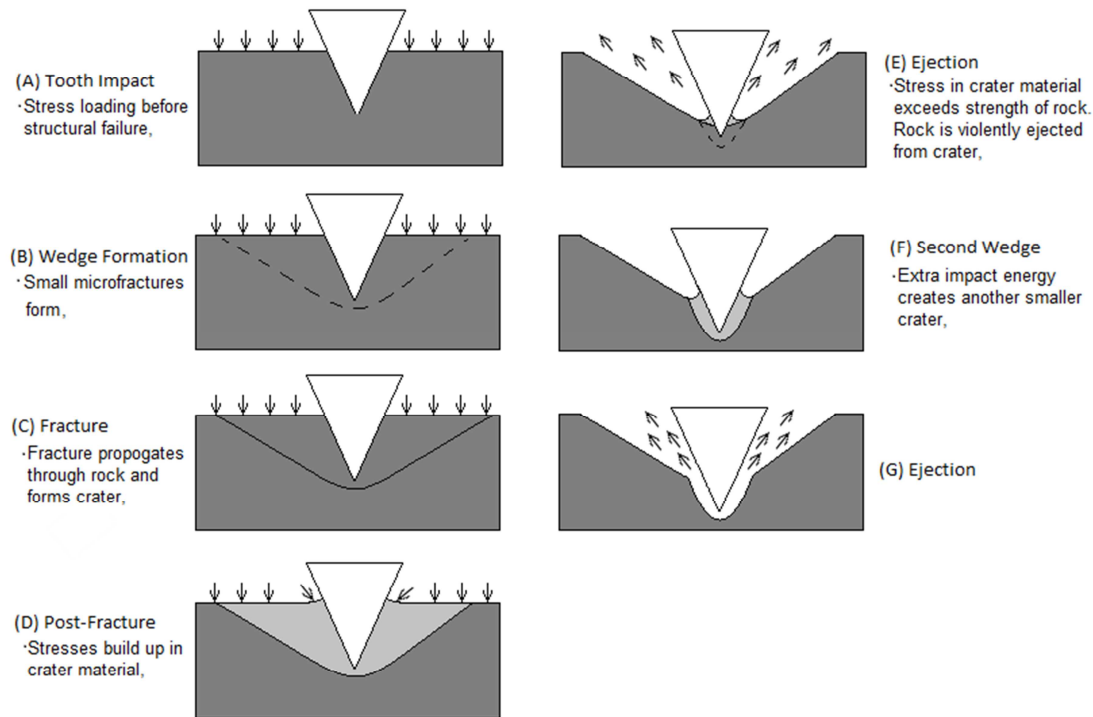


Figure 3-5: Drill bit crater mechanism (adapted from GEOE466 notes, Hawkes, 2008)

The drill bit is then rotated and the inserts are lined up at a fresh rock face ready to repeat the process. As mentioned, the process cycles nearly 40 times every second at multiple impact points on the bit. With this rapid succession of impacts coupled with a string rotation of 30 RPM, it makes sense how the ROP in a typical air hammer drilling operation will exceed the equal application of rotary drilling technology.

Weight on Bit (WOB)

The weight on bit of an air hammer drilling operation is usually much less than with rotary drilling. In rotary drilling the energy transferred by the bit into the rock is a direct result of how much weight is placed on the bit. This means that heavier drill strings need to be used in order to achieve a sufficient ROP. In contrast, most of the energy applied to the rock in a pneumatic hammer does not come from WOB but from the percussion mechanism at the bottom of the string. As discussed previously, a pneumatic piston contained in the drill assembly actuates the percussion mechanism. The energy then comes from the volume and flow rate of air supplied to the DTH hammer drill.

In fact, the DTH drill will operate better in low weight situations than in high weight situations (Melamed et al, 1997). The more WOB applied to the hammer the less likely it is to reciprocate between cycles. It is this reciprocation that causes the impact loading discussed above. If the weight on bit is too large, the bit will simply drag along the bottom of the wellbore thus increasing bit wear and decreasing ROP. For example, VNIIBT (All-Russian Scientific Research Institute of Drilling Technology) performed testing for oil and gas applications of percussion hammers showing that “in the rotary-percussion mode of drilling, ROP of 3.3 m/h was achieved with the 8-3/4 in. bit when the WOB was 4.5 [metric] tonne. To achieve the same ROP in rotary mode required 18.5 [metric] tonne” (Melamed et al, 1997).

Bit Wear

Complications in the drilling process of any technique will cause excess bit wear. However, bit wear happens during drilling even when operations are going as planned. The wear of any type of drill bit depends on the sort of contact it has with the rock and the duration of that contact. In rotary drills the contact is constant; the bit is always pressing against the formation and the teeth rotate within the bit. This rotation is good for avoiding the excess wear of the cone teeth but, as mentioned before, the bearings in the cones can become dirty or damage and therefore hinder this rotation. Without rotation the bit will wear unevenly and the problem is intensified until it requires the replacement of the drill bit. Illustrations of a new tri-cone bit, medium wear bit, and damaged bit can be seen in figure 3.6. Normal wear on the bits will be seen mainly in the teeth. They will begin to change shape by flattening out.

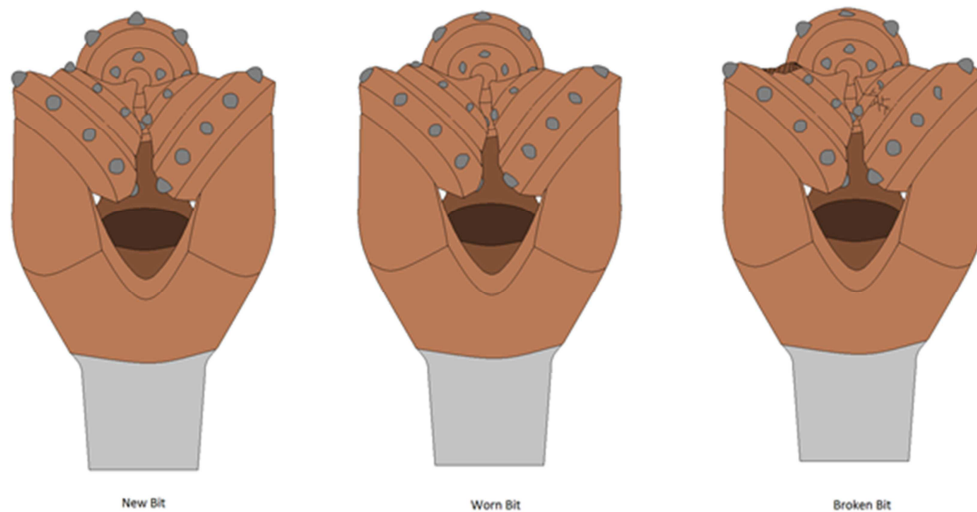


Figure 3-6: Tri-cone roller bit wear and damage visualization

The design of such bits varies and some designs have a higher wear tolerance than others. PDC (Polycrystalline Diamond Compact) insert bits have been developed along with sealed roller bearings and friction bearing bits. All of these improvements add cost and life to the service of a roller cone bit. However, the same advances in material strength that can be applied to a roller cone can be applied to a stationary DTH hammer bit.

Considering the DTH hammer bit, wear is less of a concern than with rotary bits because of the reciprocating nature of the drill. The bit will skip or jump along the bottom of the wellbore and thus only contacts the rock 2% of the time regularly seen in rotary drilling (Melamed et al, 1997). It is the reduced contact time which allows for the decreased bit wear seen on similar rotary drilling applications. Regular percussion hammer bits average nearly 500 m per bit but in some considerations have been known to drill up to 2000 m. Figure 3.7 shows a typical carbide insert hammer bit and the occurrence of a broken tooth.



Figure 3-7: DTH hammer drill bit broken carbide tooth. Other teeth have been sharpened for better bit performance (Wittig, 2010).

When considering bit consumption on PDC type hammer bits, drilling experts at the GZB (Geothermal Research Institute, Bochum, Germany) were questioned. The research institute had experience drilling with both carbide and PDC bits on a project within Bochum city limits. When the PDC bit was used, the driller was able to drill 4 drill holes without having to change the bit. In comparison the carbide bits required a bit change at least once on a 120 m drill (Wittig, 2010). The drill holes ranged from 150 m – 200 m and were drilled in a sandstone formation. The PDC bits used in this case were lasting 800 m – 1000 m in a formation considered to be quite abrasive on the equipment. In a rotary application the wear could be considerably higher.

Decreased bit wear saves time and money on a drill operation. The less time required for pulling out of hole and changing or servicing bits, the more money is saved on continuous operations.

3.1.3 Drawbacks of Air Hammer Drilling

Air hammer drilling, in most instances, is better than rotary drilling for shallow holes in hard to medium hard formations. However, there are drawbacks to this technology. The pneumatic system has limitations which can make it impossible to use in situations of increased drilling depth, unconsolidated rock, or targets lying below zone of potential hydrocarbon deposits.

Hole Stability

Because the density of air is much less than mud conventionally used in rotary drilling, there is less support on the borehole walls as the drill progresses further. The support comes from balancing or overbalancing the natural formation pore pressure with the hydraulic head of the drilling fluid. This causes problems when drilling in unconsolidated or highly fractured formations as the borehole will have a tendency to collapse. The

problem is also intensified the deeper the wellbore goes as lithostatic pressures increase the stress on the borehole walls. Problems caused by borehole failure include loss of circulation due to material plugging of the well bore, increase inflow of fluids from the formation and uneven hole geometry leading to problems with the installation of the BHE.

Dust

Although there are ways to combat dust, excessive dust is still a problem when drilling with pneumatic technology. Large volumes of air at high pressures are injected down hole. When the gases exit the drill string they expand and their velocity increases. This expansion and velocity are what carries the cuttings to surface. In dry rock the cuttings are produced along with dust. When the cuttings drop out of the air stream at surface, the dust enters the environment and can deposit on surrounding infrastructure. This problem has been partially solved with the introduction of foam drilling. Stiff foam is generated by adding water to the air. The water contains a drilling soap and when agitated by the air creates foam in the annulus. The foam traps the dust and does not let it enter the atmosphere. Foam drilling is used mainly on larger diameter holes.

Lower Explosive Limit (LEL)

Although in the geothermal industry the threat of hydrocarbon bearing zones is limited, it does happen that a driller may come across such zones. When this happens, the air sent down the drill string can act to bring the saturation of flammable gas in air to a level that exceeds the LEL. When the LEL level is exceeded, the chance of a spark igniting the gas is a danger that must be considered. An explosion down hole could lead to damages to the drill string, a rupture of the drill string, or could migrate up hole and cause dangerous issues on surface. The LEL's are a major reason for using water or oil based muds as the drilling fluid.

Drilling Depth

The ability to transport cuttings to surface is an important limiting factor in a pneumatic DTH hammer. The air used for transporting cuttings has very little density and viscosity so it relies on velocity to transport cuttings to surface. The air compressor used in the pneumatic hammer must then be able to supply enough pressure and flow rate at surface to sustain an acceptable cuttings transport velocity up the annulus. The deeper the borehole, the more air volume flow rate and compressor power is needed to sustain this velocity. The problem is intensified when water begins to enter the borehole. The back pressure of a water column may exceed the compressor rating at a certain depth. At this depth it is no longer economical to keep supplying compressor power to transport cuttings when a cheaper option is to use drilling mud and rotary drilling.

Hole Deviation

Another drawback to pneumatic hammer drilling is the deviation of boreholes. This deviation occurs because of two factors, the density of air and the vibrations of the hammer inside of the hole. In Joerg Riechers presentation of the Karlsruhe project he shows important information on the deviation of hydraulic hammers. He reports that a pneumatic system was used to drill a set of 14 boreholes to a depth of 250 m. The deviation on nearly all of the well bores was between 40 m to 110 m away from straight vertical. That means the bottom of the hole was located a horizontal distance of nearly 110 m from the top location after drilling had ceased (Riechers, 2010).

This deviation can cause problems in complex BHE arrays. If two holes were to cross one another the installation of a BHE would be impossible. Also, if the angle of deviation is too high, running in hole with steel or even PVC/PE (Polyvinylchloride/Polyethylene) tubing and casing is next to impossible due to excess friction from pipe contacting with the wellbore walls.

3.2 Hydraulic Hammer Drilling

Hydraulic hammer drilling is a technology with many similarities to pneumatic hammer drilling. The drill components look and act the same, the rock breaking mechanics are the same, and all of the benefits seen by pneumatic hammers are seen with hydraulic hammers. Increased ROP, decreased bit wear, simple equipment set up, and smaller rig sizes are all maintained with the hydraulic hammer technology. The main difference with hydraulic DTH hammer drills is the fact that water is used as the working fluid. This one difference ends up solving a lot of the problems associated with pneumatic hammer drilling.

Hydraulic hammer research started more than 70 years ago in the former Soviet Union. They began testing the hammers in an effort to increase ROP and drilling success rates. As mentioned in the paper *Hydraulic Hammer Drilling Technology: Developments and Capabilities*, “the efficiency of most hydraulic hammer designs was very low (8 percent maximum), so they were successfully used in shallow boreholes only” (Melamed et al, 2010). The VNIIBT can be credited with most of the recent and ground breaking research in the development of hydraulic DTH hammer drills. Their testing has led to hammer efficiencies greater than 40% and nearly 70 different tested designs of hydraulic hammers (Melamed et al, 1997). Most of these designs have been adapted by existing companies to create what is now considered the present hydraulic hammer technology. Companies such as Wassara have become well known for their achievements with the Hydraulic DTH hammer.

3.2.1 Present Hydraulic Hammer Technology

There are existing three main types of hydraulic hammer drills in the current industry: direct action, reverse action, and double action. Each type is actuated with a hydraulic fluid and contains the main components of a percussion hammer drill. The difference in the three hammer designs is in the power delivery system they encompass. The direct action hydraulic hammer uses the hydraulic pressure supplied by the water pumps to actuate the downwards motion of the piston-hammer assembly. The energy transfer is then fluid, to piston, to hammer, to anvil, to drill bit and finally into the rock. Part of the energy transferred by the fluid is also stored in a spring. The spring is used to return the piston back to its starting position for another cycle to take place (Melamed et al, 1997).

The reverse action hydraulic hammer is slightly different. Instead of the fluid energy being directly applied to the piston movement, it is first stored in a spring. The energy is stored during the return stroke of the piston after the hammer strikes the anvil. The energy stored in the spring is released when a valve system relieves the hydraulic pressure from the end of the piston. This stored energy forces the piston-hammer assembly to strike the anvil and transfer energy to the rock. At the bottom of the piston stroke, a hydraulic seal is returned and hydraulic pressure is used to return the piston to its starting position while simultaneously charging the spring (Melamed et al, 1997).

The double action hydraulic hammer is different than the other two technologies because it does not use an energy storage device like a spring. Instead, both strokes of the piston are controlled with hydraulic fluid and a complex valve system. During research at the GZB a hydraulic hammer from Wassera was cross sectioned and available for inspection. Pictures of the hammer are seen in figure 3.8 with an explanation of some of the important features. The entire hammer is first shown; the drill bit is the gold piece at the bottom of the assembly and the buttress joint is seen at the top. The buttress is the threaded part of the hammer where it connects to casing. Each of the discussed portions of the hammer are outlined in red and numbered from one to five.

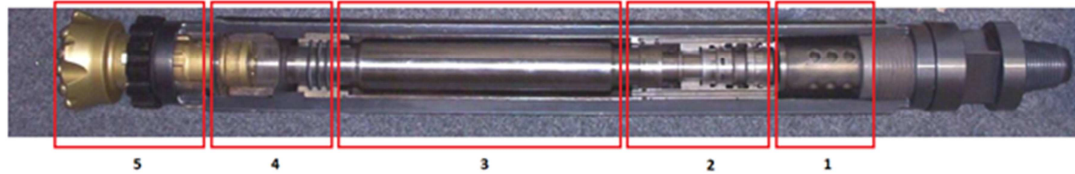


Figure 3-8: Hydraulic hammer at the GZB Geothermal Research Center in Bochum, Germany. (Wittig, 2010)

1. The Filter Screen



The first part of the double action DTH hydraulic hammer is common to all hydraulic hammers. A small mesh screen keeps any particles from the drilling fluid out of the hammer body. There are rubber seals throughout the design of the hammer. These particles could cause many excess wear of these seals if they were to enter the hammers construction. The small tolerances in the valves could become eroded if grit were to make it past the screen. This is the first part of the hammer to fail during drilling operations and can usually be replaced while the hammer is pulled out of the drill hole.

2. Hydraulic Valve system



Next the fluid passes through a system of valves used to direct fluid pressure above or below the piston. Pressure above or below the piston-hammer assembly is what actuates the piston movement and hammer striking the anvil. The movement of the piston is also what changes the position of the valves which intern redirects the flow of water. The valves friction seal against this part of the assembly and tolerances are very low. As mentioned above, any dirt or grit at this point in the hammer will hurt the performance of the drill.

3. Hammer



Attached at the end of the piston is the hammer or Jar Peen. The hammer is simply a large diameter piece of steel used to transmit mechanical energy received from the movement of the piston. The hammer tapers out at each end to maximize the momentum forces seen when it strikes the anvil.

4. Anvil, Piston, Rubber Seals



There are three components visible in this portion of the hydraulic hammer. The seals are used to isolate a pressure chamber required for the return action of the piston-hammer assembly. Near the bottom of the picture the anvil is visible. It is situated at the top of the drill bit and is used as the striking face of the hammer. Also a fluid flow path exists through the hammer and anvil. The entrance of this flow path is visible at the top of the anvil.

5. Drill bit and Anvil



Finally the drill bit, attached as part of the anvil, lies at the bottom of the drill assembly. The bit receives vibrational energy from the anvil and transfers it to the rock face. Fluid exits the bottom of the bit to clear away cuttings and debris after the impact has occurred. Fluid also helps to cool the bit from excess friction heat.

3.2.2 Advantages over Air Hammer Drilling

As mentioned before, water is used in the hydraulic hammer as the working fluid. This solves a lot of the problems which make the pneumatic hammer unable to compete with the rotary technology in drilling. Problems like the power required for deep holes, the stability of the drilled holes, efficient cuttings transport, high temperature applications and even hole deviation are improved when drilling with a hydraulic hammer.

Power Requirement

The power requirement of the water pump used to circulate water is normally lower than the air compressors used in pneumatic hammers. This has to do with the compressibility of air compared to water. It is known that water, under normal conditions, acts like an incompressible fluid while air is a compressible fluid. In each case a pump is needed in order to push the fluid into the drill string and up the hole. However, in the case of air most of the pumps energy goes into compressing the fluid and only a fraction is left to push it down the drill pipe and up the wellbore. Because water is an incompressible fluid, all of the pumps energy goes into moving water down hole as the water is not able to be compressed.

In Joerg Riechers presentation of the Karlsruhe project he mentions that for an equivalent hole of 220 m, 2.9 l/m of diesel fuel was needed during the pneumatic drilling process. In a similar 220 m hole drilled in a similar formation density, only 0.7 l/m of diesel fuel was needed to power the water pump (Riechers, 2010). His experiment shows proof that the energy required to drill with hydraulic hammer drilling is much less than drilling with air hammer drilling.

Hole Stability

Hole stability is a big problem in pneumatic hammer drilling. For this reason most pneumatic operations are done in hard rock formations where stability is not as much of an issue. When drilling with water, hole stability is no longer such a large concern. Borehole breakouts will still occur in unconsolidated formations but their severity and regularity will be reduced. The reduction is both a factor of hydraulic gradient support and reduced annular velocities.

The density of air at a pressure of 25 bar is approximately 25 kg/m^3 . This pressure is the average maximum pressure used in a pneumatic hammer drilling operation. At bottom hole, if we assume the air does not expand up hole and assume a hole depth of 100 m with acceleration of gravity equal to 10 m/s^2 , the hydraulic head will never be greater than 35 kPa. In a similar situation, assuming water as the drilling fluid (density 1000 kg/m^3), pressure at bottom hole should be approximately 1000 kPa; nearly 28 times higher than the largest conceivable air pressure. The reality is that the air, immediately after exiting the drill string begins to equalize with the atmospheric conditions at the top of the well. It will expand and decrease in density while doing so. Therefore, the real pressure down hole will be less than the proposed hypothetical situation. This further supports the claim that hydraulic hammers provide more support to the borehole walls and thus a higher hole stability.

Also, the expansion of air up the annulus increases its velocity as the volume remains constant. However, when a borehole breakout occurs the high velocity air enters the breakout along with cuttings and forms vortices. These vortices can act to blast the formation with abrasive cuttings which can in turn further damage the formation and extend the borehole breakout. In hydraulic drilling, borehole breakouts are much less common. As well, velocities are much slower in the annulus so when they do occur, damages are minimized.

Cuttings Transport

Pneumatic hammers are much less efficient in transporting cuttings to surface. This is because the density and viscosity of the air is not enough to support the weight of the cuttings. The density of a fluid imposes a buoyance force on the drill particle. This buoyance force, along with a friction force from the velocity of the fluid, is what aids in transporting cuttings to surface. In air the buoyance force is negligible but in water it is quite significant. Therefore, air relies on velocity to impose a higher friction force on the cuttings to make up for the loss in buoyance. Water does not need to rely on velocity because the buoyance force will help to lift the cuttings. For this reason, low velocity water (0.5 to 1.0 m/s) is much more effective at transporting cuttings than high velocity air.

The efficiency of cuttings transport is important for many reasons. If cuttings do not make it to surface they will eventually drop to the bottom of the drill string and lie on top of the drill. If a large enough volume of cuttings are not making it to surface the drill has the chance of getting stuck in hole. When drilling with such an expensive tool such as a DTH hammer, a stuck drill can cost many days of rig time and potentially the loss of the hammer and hole during the recovery operation. Since cuttings transport is more efficient with hydraulic hammer drills there is less of a chance of getting stuck in hole and thus less risk associated with the drilling operation.

Hole Deviation

It was previously mentioned that hole deviation in pneumatic hammer drilling can be quite significant. An example from Joerg Riechers presentation on the Karlsruhe project was used where bottom hole locations had deviated from top hole locations by a horizontal distance of nearly 110 m in some cases. In this same study, 15 holes were drilled with a hydraulic DTH hammer for comparison with the pneumatic DTH hammer wellbores. The results were a maximum deviation in hydraulic hammer boreholes of just over 40 m; a significant improvement on the 110 m deviation of the air hammers (Riechers, 2010). A chart from Riechers presentation is shown below which shows the dramatic difference in hole deviation.

DTH Water Hammer Drill
(**< 5 - 10 Deviation Angle**), Angles approximatly 5 times less than
with equivalent DTH Air Hammer

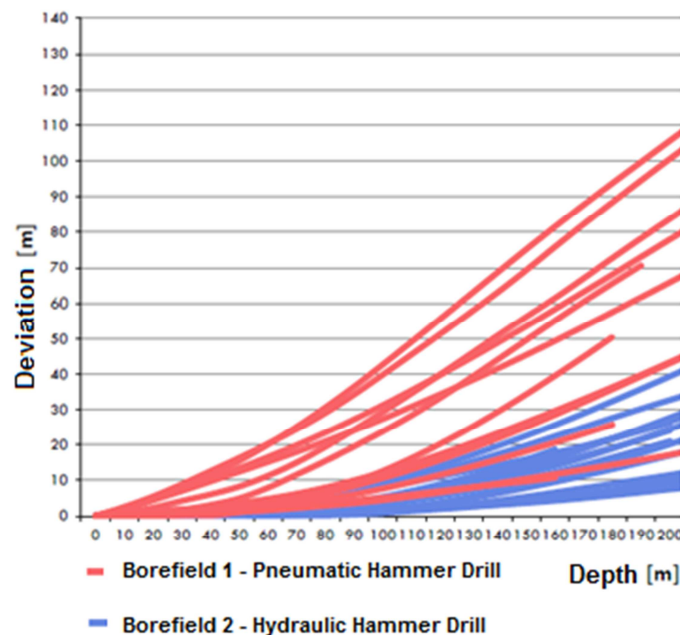


Figure 3-9: Hole deviation, Air vs Hydraulic Hammer (Riechers, 2010)

The blue colored lines represent the hydraulic hammer boreholes and the red lines represent the air hammer boreholes. On the vertical axis there is the deviation distance in meters and on the x axis the true vertical depth of the boreholes. A perfect hole would have no deviation and would lie along the x axis of this chart. It can be seen that none of the boreholes were perfectly straight. There is never a case in drilling where the final result is a perfectly strait borehole without deviation, there will always be some deviation due to density variations, fractures in the formation, or zones of higher or lower pressure.

Dust

Air hammers tend to produce a lot of dust while drilling. On modern rigs the dust is collected in filter bags. The bags minimize dust but add more equipment and clean up on site. This does not happen with water as the dust mixes with the drilling fluid before it exits the wellbore and is not given a chance to enter the air around the drill site.

3.3 Drilling Theory: Air vs. Hydraulic Hammer

It is now known that the hydraulic hammer solves many of the problems which have kept pneumatic hammers from competing directly with rotary drills. However the question still remains, is there enough benefit from the hydraulic hammer to warrant using it in the TU Darmstadt BHE project? To answer this question some important drilling calculations were transcribed into a spreadsheet for comparison of the two methods. The BHE spreadsheet was created as a tool to be used in the preliminary design of the drilling and completions in a BHE project. The drilling part of the spreadsheet will be covered below and the completions theory in chapter 4.

3.3.1 Mud Flow Rate and Density Calculations

The most important comparison between pneumatic and hydraulic DTH hammer drilling is the mud density and flow rate required to transport cuttings up the annulus. To maximize efficiency the driller must minimize the required pumping (or compressor) power while still allowing for cuttings transport. This is where the difference between the two drilling methods is evident. There are many correlations available to calculate the required mud density for drilling. Two correlations were chosen to be included in this thesis for purposes of comparing air and water as drilling fluids. The first is Moores Correlation for mud slip velocity and the second is the Walker Mayes Correlation, also used to calculate slip velocity.

Moores Correlation for Mud Slip Velocity

Moores Correlation is used in calculating mud slip velocities in the drilling industry. The slip velocity helps the drilling engineer determine if the selected drilling mud will be sufficient for cuttings transport. As previously discussed, cuttings transport is one of the most important factors of a successful drill; if the cuttings are not circulated out of hole there could be problems with the drill getting stuck thus having a negative impact on the ROP. The following section is dedicated to explaining how Moores Correlation was used in this project to structure the BHE spread sheet. It was used as a lower level approximation to mud density and also used to calculate the cuttings transport velocity in another tab.

The original formula for Moores Correlation was taken from “The On-line Computational and Graphics Website for Petroleum Engineers & Geologists” website (Harrison, 2007). This correlation appears in the “cutting slip velocity” link as:

$$v_{slip} = \frac{175(\rho_{rock} - \rho_{mud})^{0.667} \varphi_p}{\rho_{mud}^{.333} \mu^{.333}} \quad (3.1)$$

Where: ρ_{rock} = Density of the formation rock being drilled [ppg]

ρ_{mud} = Density of the drilling mud [ppg]

μ = Moores corelation constant

φ_p = particle diameter [in]

v_{slip} = Velocity cuttings through the drilling fluid [ft/min]

By rearranging the formula to get rid of the 1/3 roots it is transformed to the following step in this derivation:

$$\mu \left(\frac{v_{slip}}{175\phi_p} \right)^3 = \frac{(\rho_{rock} - \rho_{mud})^2}{\rho_{mud}}$$

Simplifying the right hand side further we get a formula that resembles a quadratic equation. Letting X and Y equal their respective parts and then creating a quadratic equation shows the need to redefine the Y variable.

$$\mu \left(\frac{v_{slip}}{175\phi_p} \right)^3 = \frac{(\rho_{rock} - \rho_{mud})(\rho_{rock} - \rho_{mud})}{\rho_{mud}}$$

$$\mu \left(\frac{v_{slip}}{175\phi_p} \right)^3 = \left(\frac{\rho_{rock}}{\rho_{mud}} - 1 \right) \left(\frac{\rho_{rock}}{\rho_{mud}} - 1 \right)$$

Let... $X = \frac{\rho_{rock}}{\rho_{mud}}$ and $Y_0 = \mu \left(\frac{v_{slip}}{175\phi_p} \right)^3$

Therefore... $Y_0 = (X - 1)(X - 1) = X^2 - 2X + 1$

Redefine Y as... $Y_1 = Y_0 + 1$

Therefore... $0 = X^2 - 2X + Y_1$

With the redefined Y variable we can use the quadratic formula to solve the roots of the equation.

$$X = \frac{-b \pm \sqrt{b^2 - 4ac}}{2a} ; 0 = aX^2 + bX + c$$

Where: $a = 1$

$b = -2$

$c = Y_1 = \mu \left(\frac{v_{slip}}{175\phi_p} \right)^3 + 1$

Substituting the definitions of X and Y back into the solved roots, and rearranging to isolate the mud density, we end up with an equation to solve for the mud density. This equation is dependent on the rock density, the slip velocity, a correlation constant μ , and the size of the cuttings.

$$\frac{\rho_{rock}}{\rho_{mud}} = \frac{2 \pm \sqrt{(-2)^2 - 4(1)(\mu \left(\frac{v_{slip}}{175\phi_p} \right)^3 + 1)}}{2(1)}$$

Finally...

$$\rho_{mud} = \frac{2\rho_{rock}}{2 \pm \sqrt{(-2)^2 - 4(1)(\mu(\frac{v_{slip}}{175\phi_p})^3 + 1)}} \quad (3.2)$$

Moores Correlation Constant μ

The correlation constant was used by Moore in order to include the diameter, velocity of the drilling fluid and the plastic viscosity/yield point (PV/YP) into the calculation of the slip velocity. Looking at the original correlation this makes sense; the only governing terms in the equation are density and cutting size. Further information is then needed for how the cuttings move through the fluid. The correlation constant takes into consideration how the cuttings move through the fluid and how much of the fluid they have to move through.

The equation for the correlation constant is shown below, as found in the online calculator:

$$\mu = \left(\frac{2.4v}{D_h - D_p} \frac{2n-1}{3n} \right)^n \left(\frac{200K(D_h - D_p)}{v} \right) \quad (3.3)$$

Where: $v = \text{annular velocity [ft/min]}$

$D_h = \text{hole diameter [in]}$

$D_p = \text{drill pipe diameter [in]}$

$n = \text{viscometer constant}$

$\mu = \text{correlation constant}$

Two important variables included in this equation are the K value, not to be confused with conductivity, and the n value. These two variables each have their own correlations based on the viscometer readings of PV/YP. Each of the equations can be seen below. Please note that the K value depends on the calculation of n.

$$K = \frac{\theta_{300}}{511^n} \quad (3.4)$$

$$n = 3.32 \log \frac{\theta_{600}}{\theta_{300}} \quad (3.5)$$

Where: $\theta_{300} = 300 \text{ viscometer dial reading} = PV + YP$

$\theta_{600} = 600 \text{ viscometer dial reading} = \theta_{300} + PV$

Walker Mayes Correlation Theory

As a comparison to the Moores Correlation, the Walker Mayes correlation was used. This formula calculates a slip velocity based on mud/rock density and cutting thickness alone. It was developed for disk shaped cuttings and assumes fully turbulent flow conditions. The formula is given on the next page (Hawkes, 2008).

$$v_{slip} = [1.79gT \frac{(\rho_{rock}-\rho_{mud})}{\rho_{mud}}]^{\frac{1}{2}} \quad (3.6)$$

Where: g = acceleration due to gravity [$9.81 \text{ m} / \text{s}^2$]

T = thickness of the disc shaped cuttings [m]

In order to compare with the adaptation of Moores equation derived previously, the Walker Mayes correlation was formulated to calculate the mud density dependant on the slip velocity, the cutting thickness, and the rock density. To do this, each side of the equation is squared in order to get rid of the square root.

$$v_{slip}^2 = 1.79gT \frac{(\rho_{rock}-\rho_{mud})}{\rho_{mud}}$$

By expanding the density ratio and dividing v_{slip}^2 by $(1.79gT)$, the equation is simplified in preparation for isolating ρ_{mud} .

$$\frac{v_{slip}^2}{1.79gT} = \left(\frac{\rho_{rock}}{\rho_{mud}} - 1 \right)$$

Finally, ρ_{mud} can be isolated on the left hand side of the equation; thus formulating an equation for the mud density based on the Walker Mayes correlation.

$$\rho_{mud} = \left(\frac{\rho_{rock}}{\left(\frac{v_{slip}^2}{1.79gT} + 1 \right)} \right) \quad (3.7)$$

In the BHE spreadsheet this equation is used along with the original Walker Mayes correlation as an upper level approximation for acceptable drilling mud density and to calculate the slip velocity if the chosen mud density.

3.4 The Comparison

In order to calculate values for each of the drilling techniques, a standard set of inputs was required. These inputs are the same variables as required by equations 3.2 and 3.7 and are required to be site specific when entering into the spreadsheet. The variables, as listed by

the equations, are: the mud circulation rate, the borehole drift diameter, the drill string outer diameter, the density of the rock formation, the thickness of the cuttings, the diameter of the cuttings (spherical), the yield point of the fluid (YP), and the plastic viscosity of the fluid (PV). One must consider that these calculations do not take into consideration the compressibility of air; however an average density of the pressurized air in the wellbore can be easily calculated. This calculation will be discussed below along with the other variables.

Flow Rate

The flow rates seen in typical pneumatic and water hammer applications were acquired during study at the GZB in Bochum. According to Prof. Volker Wittig at the GZB the average circulation rate of a typical hydraulic hammer is approximately 5 l/s depending on borehole size and how well the drill is progressing. Flow rate is monitored very closely and is increased or decreased to maximize the ROP. A literature search on the flow rates typically seen in pneumatic DTH hammer drilling turned up values in between 15 l/s – 40 l/s. These rates varied a lot in the publications searched. The variance on flow rate is no surprise as a skilled driller will adapt his flow rates and pressures to how hard the drill is working in order to maximize its ROP. For purpose of analysis, a flow rate of 5 l/s in the water hammer and 25 l/s in the pneumatic hammer will be used.

Borehole Size

The end result of the TU Darmstadt BHE project is to drill and produce two to four deep wellbore heat exchangers for the district heating of the renovated building. This means that the efficiency of this system will rely on the design of the wellbores. In order to maximize the amount of heat transfer to the reservoir, and assuming an unlimited supply of waste hot water, the casing diameters should be maximized for the prospective drill. Currently available in Germany, and for use in the TU Darmstadt BHE project, are 6 inch hydraulic hammers. This means that the largest drilled borehole diameter is a 6 inch or 0.1524 m. For this reason a borehole drift diameter of 0.1524 m will be assumed in the calculations.

Drill String Outer Diameter

In order to attach and properly drill with the 6 inch drill, a 4 inch (0.1016 m) drill pipe is required. This pipe will likely be tapered slightly on its way to surface but for the purpose of analysis a constant diameter will be used. Casing measuring 0.1016 m in outer diameter will be used as an input for the Walker Mayes and Moores correlations.

Density of the Rock Formation

Density measurements of the granodiorite were not able to be performed during the research period set aside for this thesis project. However there is already a collection of data existing on the mechanical properties of granodiorite all over the world. *Mechanical Properties of Granodiorite from Laboratory Tests* is a publication which studied and tested granodiorite samples from five areas of the world. They collected information on the rock and compiled the results into the table seen below. For the TU Darmstadt BHE project, the values for Louvigne-du-Desert, France will be chosen because of its geographical proximity in relation to the other locations.

Table 3-1: Properties of the granodiorite formation (Dayre, Giraud, 1986)

Physico-mechanical properties of some granodiorites				
Location	Density (kg/dm ³)	Compressive strength σ_c (MPa)	Tensile strength σ_{tb} (MPa)	Modulus of elasticity (MPa)
Bridge Canyon Dam, Ariz., U.S.A.	2.71	118.59	8.20	46 880
Tumut Pont Dam, Australia	2.71	126.86	1.45	63 090
Louvigné-du- Désert, France	2.71	158	10	72 000
Wadi Buwwah, Saudi Arabia	2.80	133	20.4	84 000
Wadi Aridah, Saudi Arabia	2.80	230	17	69 000

Thickness and diameter of the cuttings

The final input parameter for the cuttings transport equations is the thickness and diameter of the cuttings. See below is a picture taken of actual sandstone cuttings harvested from a hydraulic hammer drilling operation in Bochum, Germany. The cuttings are quite uniform in shape and size which is characteristic of percussion hammer drilling. The impacts occur at such a high frequency that even if larger rock particles are broken off the rock face they get ground down to this size within a few cycles. By the time the cuttings exit from underneath the drill bit they are small and disc shaped. Input parameters for the BHE spreadsheet will be a disc diameter of 2 mm and a spherical thickness of 2 mm; assuming a perfectly round, 2 mm diameter ball. In reality the cuttings are more disked shaped but for the Walker Mayes correlation a spherical approximation is necessary.

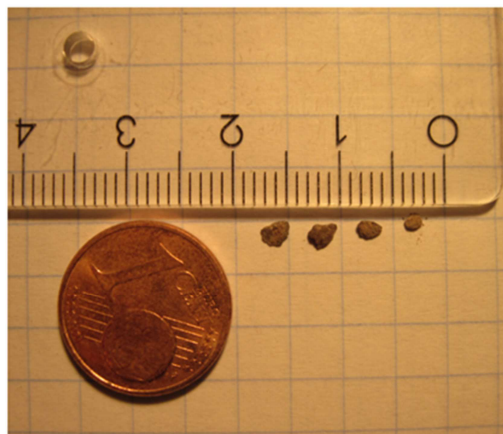


Figure 3-10: Diameter and thickness of cuttings

PV and YP of Air Water

These values are the most difficult to approximate for the Walker Mayes correlation. YP is the resistance of a fluid to flow, and as most fluids will not flow out of a container by themselves, they all have a value. However, the YP of water is so small that it flows with little to no natural resistance. This value can be approximated as 1 but due to the sensitivity of measurement devices is hard to get a closer estimate. It is impossible to consider the YP of air because in a certain consideration it does not exist; air essentially has no resistance to flow and in a normal environment it will freely flow out of its container. The PV of these substances also does not exist. There are very few if any particles in water and so by definition the water cannot have a plastic viscosity; the same goes for air. Therefore, a Walker Mayes correlation is not possible for air and can only be considered an estimate for water. The process involves using a viscometer and gathering readings of the shear rates at 600 RPM and 300 RPM. These shear rates are used to calculate the PV and YP (ASHME, 2004). For the Walker Mayes correlation the assumed values of YP and PV will be used to calculate the shear rates at 300 RPM and 600 RPM instead. PV will be estimated at 0, and YP at 1 for water as a drilling fluid. The correlation will not be performed for air.

Calculated Values for Density and Slip Velocity

Finally the values mentioned are input into the spreadsheet for calculation. Using each of the correlations the following results were calculated for air and water drilling fluids.

Table 3-2: Output data for water

Mud Weight Calculations Spreadsheet OUTPUT DATA - Water			
Equation #	Calculated Values		Description
1	V_mud =	0.490299	Mud Circulation annular velocity [m/s]
2	p_rock =	3.145	Average Rock Density for cutting transport calculation (g/cm ³)
3	p_mud =	823.6265	Walker Mays Mud density [kg/m ³]
4	n =	0.99942	↑
	K =	0.001964	
	μ =	0.940331	↓
	p_mud =	540.1394	Moore's Mud density [kg/m ³]

The calculated values show an approximated minimum mud density of 540.1 kg/m³ (Moore's equation) and minimum 823.6 kg/m³ (Walker Mayes Correlation). The equation is telling us that if we circulate a fluid at 5 l/s through the specified drill string set up, we need a minimum mud density of between 540.1 kg/m³ and 823.6 kg/m³ in order to maintain a net transport velocity of 0.2 m/s. The mud density approximated through calculation is much less than the density to be used during actual hydraulic drilling. Therefore, if water is used as the drilling fluid (density 995 kg/m³) both approximations are exceeded by factors of 120% and 180% respectively. In this instance it would be safe to say that under the given drilling conditions, water flowing at a flow rate of 5 l/m is sufficient to circulate cuttings to surface.

In order to compare air as a drilling fluid, the Walker Mayes correlation was used in its original form to calculate a slip velocity of cuttings in the annulus. The results are shown below.

Table 3-3: Output data for air

Cuttings Velocity Calculations Spreadsheet INPUT - Air		
Equation #	Calculated Values	Description
	Q = 5.62475	Mud Circulation Rate [m ³ /min]
1	V _{mud} = 9.250488	Mud Circulation annular velocity [m/s]
2	ρ _{rock} = 3.145	Average Rock Density for cutting transport calculation (g/cm ³)
3	V _{Slip} = 9.050474	Walker Mays Slip Velocity [m/s]
	V _{net} = 0.2000	Net Cuttings Velocity[m/s]

The above table shows the calculations performed for air as the drilling fluid. It can be seen for an equal net transport velocity of 0.2 m/s an air circulation rate of 5.62 m³/min is necessary. Comparing 5.62 m³/min to the flow rate of 0.3 m³/s (5 l/min) of water, it can be seen that the flow rate of air dwarfs the flow rate seen with water transport. Air is obviously the less efficient transport mechanism and therefore will not be used as the primary drilling fluid in the TU Darmstadt BHE project.

3.5 Drilling Design

All things considered a preliminary design for the drilling of the BHE boreholes can be created. This design is stated below in step by step form followed by a simple stick diagram. Before the project is to commence all volumes and hole diameters should be checked with the prepared BHE design. The dimensions in the stick diagram have been specifically designed to fit together with minimal tolerances. Any changes to the design of the bore hole or the BHE should be made clear and tolerances of the planned operations double checked. Also have the drilling engineer check the design and the program before implementing its procedures. The drafted plan is only a preliminary design and some aspects may have been missed or overlooked.

1. Drill hole for conductor casing: This casing will isolate the BHE from the upper most layers of the formation (red bed, weathered granodiorite).
 - a. 8 inch total hole diameter (6 inch hammer drill bit with 8 inch reamer bit attached)
 - b. Drill should progress to a depth of approximately 60 m. For the final 15 m to 10 m of drilled depth the geologist should be onsite in order to examine the rock cuttings. Evidence of granodiorite weathering will be looked for. If any evidence exists extend the drilled depth 5 m and examine cuttings further. Weathering evidence could be the existence large mineral crystals, rust staining, melaphyre present, red bed present.
2. Pull out of hole (POOH) with drill string and perform a wiper trip to bottom to ensure a clean bore hole.
3. Run in hole (RIH) with 7 inch conductor casing to total drilled depth and prepare for cementing operations by filling hole with water. Have a surplus of casing on location in case the consolidated granodiorite is deeper than expected. 100 m of the specified casing should be adequate.

4. Cement in conduction casing
 - a. Cement should be designed to insulate against the relatively colder ground and also to seal off any fluid transport within the ground water zone. The cementing company Dyckerhoff in Germany offers cement solutions fitting to this application. One stage cementing job will be sufficient. Visit their website <http://www.dyckerhoff.com/online/en/Home.html> for a complete product listing.
5. RIH with main drilling assembly. 6 inch hydraulic hammer on 4 inch casing to be drilled through the granodiorite formation. Drill string will consist of a few joints of heavy walled pipe at the bottom to weigh down the drill string and then regular grade pipe to surface. Weight on bit (WOB) should be minimized in the operation but is to be applied at the driller's discretion.
 - a. 6 inch total hole diameter
 - b. Drill should progress to specified BHE setting depth and then extend past 5 m TVD. The 5 m is to make up for back fill and leave room for cementing operations.
6. POOH with drill string and perform 2 wiper trips in the wellbore. This will ensure a drift diameter equal to the radius of the drill bit and will ensure proper running of casing. Ensure hole is filled with fresh water for the casing running procedures. In order to cement, the casing will have to be hung from the rig. Extra support may need to be present when running in hole and hanging casing.
7. RIH with specified 5 inch casing string on slim hole connections and prepare for cementing procedure.
 - a. Drilled length of the borehole will be slightly larger than 800 m but each BHE will be required to have length of 800 m. Casing for the main hole should be budgeted at 900 m per wellbore to make up for damaged joints or running complications. All casing should be inspected and drifted before running in hole. Check these against factory specifications and ensure adequate dimensions.
8. Cement casing string in hole as per cementing company's instructions.
 - a. Cement program should include a two stage cementing procedure where insulating cement is used at the top of the borehole and conductive cement at the bottom. The exact separation depth of the two stages has not yet been calculated and should be done before talking to the cement company for estimates on the cements to be used and on the two stage cementing job.

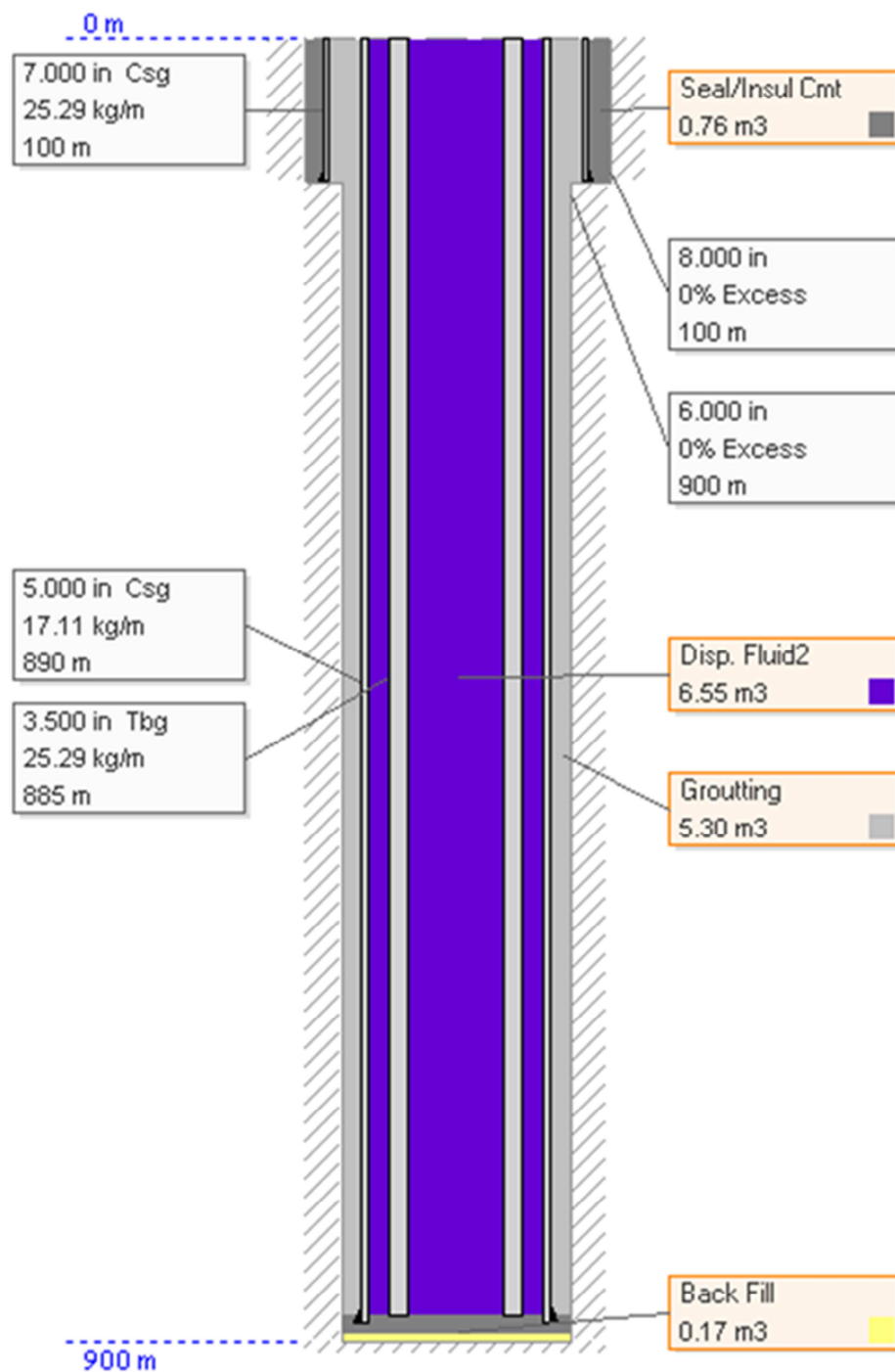


Figure 3-11: Borehole stick diagram correlating to drilling design

3.6 Environmental Impact / Risk Identification

There is a limited amount of information available about the geology underneath the TU Darmstadt Geosciences building. Any evidence of potential environmental impact will be purely speculative and is based on the information provided in the geological background of this report. There are different impacts and risks associated with the drilling procedure in the uppermost 60 m and the lower heat reservoir. Each section will be discussed separately below.

In the upper most 60 m of wellbore there is three distinguishable layers apart from the top soil. The Red Bed layer, as mentioned before, consists of alternating stratified layers of siltstone and sandstone. This zone is highly porous and has fluid conductivity values in the range of $10^{-5} - 10^{-7}$ m/s. Environmental concern comes from the existing ground water table in this region. The water table has been tested at a depth of 4 m below surface and will saturate this part of the ground. Since hydraulic connectivity should exist between the Red Bed and weathered granodiorite layer, these layers will be considered together for the potential contamination of the ground water table. The ground water table must not be contaminated. It may potentially flows away from the campus in a SW to W direction towards the city center and existing potable water source wells. Care should be taken in the drilling at this area to not introduce contaminating agents into the ground water. Temperature contamination is not expected to matter however chemical contamination should be a concern. Prior to the drill, the geologist in charge of drilling operations should have samples taken of the ground water in the area to ensure the drilling fluid will not interact negatively with the existing ground water. Negative actions could include changes to microbiological cultures and chemical concentrations. Losses of drilling fluid are expected in this area.

Care should also be taken in the first ten meters of drilled depth to ensure underground contamination zones are not intersected. Since the drill will be traveling through old construction zones (from the past work done at the university), existing contamination of the formation is a potential. At any signs of oil staining, debris, or unusual/unexpected geological conditions, drilling progress should be halted and an assessment of the contaminated zone be performed. If the drilling operations are at risk of spreading the existing contamination, the local regulating authorities should be contacted and the decision made on whether to proceed with the planned project.

Drilling risks in the uppermost 60 m of drilled borehole include wellbore instability and potential inflow of ground water.

In the main drill hole, set in the granodiorite formation, there are no real concerning environmental or drilling risks. Drill cores from outcrops in the region confirm a fracture system which shows the potential existence of small openings every 1 m – 5 m. These fractures will become less frequent as depth increases. The chance for loss of circulation or fluid losses in these zones does exist, however total loss of circulation should not occur.

4 COMPLETIONS THEORY – COAXIAL VS DOUBLE U-TUBE

For reasons already discussed, the coaxial heat exchanger was chosen for the model of the borehole heat exchanger. An analytical approach for modeling the BHE was used and integrated into a spreadsheet for reproducible results. In this chapter, theory behind the design of the BHE and the BHE spreadsheet will be discussed in detail. The theory is comprised of thermodynamics in order to calculate values for steady state operation. The final goal is to calculate a reasonable heat transfer rate per meter of wellbore. This is done in order to approximate the total number and the length of each BHE needed to supply the 300 kW heating system of the renovated building.

Assumptions have been made in the processing of the spreadsheet results which affect their final outcome. These assumptions will be clearly stated in the discussion however the purpose of these results should not be lost. The spreadsheet was designed as a tool for engineers to quickly apply accurate thermodynamic theory in the preliminary design of a wellbore heat exchanger. The results obtained in this thesis are applicable for one design and a certain assumed environment. The results should not be used as final numbers when designing a coaxial BHE system.

When designing such systems, one should turn to the aid of FEM programs such as FEFLOW. FEFLOW is a finite element modeling (FEM) program designed to be used in geothermal modeling. FEM programs are better used to calculate the transient response of the thermal storage reservoir but take time to build and run. As a check, a FEFLOW model was used to verify the results of the spreadsheet. These two models will be compared beside one another in this chapter in an effort to validate the spreadsheet results.

4.1 BHE Materials Design

The materials used in a typical BHE are a polyvinyl chloride (PVC) or a polyethylene (PE) pipe. Material specifications of these pipes put the collapse pressure rating at approximately 581 kPa and 615 kPa respectively. The inner diameter of the pipe was considered to be 0.127 m with a wall thickness of 0.0056 m. These dimensions were kept the same for comparison of PVC/PE and steel pipe in the proposed design. The equation used to calculate the collapse pressures came from the ASTM F480 standard, which covers “water well casing pipe and couplings made from thermoplastic materials in standard dimension ratios SCH 40 and SCH 80” (ASTM international, 2010). This equation and its variables can be seen below.

$$P_c = \left(\frac{2E}{1-u^2} \right) \left\{ \frac{1}{\left[\frac{D_o}{t} \right] \left[\frac{D_o}{t} - 1 \right]^2} \right\} \quad (4.1)$$

Where: P_c = Collapse pressure rating

u = Poissons Ratio

E = Youngs Modulus

D_o = Outer diameter of pipe

t = thickness of pipe

The only variation from the standard was the assumption that the PVC and PE pipe had reduced wall thickness. This reduced wall thickness came from the need to have identical dimensions for comparison to steel pipe with an identical well design. Had the thickness of the PVC and PE pipe been nominal, the inner diameter would have been greatly reduced in the casing and the tubing thus requiring the redesign of all borehole dimensions. Also, the spreadsheet variables are kept constant for other calculations and thus should not be modified for the collapse pressure calculation.

The collapse pressure is critical when choosing a pipe for the design of the casing. This pressure dictates whether the pipe will hold its form when exposed to a certain pressure. If the down hole pressure is to become at any point larger than this calculated collapse pressure, the pipe is susceptible to failure. A failure of this type would be catastrophic for the flow of the BHE and would be quite costly to fix. In order to fix a problem such as this, pipe would have to be taken out of the hole and the collapsed sections replaced before running back in hole.

To determine if the PVC or PE pipes are acceptable choices in the design of the TU Darmstadt BHE project, a maximum pressure calculation must be performed. Because over pressured zones are not expected in the granodiorite, the maximum pressure to be expected should come via hydraulic gradient. The fluids which will be seen by the casing and the tubing are the refrigerant and the grouting material. Since the grout will be the denser of the two fluids, the maximum pressure calculation was done assuming a hydraulic gradient caused by a grouting material with a density of 1800 kg/m^3 . This calculation was also done at a depth of 800 m. The density of 1800 kg/m^3 is that of mortar cement and the depth of 800 m is the potential drilled depth limit of our considered hydraulic DTH hammer drill. The reason for choosing to use mortar cement is because the actual grout used will range from 0.9 g/cm^3 to 1.8 g/cm^3 density (Dykerhoff, 2008). Because the possibility exists to have a grout as heavy as mortar cement, the values and properties of such cement will be used.

The following formula was used to calculate the pressure seen at a depth of 800 m on the pipe. Consideration was made towards the actual conditions that may exist at that depth during a well cementing process. Usually the cementing company will fill the casing with a calculated annular volume plus excess. Then, following a special type of plug, water and pressure is used to force this volume of cement up into the annulus to fill the space between the casing and formation. Therefore at the bottom of the casing there exists a pressure imbalance between water hydraulic head and cement hydraulic head. This imbalance will be thought of as the collapse pressure seen by the casing.

$$P_{C,actual} = gh(\rho_{cement} - \rho_{water}) \quad (4.2)$$

Where: $g = \text{Acceleration due to gravity } [9.81 \text{ m/s}^2]$

$h = \text{Depth } [m]$

$\rho_{(cement)} = \text{Density of the cement slurry } [kg/m^3]$

$\rho_{(water)} = \text{Density of water } [kg/m^3]$

The pressure calculated with the formula above was 6,278.4 kPa. The acceptable collapse pressure of the PVC and PE pipes was calculated to be 581 kPa and 615 kPa respectively. The actual collapse pressure exceeds the recommended maximum allowable values by a factor of nearly 10. The pipe to be used in the TU Darmstadt BHE project must be one which withstands a much higher pressure than the PVC and PE pipes with similar dimensions. In addition to the stress criterion, the PE and PVC pipe are in most cases not able to withstand the higher temperature demand of the TU Darmstadt BHE system. There are some high temperature PVC options however they do not meet the strength criterion of the project.

Steel was the next logical choice for a pipe material. Oilfield tubing and casing is readily available from service industries catering to the oil and gas industry. The down hole pressures seen in most oil and gas wells dwarf the hydraulic pressures which may be seen in the TU Darmstadt BHE project. For this reason the material specifications of an API standard J-55 steel casing should give more than enough strength in order to withstand the mentioned bottom hole pressure of 6,278.4 kPa. In order to verify this assumption the following formula was adopted from the Roscoe Moss Companies website in order to calculate the collapse pressure specification of steel (Roscoe Moss Company, 2008).

$$P_c = \left(\frac{2E}{1-u^2} \right) \left\{ \frac{1}{\left[\frac{D_o}{t} - 1 \right]} \right\}^3 \quad (4.3)$$

Where: The variables are the same as described in Eq (4.1)

The result of the calculation was a collapse pressure of 42,601.6 kPa for an outer diameter of 127 mm and a wall thickness of 6 mm; a value nearly 8 times greater than the actual maximum pressure to be seen at bottom hole conditions. For this reason steel pipe will be used in the design of the BHE. If steel is chosen, a cost saving measure could be in the acquiring of yellow or green band tubing from used tubing suppliers. An inspection classification chart is shown in figure 4.1. The chart explains the meaning behind inspection banding and its implications on tubing strength.

INSPECTION CLASSIFICATIONS		
Used Tubing/Casing	New Tubing/Casing (and Plain End Drill Pipe)	Used Drill Pipe
*Yellow Band: 0-15% body wall reduction (85% min. remaining)	*White Band: suitable for all inspections performed (incl. min. 87.5% body wall).	Double White Band (Premium): 80% minimum wall remaining
*Blue Band: 16-30% body wall reduction (70% min. remaining)	*Yellow Band: Repairable reject. 87.5% body wall remaining after repair. Locate bands on either side and circle around defect.	Yellow Band: 70% to 80% (min.) of nominal wall remaining.
*Green Band: 31-50% body wall reduction (50% min. remaining)	*Blue Band: Imperfections of undetermined depth. Identified as above.	Orange Band: <70% (min.) of nominal wall remaining.
*Red Band: 50%+ body wall reduction (<50% remaining)	*Red Band: Defective length. Identified as above. Body wall defects must be cut out of tube.	Red Band: Any tube with a hole or a fatigue crack.
Damaged pin or box ends marked with red bands next to pin or on coupling	Damaged pin or box ends marked with red bands next to pin or on coupling	Tool joint classification color bands appear on the pin or box. Shoulder condition color codes are adjacent to the threads.
Drift restrictions indicated by green bands on either side of restriction and another next to body wall color band near box	Drift restrictions indicated by red bands on either side of restriction - just like other defects.	N/A
*Bands on tube body next to box end or coupling	Tube classification bands appear in same location (box end) as on used material.	Tube classification color bands appear next to the pin

Figure 4-1: Inspection classifications chart (www.inter-mountain.com/octg.htm, 2010)

4.2 BHE Fluid Flow Design

Physical Characteristics

When designing the fluid flow through the BHE there are two separate phases to consider. These phases are the charging phase and the extraction phase. During the charging phase hot water is put into the well to heat up the reservoir. Alternately in the extraction phase, cold water is pumped into the well in order to exchange energy with the relatively hot formation and bring that energy back to the surface as heat. During the design of the BHE it is important to consider this flow path.

During the charging phase, the aim is to exchange as much heat with the formation as possible. This means that the flow conditions should be turbulent and the surface area at a maximum. This condition is the best for heat transfer to allow for fluid mixing as it flows past the heat transfer area.

Surface area is also important when exchanging heat. In the book “*Fundamentals of Heat and Mass Transfer*” (Incropera et al, 2009) it states that there are three ways to increase the rate of heat transfer across a solid medium. These three ways are: increasing the fluid velocity to increase the surface heat transfer coefficient (h), increasing the difference in temperature between the solid and the fluid, or increasing the surface area. Incropera uses the example of fins as a cheap and effective way of increasing the surface area. In the TU Darmstadt BHE project extended fins are not an option for increasing the heat transfer surface area. However, this same effect can be done by decreasing the size of annulus. The smaller the annulus between the tubing and the casing the more surface area is exposed per unit volume of fluid; as can be seen by the following mathematical proof.

$$\text{Annular Volume} = \pi r_2^2 h - \pi r_1^2 h \quad (4.4)$$

$$\text{Surface Area} = 2\pi r_2 h \quad (4.5)$$

By isolating h in equation 4.4 the solution for h will give the respective surface area for a chosen set of r values. For arguments case r_2 will be set to 0.1524 m (6 inches) and r_1 will vary between two values, 0.0762 m (3 inches) in one case and 0.127 m (5 inches) in the other. To standardize each case the solution for h will be calculated for an annular volume of 1 m³.

After plugging in each set of variables an h value of 18.27 m results from the 0.0762 m (3 inch) case and a value of 44.85 m for the 0.127 m (5 inch) case. The values for h are then input into formula 4.5 where a surface area is calculated. The resulting surface area for the 0.127 m case is 42.95 m² and for the 0.0762 m case is 17.49 m²; the 0.127 m surface area is 2.5 times larger than in the 0.0762 m case. This proves that by simply decreasing the annular size the heat transfer can be increased due to increasing heat transfer area.

Therefore, for the charging flow we want a wellbore designed to minimize annular space between the casing inner wall and the pipe outer wall; the same applies in the extraction flow. An added effect of the decreased annular space is to cause the flow to be more turbulent. Turbulent flow increases the ability of the BHE to transfer heat. With a casing inner diameter of 115.8 mm, and a pipe outer diameter of 88.9 mm, the Reynolds number equates to approximately 65,000 at a circulation velocity of .24 m/s. Since it is known that in pipe flow a Reynolds number of greater than 4000 means turbulent flow conditions, we can say that in the annulus there exists turbulent flow. Similarly with a tubing inner diameter of 77.9 mm the Reynolds number is approximately 50,000; this is also far above the threshold of turbulent flow. The downside to a smaller annulus is the increased pumping power needed to push the same volume flow rate of fluid through the space. Since economics have not been considered in this publication the efficiency of the heat transfer will be the number one priority. Therefore, due to restrictions in the pipe connectors, for a casing size of 127.0 mm tubing will be inserted with a diameter of 88.9 mm. This is the largest casing that can be fit into the 6 inch (152.2 mm) hole and the largest tubing that can be fit into the 127.0 mm casing.

Flow Direction

The next consideration to make is the direction of flow through the BHE. There are two possibilities to this direction; down the center pipe and up the annulus or down the annulus and up the center pipe. In the charging phase hot water needs to reach the bottom of the wellbore before exchanging the bulk of its heat with the surroundings. In the extracting phase cold water must have as much heat transferred as possible at the bottom of the wellbore where charged formation temperatures are the highest. To consider these points it is beneficial to calculate the thermal resistances in the borehole. These resistances will also be needed when calculating the heat transfer per meter of wellbore.

The first step in calculating the thermal resistances of the borehole is conceptualizing a model. This model must include a few key features which will be present in the actual BHE. Features like a central pipe wall, an outer pipe wall, a volume filled with grout, a skin zone and the formation are all to be included in the conceptual model. A schematic of the model used in this thesis is pictured below. Notice all of the dimensions are left as variables.

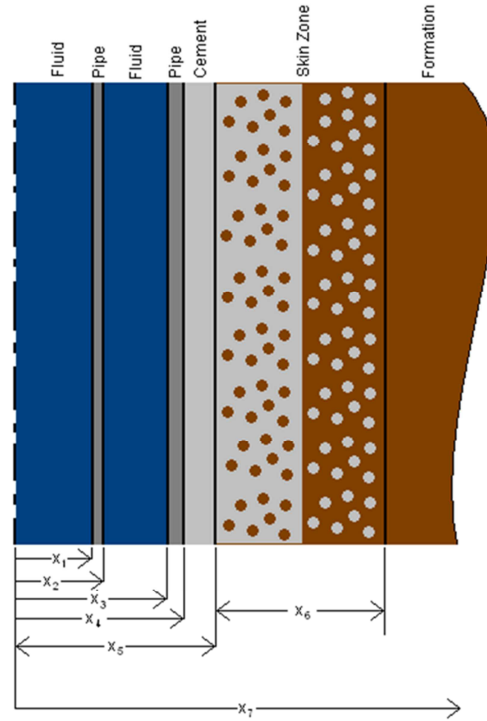


Figure 4-2: Conceptual model of the BHE

The diagram labels a few important dimensions that will be clarified at this point in the thesis paper. X_1 is the distance to the inner radius of the pipe wall and X_2 is the distance to the outside radius. X_3 and X_4 are the inner and outer radii of the casing and X_5 represents the average borehole radius. X_5 can be approximated with the radius of the drill bit used to drill the bore hole. X_6 is the thickness of the skin zone. Since the skin zone thickness is next to impossible to estimate before drilling, a reasonable guess will need to be supplied. Finally, X_7 is the distance into formation. When formulating the thermodynamics tab on the BHE spreadsheet X_7 is set to the acceptable radius for the heat reservoir. The acceptable radius will change depending on the well placement and its proximity to other properties. It will not be acceptable for the heat affected zone to reach past the property line of the botanical garden campus.

The formulas for the thermal resistances of the BHE wall components are based on Fourier's Law. This law states that the heat flow is dependent on the thermal conductivity of the substance multiplied by the heat transfer area and finally by the temperature gradient through the sample. The formula for Fourier's Law can be seen written below.

$$\dot{q} = -\lambda * A * \left[\frac{\delta T}{\delta x} + \frac{\delta T}{\delta y} + \frac{\delta T}{\delta z} \right] \quad (4.6)$$

Where: \dot{q} = Heat transfer rate

λ = Thermal conductivity of substance

A = Heat transfer area

$\left[\frac{\delta T}{\delta x} + \frac{\delta T}{\delta y} + \frac{\delta T}{\delta z} \right]$ = 3D temperature gradient

Because we will use the analytical approach, it is beneficial to simplify this equation and call the problem one dimensional; in reality a vertical temperature gradient will exist. However for preliminary design of the BHE via spreadsheet calculation, we can assume that the importance of the horizontal temperature gradient is much higher than the vertical gradient. This assumption should be remembered as it will explain some of the difference between the spreadsheet and the FEFLOW model approximations. A simplified version of Fourier's law can be seen in formula 4.7 below.

$$\begin{aligned}\dot{q} &= -\lambda * A * \left[\frac{\delta T}{\delta x} \right] \\ \dot{q} &= -\lambda * A * \frac{dT}{dx} \\ \dot{q} &= -\lambda * A * \frac{\Delta T}{L}\end{aligned}\tag{4.7}$$

Where: $\Delta T = \text{Temperature difference}$

$L = \text{Thickness of wall}$

At this point the important terms to notice are the thermal conductivity, the heat transfer area and the wall thickness. Together they make up the inverse of the bulk thermal resistance of the formation. This bulk thermal resistance is the sum of all component thermal resistances as can be seen in the following formulation.

$$\frac{-\lambda * A}{L} = \frac{1}{R_{bulk}} = \frac{1}{R_{form} + R_{sk} + R_{cm} + R_{cst} + R_{fl} + R_{pst} + R_{cid} + R_{pod} + R_{pid}}\tag{4.8}$$

Where: $R_{form} = \text{Formation thermal resistance}$

$R_{sk} = \text{Skin zone thermal resistance}$

$R_{cm} = \text{Cement thermal resistance}$

$R_{cst} = \text{Casing steel thermal resistance}$

$R_{fl} = \text{Fluid thermal resistance}$

$R_{pst} = \text{Pipe steel thermal resistance}$

$R_{cid} = \text{Casing inner diameter convective thermal resistance}$

$R_{pod} = \text{Casing outer diameter convective thermal resistance}$

$R_{pid} = \text{Pipe inner diameter convective thermal resistance}$

For the discussion involving flow direction the important resistances are those close to the center of the wellbore; these are namely the skin zone, cement, steel, and fluid thermal resistances. Each of these resistances, for the case of a plane wall, can be calculated by applying the general formula mentioned in equation 4.8. The only difference is the use of a component specific thickness and thermal conductivity (area will be the same in each case). However a radial coordinate system exists in the considered wellbore model. The formulas below were taken from the *Fundamentals of Heat and Mass Transfer* on the formulation of a radial heat transfer model.

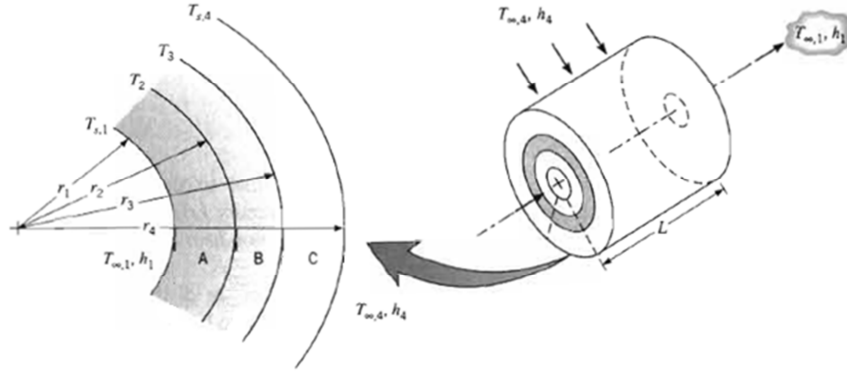


Figure 4-3: Radial thermal resistance model. (modified from Incropera et al, 2007).

For the cylinder pictured in figure 4.3 the formulation of the component thermal resistances comes from application of the general energy equation and Fourier's law in a radial coordinate system. The result is the following resistance model and component resistance formulas. Again, for a detailed proof and explanation of resistance models please see Incropera's "*Fundamentals of Heat and Mass Transfer*" chapters 3.2 and 3.3.

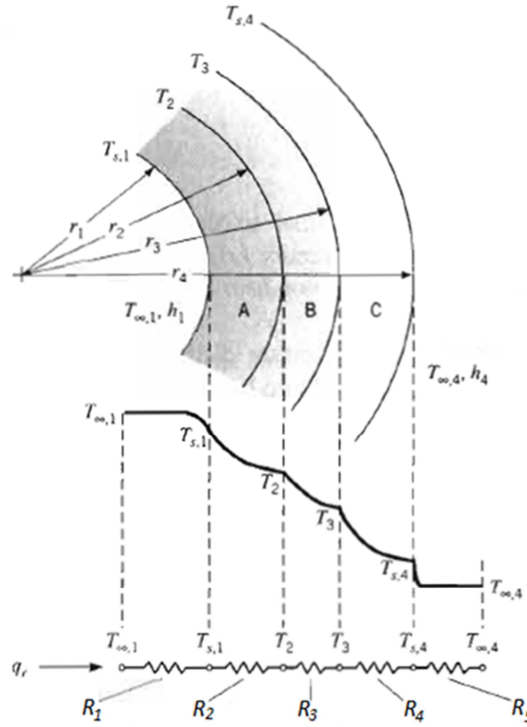


Figure 4-4: Theory resistance model (modified from Incropera et al, 2007).

Where: $R_1 = \frac{1}{h_1 2\pi r_1 L} = \text{conductive thermal resistance}$

$$R_2 = \frac{\ln(r_2/r_1)}{2\pi\lambda_A L} = \text{thermal resistance}$$

$$R_3 = \frac{\ln(r_3/r_2)}{2\pi\lambda_B L} = \text{thermal resistance}$$

$$R_4 = \frac{\ln(r_4/r_3)}{2\pi\lambda_c L} = \text{thermal resistance}$$

$$R_5 = \frac{1}{h_4 2\pi r_4 L} = \text{conductive thermal resistance}$$

h = the convective heat transfer coefficient

Now that general formulas for convective thermal resistance and material thermal resistances have been established, they can be applied to the BHE model used in this thesis. Below are the formulas for calculating the thermal resistances in the radial BHE model. The new term that has been introduced is the convective heat transfer coefficient (h). This term represents the apparent resistance to heat flow created by convective cooling existing because of the velocity of the fluid as it passes over a wall.

$$R_{pid} = \frac{1}{h_{pid} 2\pi x_1 d_{slice}} = \text{Convec. thermal resistance of inner pipe wall} \quad (4.9)$$

$$R_{pst} = \frac{\ln(x_2/x_1)}{2\pi\lambda_{pst} d_{slice}} = \text{Thermal resistance of the pipe steel} \quad (4.10)$$

$$R_{pod} = \frac{1}{h_{pod} 2\pi x_2 d_{slice}} = \text{Convec. thermal resistance of outer pipe wall} \quad (4.11)$$

$$R_{fl} = \frac{\ln(x_3/x_2)}{2\pi\lambda_{pst} d_{slice}} = \text{Thermal resistance of the fluid} \quad (4.12)$$

$$R_{cid} = \frac{1}{h_{cid} 2\pi x_3 d_{slice}} = \text{Convec. thermal resistance of inner casing wall} \quad (4.13)$$

$$R_{cst} = \frac{\ln(x_4/x_3)}{2\pi\lambda_{cst} d_{slice}} = \text{Thermal resistance of the casing steel} \quad (4.14)$$

$$R_{cm} = \frac{\ln(x_4/x_5)}{2\pi\lambda_{cm} d_{slice}} = \text{Thermal resistance of the cement} \quad (4.15)$$

$$R_{sk} = \frac{\ln(x_5+x_6/x_5)}{2\pi\lambda_{sk} d_{slice}} = \text{Thermal resistance of the skin zone} \quad (4.16)$$

And later the formation resistance will become important...

$$R_{form} = \frac{\ln(x_7/x_5+x_6)}{2\pi\lambda_{form} d_{slice}} = \text{Thermal resistance of the formation} \quad (4.17)$$

Formulas 4.9 to 4.17 are used in the thermodynamics tab of the BHE spreadsheet to calculate the thermal resistances of each component of the BHE model. In figure 4.6 below the radial cross section can be seen and its respective one dimensional resistance network shown. Input variables for x are input in millimeters except for x_7 which is in meters. Input variables for k are referring to the thermal conductivity and units are [W/mK].

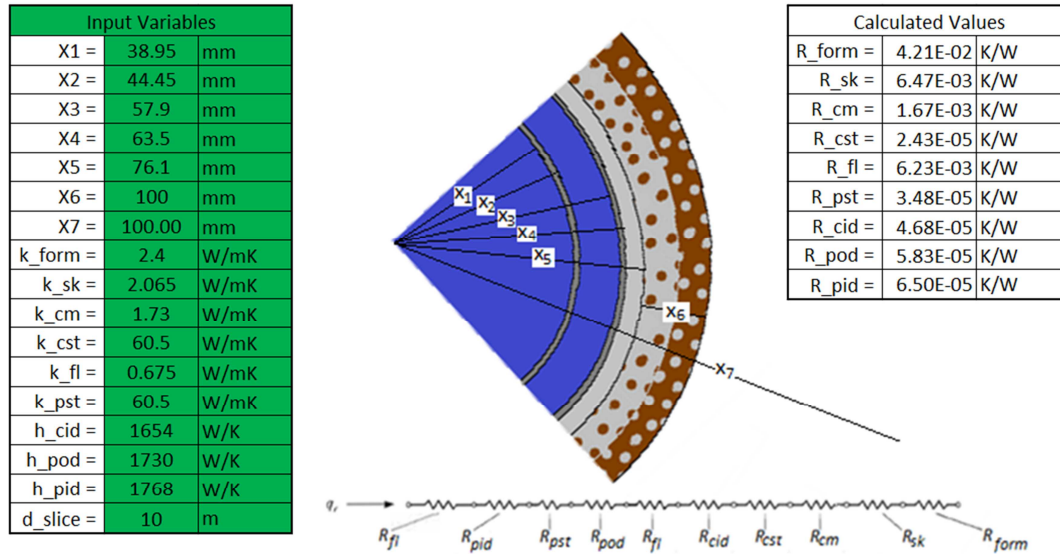


Figure 4-5: Radial BHE model and respective resistance network

A list variables and results can be seen in figure 4.5. The list includes the values which have been chosen for use in the modeling of the BHE spreadsheet. These values will serve as the preliminary design of the BHE. The resulting resistances, also included in the figure, will guide the reasoning behind the fluid flow direction. Notice the value for x_7 ; this will change as we consider the heat transfer rate.

Meanwhile, certain considerations can be made on the flow path through the BHE. It can be seen that the thermal resistance of the fluid compared to the casing and pipe steel is much larger. The skin zone also has a large thermal resistance compared to the steel pipes. A large thermal resistance means that the layer acts more like an insulator and less like a conductor; subsequently a conducting material will always have a low thermal resistivity. The fact that the fluid layers act to resist temperature change can be used to plan the most beneficial flow path through the wellbore. In the charging phase, hot water needs to reach the bottom of the wellbore before exchanging the bulk of its heat with the surroundings. By injecting water in the center pipe it will be best insulated from the formation before reaching the bottom and charging the wellbore. In the extracting phase cold water must have as much heat transferred as possible at the bottom of the wellbore where charged formation temperatures are the highest. A similar flow path, down the pipe and up the annulus, allows the fluid to reach bottom at the coldest possible temperature. This allows for a higher heat transfer rate at the bottom of the well where the temperature difference is the greatest. The significance of temperature difference in regards to heat transfer will be covered later in this publication.

As an added advantage there have been interesting developments in tubing technology for use in coaxial heat exchangers. The study done by Morita et al. (2005) states that an insulated down pipe can be used for small scale power generation with deep coaxial heat exchangers. The insulated pipe being considered is a double walled pipe; the wall gap is filled with argon gas. The estimated equivalent thermal conductivity of the pipe may be close to 0.07 W/mK. This compares to 40-60 W/mK in regular steel pipe.

4.3 BHE Grouting Design

The efficiency of the BHE depends largely on the grout or cement used to secure the casing in the ground. This grout can act as an insulator, a conductor, or a barrier to flow within the formation. In the case of the TU Darmstadt BHE project, the grouting design is a crucial step which must be thought about before consulting with the cementing service company. It needs to be installed for environmental reasons as well as to improve the efficiency of the BHE.

One important consideration is the vertical temperature gradient which will exist after the formation has been thermally charged. The highest temperatures will be seen near the bottom of the wellbore with a vertical gradient quickly cooling to a temperature near the natural formation temperature. The important point to consider is at what depth the heat transfer fluid will begin to lose too much heat to the formation. At this depth it will be beneficial to have an insulating grout which can act to shield the fluid from unnecessary losses. When moving down from this point it would be beneficial to have a conductive grout which allows for the maximum possible amount of heat to enter the working fluid stream.

Another consideration, not for the benefit of the BHE but for the benefit of the environment, is the grout used to isolate the first 8" section of well bore. It has already been established that this section will be cased with 7" casing and placed approximately 5 m into the consolidated granodiorite. The reason for this precautionary measure is to ensure that ground water does not find a flow path from its place within the Red Bed and weathered granodiorite into the consolidated formation below. An intrusion of this kind would result in the disruption of the original ground water flow and potentially cause the contamination of the ground water table. Therefore, the cement which lies between the surface casing and the top rock formations should be designed to hydraulically isolate the 7" hole from the 6" hole required for the BHE.

The first cementing job can be done in a single stage. This job involves cementing the 7" casing in place and isolating the Red Bed and weathered granodiorite from the consolidated granodiorite formation. The cement or grout to be chosen for this operation should be resistant to ground water flow and thus carry a high weight and low porosity once set.

The grouting of the BHE casing into the 6" borehole is more difficult. The cement job will have to be a two stage operation and will involve special consideration on the casing design. Two stage operations are being done regularly on deeper wells and thus the cementing service company should be able to carry out such a task. Essentially the conducting grout is forced into the annulus via hydraulic pressure in the casing. By volume calculation the cement top is placed at an approximate depth specified by the design of the BHE. Once the first stage has set the cementing company will enter the wellbore once again, and through either casing perforations or a sliding sleeve, inject the second stage of cement into the remaining annulus via the casing. In a perfect world the two stages will lie on top of one another and returns from the second stage will reach surface. Grout used in the bottom stage should have thermal conductivity maximized while grout used in the top stage should have thermal conductivity minimized. This will provide the region of insulation and the region of conduction necessary for efficient running of the BHE.

The point at which the second cementing stage is set will depend on a detailed numerical analysis of the BHE environment under extraction conditions. Since a detailed 3D model is not within the scope of this thesis, further work should be done in order to approximate the stage depth. The approximation can be made via 3D FEFLOW heat transfer modeling and may be an opportunity for another master's thesis.

4.4 Borehole Heat Exchanger Length Design

The parameters already set in the BHE design are the cross sectional dimensions, the pipe material selection, and the grouting design. It is known that the recommended maximum depth for the DTH hammer drill in question is limited to around 800 m so this can be set as a constant in the design of the TU Darmstadt BHE. The last design question to be addressed in this chapter is the potential total length of geothermal boreholes. This will in turn give a number of required boreholes for the project. The combined length of BHE will be calculated with Fourier's law along with the determination of an average heat transfer per meter of well [\dot{q} , W/m]; in reality this heat transfer will vary along the length of the well. This number, when multiplied by the assumed BHE depth of 800 m per wellbore and divided by a total system power requirement of 300 kW, will give the needed number of boreholes for the project. The numbers received from the thermodynamics spreadsheet must be taken lightly; the model assumes one dimensional behavior, a constant bore hole length of 800 m, and is only able to calculate the heat transfer at a single depth. This heat transfer also depends on the assumption of thermal storage area or the maximum allowable depth into formation of the effected temperature gradient.

As already mentioned, the heat transfer will be calculated using Fourier's law. The mathematical law has already been introduced in this chapter with equation 4.7. When calculating the thermal resistances it was shown that...

$$\frac{-\lambda \cdot A}{L} = \frac{1}{R_{bulk}} = \frac{1}{R_{form} + R_{sk} + R_{cm} + R_{cst} + R_{fl} + R_{pst} + R_{cid} + R_{pod} + R_{pid}}$$

Therefore it can be said that...

$$\dot{q} = \Delta T / R_{bulk} \quad (4.18)$$

Where: ΔT = temperature difference between pipe fluid and formation

Since the values needed for R_{Bulk} were calculated in the flow direction analysis they can be utilized for the determination of the heat transfer rate. The difference between the pipe fluid and the formation temperatures are not so easy to realize. The two scenarios, charging and extracting, will require different considerations in order to properly analyze within the one dimensional thermodynamic theory covered thus far.

Thermal Charging Phase

The end result is to be able to calculate an average heat recovery rate from the charged thermal reservoir. In order to do this, the temperature distribution of the reservoir after charging must be known. This temperature distribution can be calculated using the equations, theory, and methodology discussed up to this point.

Remembering back to the resistance calculations, an answer for the resistance of the formation was not supplied. This is because the distance x_7 has to be defined for each phase. The value for x_7 in the charging phase is the distance of the effected thermal radius in the formation. In the spreadsheet and in this thesis it will be assumed at 100 m for calculation of the charged temperature distribution. Therefore with an x_7 of 100 m input into formula 4.17, the thermal resistance of the formation is calculated to be 4.206×10^{-2} K/W. It can be seen that at this distance the thermal resistance of the formation dominates the bulk thermal resistance as it is the largest of the calculated values.

The temperature difference between the fluid and the reservoir is known during the charging phase. Fluid at a constant temperature is injected into the wellbore at 90 degrees Celsius. It has also been discussed that the thermal resistance of the fluid surrounding the injection pipe (down pipe) acts to insulate it from the formation. For these reasons it will be assumed that after steady state has been reached, for a thermally effected radius of 100 m, the fluid in the down pipe will reach the bottom at or very close to the injection temperature of 90 degrees Celsius. Therefore, when calculating a heat transfer rate at the bottom of the wellbore the temperature difference between the fluid and the formation at 100 m will be 55 degrees Celsius (90 minus 35 degrees Celsius).

The determination of formation temperature gradient is rather quite simple. In the definition of the geology under the TU Darmstadt geoscience building, it was mentioned that the neutral zone lies at a depth of approximately 40 m. This means that at a depth of 40 m we have a temperature of 12 degrees Celsius. If there is a thermal gradient of 3 degrees Celsius per 100m TVD, the temperature at 800m is easily calculated with the following formula:

$$T = 12^{\circ}\text{C} + (z - 40\text{m}) 3^{\circ}\text{C}/100\text{m} \quad (4.19)$$

Where: $z = 800\text{m}$

The resulting temperature is indeed 35 degrees Celsius and represents the formation temperature at a depth z . The temperature difference of 55 degrees Celsius and the thermal resistivity of 4.206×10^{-2} K/W are combined together in equation 4.18 to give a heat transfer rate (\dot{q}) of 97.2 W/m of wellbore. According to the theory from Incropera et al, the temperature distribution through the reservoir can be calculated with a generic assumption. Because the heat transfer rate is constant throughout the formation components, the temperatures at each component boundary can be calculated through the following formula (Incropera et al, 2007):

$$T_i = T_{i-1} - \dot{q}R_i \quad (4.20)$$

Where: i = the temperature at the boundary of interest
 $i - 1$ = the known temperature at the previous boundary
 R_i = the thermal resistance of material between boundaries

Therefore, starting at the down pipe fluid temperature and working towards the 100 m formation boundary, the temperatures of any point within this zone can be calculated with the above formula for points i-n (n is the number of temperature points spaced throughout the reservoir). All one needs to know is the thermal resistance of the zone and the heat transfer through it. The following table is taken from the spreadsheet where this formula has been applied. Temperatures through each borehole wall component, as well as points through the formation, have been calculated.

Table 4-1: Temperature dist.

Radial Model [degC]		Distance [m]
T_pid =	89.9	.0779
T_pod =	89.8	.0889
T_cid =	83.1	.1158
T_cod =	83.1	.1270
T_ski =	81.3	.1522
T_sko =	77.2	.2522
T_1 =	62.6	2.0000
T_2 =	54.9	6.0000
T_3 =	52.9	8.0000
T_4 =	51.3	10.0000
T_5 =	45.7	22.0000
T_6 =	43.1	32.0000
T_7 =	40.4	47.0000
T_8 =	37.9	67.0000
T_9 =	36.0	87.0000
T_10 =	35.3	97.0000
T_11 =	35.0	100.2522

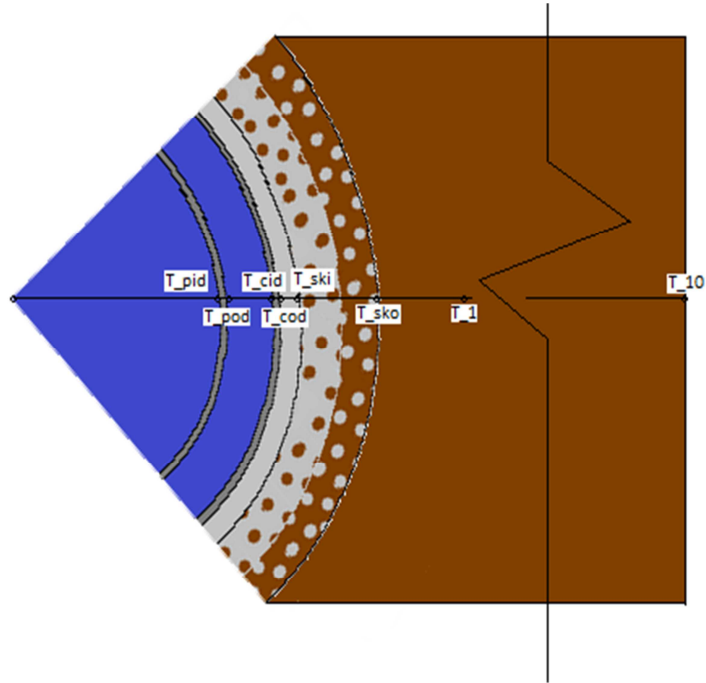


Figure 4-6: Figure Showing variables for Table 4.1

Extraction Phase

Now that the temperature distribution after charging is known, the methodology of how the problem is perceived must be restructured. The aim of the extraction phase is to interact with the near wellbore rock in order to exchange heat with a cooler wellbore fluid. In this case the heat transfer rate will occur between the hottest temperature outside the wellbore and the wellbore fluid. At the same time, this same hottest temperature will experience a gradient towards the formation as the cooler formation attempts to equalize with the thermal reservoir. In order to calculate heat transfer per unit length, an assumption has to be made that the calculated rate is the rate immediately after charging. As time progresses

the formation will attempt to even out the temperature and the heat exchanger fluid will also try to bring the temperature of the near wellbore down. The hope is that after a long enough charging period the time it takes for the reservoir to cool down will be greater than time at which the heating load in the building is required. This transient analysis is best done with software such as FEFLOW and is out of the scope of this project.

The instantaneous heat transfer from the radius occurs between the highest temperature in the near well bore and the heat transfer fluid. In the TU Darmstadt BHE project, the highest temperature occurs at the outer radius of the skin zone. This observation is due to the thermal conductivities of the component layers between the skin zone and the well bore fluid. The layers closer to the borehole are more likely to equalize with the heat transfer fluid in a shorter time. However, due to the high thermal resistivity of the skin zone and the formation, the point between these two layers should hold a stable high temperature longer than anywhere else. Therefore, for this instance of heat transfer the temperature difference is going to be a maximum of 22 degrees Celsius (77.2 degrees Celsius minus 55 degrees Celsius).

The value for bulk resistance must also be reconsidered. The new bulk value will include all those resistances in between the temperatures of interest. This includes the pipe steel, the casing steel, the cement zone, the skin zone and the convective thermal resistivities. Since the bulk resistivity is just a sum of all components, the new bulk thermal resistivity is equal to 1.459×10^{-2} K/W.

Applying formula 4.18 as before, the extraction heat transfer rate per meter of wellbore comes out to be a maximum of 150.7 W/m of wellbore. When the average formation temperature is considered (18.75°C) the heat transfer calculates to 128.5 W/m of wellbore. This average number divided by the 300 kW of required power equals a total of 2334.5 m of installed wellbore or the installation of three 800 meter wellbores.

4.5 Introduction to the Thermo Tab of the BHE Spreadsheet

The results obtained in the thermodynamic simulation are weighted heavily on the assumptions made during the processing of results. When planning for such a design, the designer may want to make different assumptions as those made in the thesis analysis. For this reason the BHE spreadsheet was created. The following section will introduce each of the thermodynamic tabs of the spreadsheet and explain how future designers can modify the inputs to obtain their own approximation of the results.

The spreadsheet would be a good choice for preliminary design of such a system. This design work would take place before time consuming numerical computer models needed to be built. Additionally, the inputs and results in the spreadsheet will help to expedite the numerical input process and have been designed in such a way as to compliment the input data required for building a FEFLOW model.

Borehole Heat Transfer - Charge

The following spreadsheet in figure 4.7 is used to calculate the steady state temperature distribution in the formation existing after charging.

Borehole Heat Transfer - Charge Spreadsheet INPUT						
Equation #	Input Variables		Input Variables		Description	
1	77.9	Downpipe Inner Diameter [mm]	X1=	38.95	Downpipe Inner Radius [mm]	Input Values are used to calculate all of the required Lx and Ax values for calculating the overall heat transfer constant. Ax values for heat transfer through conductive layers is estimated at the center of the layer.
	88.9	Downpipe Outer Diameter [mm]	X2=	44.45	Downpipe Outer Radius [mm]	
	115.8	Casing Inner Diameter [mm]	X3=	57.9	Casing Inner Radius [mm]	
	127	Casing Outer Diameter [mm]	X4=	63.5	Casing Outer Radius [mm]	
	152.2	Borehole Drift Diameter [mm]	X5=	76.1	Borehole Drift Radius [mm]	
	X6 =	100	Skin Zone Thickness [mm]			
	X7 =	100.00	Effective Borehole Thermal Radius [m]			
2	k_form =	2.4	Thermal Conductivity of Formation [W/mK]		Equation is to calculate the overall heat transfer coefficient. This value will be used when solving for the Heat transfer from formation to wellbore or wellbore to formation. - Referenced formula from Incropera, <i>The Fundamentals of Heat and Mass Transfer</i> . Values from this text can be found for reference in the "Heat Transfer useful values" table.	
	k_sk =	2.1	Thermal Conductivity of Skin Zone [W/mK]			
	k_cm =	1.73	Thermal Conductivity of Cement/Grout [W/mK]			
	k_cst =	60.5	Thermal Conductivity of Casing Steel [W/mK]			
	k_fl =	0.675	Thermal Conductivity of Fluid [W/mK]			
	k_pst =	60.5	Thermal Conductivity of Pipe Steel [W/mK]			
	T_form =	307.95	Average Temperature of Formation [K]			
2 SubRoutine	T_fl =	363	Average Temperature of Pipe Fluid [K]		Because we are approximating 1-D heat transfer we must assume a constant vertical temperature distribution over the heat transfer area. For this reason the calculation will be done in vertical sections or "Model Slice Distances".	
	d_slice =	10	Model Slice Vertical Distance [m]			
	h_cid =	5872	Convec. Coefficient of Casing inner diam. [W/mK]			
SubRoutine Inputs	h_pod =	6144	Convec. Coefficient of Pipe outer diam. [W/mK]		Input Values are used to calculate all of the required Values for the Convective Heat Transfer Coefficient Sub Routine	
	h_pid =	6286	Convec. Coefficient of Pipe inner diam. [W/mK]			
	Q =	0.017	Fluid Flow Rate [m^3 / s]			
	p_fluid =	1000	Density of the Fluid [kg/m^3]			
	μ_fluid =	3.60E-04	Viscosity of the Fluid [N-s/m^2]			
	c_p =	4.209	Specific Heat of the Fluid [kJ/kg]			
	T_avgwall =	90	Average Wall Temperature [deg C]			
T_form Variables	V_avgp =	0.262058142	Average Fluid Velocity Pipe [m/s]		Input values are used to calculate the formation temperature at the depth of which the temperature observation points are placed into the formation. These probes must all lie at the same depth as the spread sheet is a 1-D model.	
	V_avga =	0.237789605	Average Fluid Velocity Annulus [m/s]			
	T_yearavg =	12	Yearly Average Temperature in climate [deg C]			
	T_geograd =	3	Geothermal Gradient in Region [deg C/100m]			
	depth_NZ =	40	Approximate Depth of Neutral Zone in Region [m]			
	depth_slice =	800	Depth of sample slice [m]			

Figure 4-7: Input spreadsheet for thermodynamic calculations of charging phase

Visible in this diagram are inputs for the BHE dimensions, thermal conductivities (k values on spreadsheet), fluid properties, fluid flow rates and geothermal gradient inputs. These inputs are used to calculate the formation temperature gradient. The green cells are user inputs, the gray cells represent referenced values, and the orange cells represent input calculations.

Notice the red "subroutine" input cells. These cells reference to a subroutine within the spreadsheet which calculates the convective heat transfer coefficients (h). The coefficients return on the input page as gray cells and are used in the calculation of thermal resistances in the spreadsheet. The subroutine was adopted from Harlan Bengtson and his article about the calculation of forced convection heat transfer coefficients (Bengtson, 2010).

The most controversial input parameters are the x_7 input (effective borehole thermal radius) and the model slice vertical distance. The effective borehole thermal radius has already been discussed but the model slice vertical distance has not. The larger this slice the larger the vertical section of wellbore you assume to be constant. For more accurate results the slice distance can be minimized and for more average results the slice distance can be maximized. The user must always remember to modify his formation temperature inputs if a large slice is going to be used. For instance a slice of 800 m would warrant an average formation temperature of approximately 24 degrees Celsius; a value in between the neutral zone temperature and the temperature at 800 m.

Borehole Heat Transfer - Charge Spreadsheet INPUT					
3	T_inletwater	363	Average Temperature of Pipe Fluid [K]		The input values will be used in OUTPUT 3. This section uses the calculated heat transfer rate to calculate temperatures throughout the model at given temperature probe distances. Probe distances are entered into the INPUT variables to the right. Please see the diagram to the right for visual variable representation. PLEASE NOTE the distance d_T11 is located at the edge of the considered heat reservoir where the temperature is at the normal geothermal gradient. Values calculated are compared to a reference FEFLOW model. Please input own values for the FEFLOW approximations if available.
	d_T1 =	1.8239	2.0000	Distance of Temperature Probe into formation from edge of defined skin zone [m] / Distance from center of wellbore [m]	
	d_T2 =	5.8239	6.0000		
	d_T3 =	7.8239	8.0000		
	d_T4 =	9.8239	10.0000		
	d_T5 =	21.8239	22.0000		
	d_T6 =	31.8239	32.0000		
	d_T7 =	46.8239	47.0000		
	d_T8 =	66.8239	67.0000		
	d_T9 =	86.8239	87.0000		
	d_T10 =	96.8239	97.0000		
	d_T11 =	100.00	100.1761		
	T_form =	307.95	Temperature of Formation [K]		

Figure 4-8: Temperature distribution input parameters

Figure 4.8 is of the distance input cells for calculating the temperature distribution through the formation to the thermally effected boundary. These values can be placed anywhere within the formation (outside of 0.250 m). The user should be aware that the estimation of a temperature profile depends on the position of the temperature probe points. More points should be placed closer to the wellbore and less points placed further away from the wellbore. This is the ideal arrangement of nodes as tested during the thesis. For instance, in the above figure one can see there are 7 temperature probes placed within the first 50 m of distance and only 4 placed in the remaining 50 m.

Borehole Heat Transfer Spreadsheet OUTPUT						
Equation #	Calculated Values		Description			
2	Radial Model					
	R_form =	4.206E-02	Resistance of the formation [K/W]			
	R_sk =	6.466E-03	Resistance of the Skin Zone [K/W]			
	R_cm =	1.665E-03	Resistance of the Cement [K/W]			
	R_cst =	2.429E-05	Resistance of the Casing Steel [K/W]			
	R_fl =	6.233E-03	Resistance of the Fluid [K/W]			
	R_pst =	3.475E-05	Resistance of the Pipe Steel [K/W]			
	R_cld =	4.681E-05	Resistance from the convective effect on the Casing Inner Diameter [K/W]			
	R_pod =	5.827E-05	Resistance from the convective effect on the Pipe Outer Diameter [K/W]			
	R_pid =	6.501E-05	Resistance from the convective effect on the Pipe Inner Diameter [K/W]			
	R_Tot =	5.665E-02	Total Thermal Resistance [K/W]			
	ΔT =	55.05	Temperature Difference from T_form to T_fl [K]			
3	q_x =	97.17621848	Instantaneous Heat Transfer [W/m]			
	FEFLOW Temp Probes [m]		FEFLOW Temp Probes [degC]		Radial Model [K]	
	d1 =	0	T1 =	88.6	T_pid =	362.9
	d19 =	0.462	T19 =	74.6	T_pod =	362.9
	d2 =	2	T2 =	64.6	T_cld =	356.8
	d3 =	4	T3 =	59.7	T_cod =	356.8
	d4 =	6	T4 =	56.9	T_ski =	355.2
	d5 =	8	T5 =	54.8	T_sko =	348.9
	d6 =	10	T6 =	53.0	T_1 =	335.5
	d7 =	12	T7 =	51.5	T_2 =	328.5
	d8 =	17	T8 =	48.8	T_3 =	326.6
	d9 =	22	T9 =	46.9	T_4 =	325.2
	d10 =	27	T10 =	45.3	T_5 =	320.1
	d11 =	32	T11 =	43.9	T_6 =	317.7
	d12 =	37	T12 =	42.9	T_7 =	315.2
	d13 =	47	T13 =	41.0	T_8 =	312.9
	d14 =	57	T14 =	39.6	T_9 =	311.2
	d15 =	67	T15 =	38.3	T_10 =	310.5
	d16 =	77	T16 =	37.2	T_11 =	310.3
	d17 =	87	T17 =	36.2		
	d18 =	97	T18 =	35.3		

Figure 4-9: BHE thermodynamics spreadsheet output for charging phase

This output screen (figure 4.9) shows the calculated component resistances, bulk thermal resistance, temperature difference, and instantaneous heat transfer as discussed before. The results of instantaneous heat transfer are used to populate the temperature distribution spreadsheet. This spreadsheet is set up to calculate the horizontal temperature distribution at the user defined observation probes for every depth of the wellbore from 40 m down to 1000 m TVD depth. The distribution uses equation 4.20 with the parameters modified to calculate every 5 m up to total TVD.

The populated table allows the engineer to choose a depth at which the temperature distribution is optimal for their BHE environment and design. It also supplies the engineer with an approximate steady state charged reservoir temperature profile. The profile as calculated by the spreadsheet can be seen in figure 4.11.

Temperature Field, Surface to bottom													
Depth	Formation Temperature	Skin Zone Temperature	Tempearture Probes [m into formation from wellbore]										
			2	6	8	10	22	32	47	67	87	97	100.3
40	12	71.8	51.2	40.2	37.3	35.1	27.2	23.5	19.7	16.1	13.5	12.4	12.1
45	12.15	71.9	51.3	40.3	37.4	35.2	27.4	23.6	19.8	16.3	13.7	12.6	12.3
50	12.3	71.9	51.3	40.4	37.5	35.3	27.5	23.8	19.9	16.4	13.8	12.7	12.4
55	12.45	72.0	51.4	40.5	37.6	35.4	27.6	23.9	20.1	16.6	14.0	12.9	12.6
60	12.6	72.0	51.5	40.6	37.7	35.5	27.7	24.0	20.2	16.7	14.1	13.0	12.7
65	12.75	72.0	51.6	40.7	37.9	35.6	27.9	24.1	20.3	16.8	14.3	13.2	12.9
70	12.9	72.1	51.6	40.8	38.0	35.8	28.0	24.3	20.5	17.0	14.4	13.3	13.0
75	13.05	72.1	51.7	40.9	38.1	35.9	28.1	24.4	20.6	17.1	14.6	13.5	13.2
80	13.2	72.1	51.8	41.0	38.2	36.0	28.2	24.5	20.8	17.3	14.7	13.6	13.3
85	13.35	72.2	51.9	41.1	38.3	36.1	28.3	24.7	20.9	17.4	14.9	13.8	13.5
90	13.5	72.2	51.9	41.2	38.4	36.2	28.5	24.8	21.0	17.6	15.0	13.9	13.6
95	13.65	72.2	52.0	41.3	38.5	36.3	28.6	24.9	21.2	17.7	15.1	14.1	13.8
800	34.8	77.2	62.6	54.8	52.8	51.2	45.6	43.0	40.3	37.8	35.9	35.2	34.9
805	34.95	77.2	62.6	54.9	52.9	51.3	45.8	43.1	40.4	37.9	36.1	35.3	35.1
810	35.1	77.3	62.7	55.0	53.0	51.4	45.9	43.2	40.5	38.0	36.2	35.4	35.2
815	35.25	77.3	62.8	55.1	53.1	51.5	46.0	43.4	40.7	38.2	36.4	35.6	35.4

Figure 4-10: Horizontal temperature field at varying depths

The figure 4.10 has been minimized to hide depth cells ranging from 100 m to 800 m. This has been done to save space in this publication. The actual spreadsheet program will include all values between 40 m and 800 m in 5 meter increments and can be seen in appendix A.

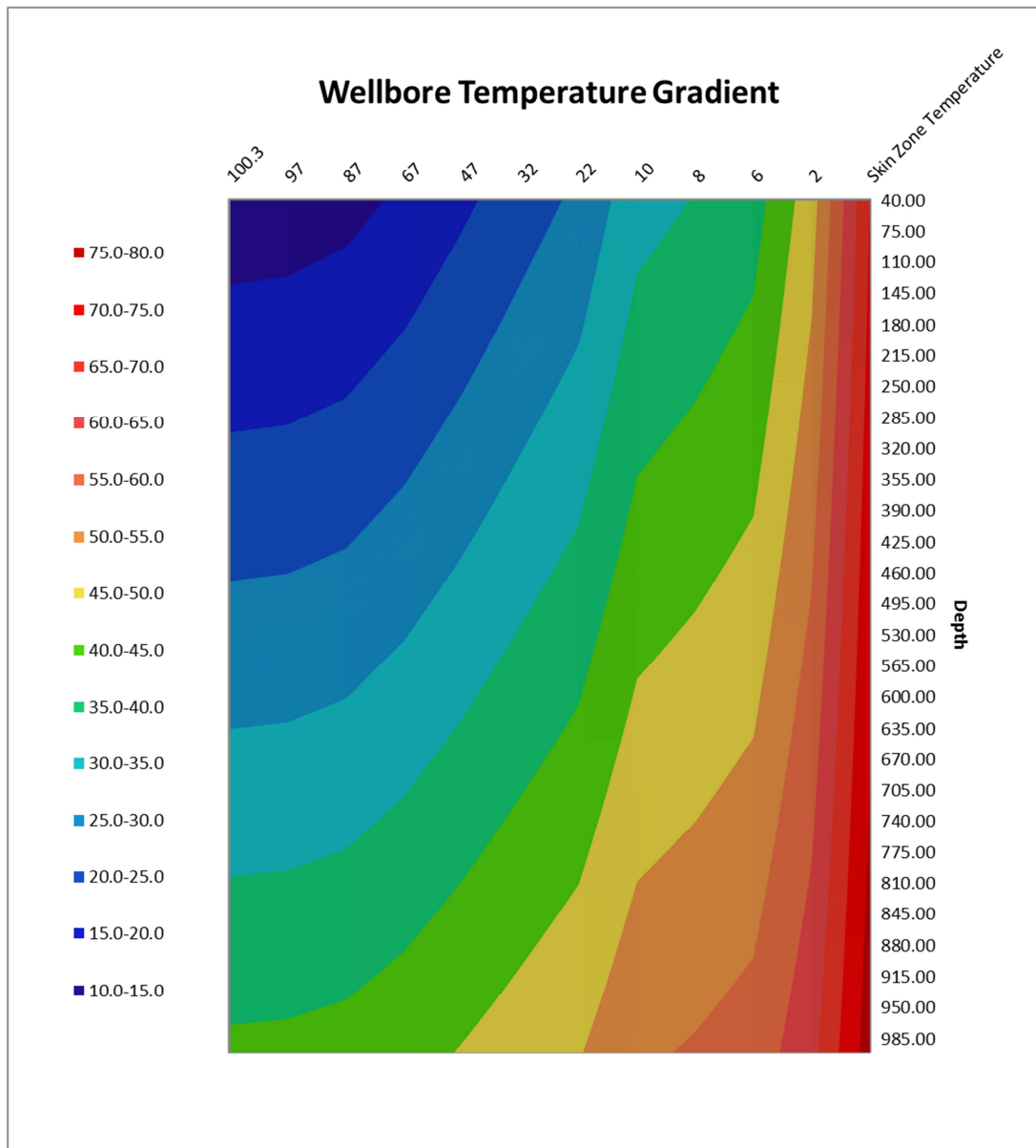


Figure 4-11: Reservoir temperature gradient approximation after charging.

Borehole Heat Transfer – Extract

On the next page, Figure 4.12 shows the screen view of the input spreadsheet for the extraction thermodynamic calculation. The input parameters remain the same as in the charging spreadsheet except for the absence of setting depth. Another change to the input parameters is the T_{form} variable. In the “Borehole Heat Transfer – Charge” spreadsheet, T_{form} represents the formation temperature at a distance x_7 from the center of the wellbore. The borehole dimensions (x values) are left as inputs in this spreadsheet incase the engineer would like to segregate the boreholes for extraction and for charging. If this condition exists the T_{form} variable must be checked for its accuracy as it references the charging spreadsheet at a distance x_5 plus x_6 from the center of the wellbore; this reference point may need to be moved.

Borehole Heat Transfer - Charge Spreadsheet INPUT						
Equation #	Input Variables			Description		
1	77.9	Downpipe Inner Diameter [mm]	X1 = 38.95	Downpipe Inner Radius [mm]	Input Values are used to calculate all of the required Lx and Ax values for calculating the overall heat transfer constant. Ax values for heat transfer through conductive layers is estimated at the center or the layer.	
	88.9	Downpipe Outer Diameter [mm]	X2 = 44.45	Downpipe Outer Radius [mm]		
	115.8	Casing Inner Diameter [mm]	X3 = 57.9	Casing Inner Radius [mm]		
	127	Casing Outer Diameter [mm]	X4 = 63.5	Casing Outer Radius [mm]		
	152.2	Borehole Drift Diameter [mm]	X5 = 76.1	Borehole Drift Radius [mm]		
	X6 = 100	Skin Zone Thickness [mm]				
	X7 = 100.00	Effective Borehole Thermal Radius [m]				
2	k_form = 2.4	Thermal Conductivity of Formation [W/mK]		Equation is to calculate the overall heat transfer coefficient. This value will be used when solving for the Heat transfer from formation to wellbore or wellbore to formation. - Referenced formula from Incropera, <i>The Fundamentals of Heat and Mass Transfer</i> . Values from this text can be found for reference in the "Heat Transfer useful"		
	k_sk = 2.1	Thermal Conductivity of Skin Zone [W/mK]				
	k_cm = 1.73	Thermal Conductivity of Cement/Grout [W/mK]				
	k_cst = 60.5	Thermal Conductivity of Casing Steel [W/mK]				
	k_fl = 0.675	Thermal Conductivity of Fluid [W/mK]		Because we are approximating 1-D heat transfer we must assume a constant vertical temperature distribution over the heat transfer area. For this reason the calculation will be done in vertical sections or "Model Slice Distances".		
	k_pst = 60.5	Thermal Conductivity of Pipe Steel [W/mK]				
	T_form = 347	Average Temperature of Formation [K]				
	T_fl = 328.15	Average Temperature of Pipe Fluid [K]				
d_slice = 10	Model Slice Vertical Distance [m]					
2 SubRoutine	h_cld = 5872	Convec. Coefficient of Casing inner diam. [W/mK]				
	h_pod = 6144	Convec. Coefficient of Pipe outer diam. [W/mK]				
	h_pid = 6286	Convec. Coefficient of Pipe inner diam. [W/mK]				
SubRoutine Inputs	Q = 0.017	Fluid Flow Rate [m³ / s]		Input Values are used to calculate all of the required Values for the Convective Heat Transfer Coefficient Sub Routine		
	ρFluid = 1000	Density of the Fluid [kg/m³]				
	μFluid = 3.60E-04	Viscosity of the Fluid [N-s/m²]				
	c_p = 4.209	Specific Heat of the Fluid [kJ/kg]				
	T_avgwall = 90	Average Wall Temperature [deg C]				
	V_avgp = 0.262058142	Average Fluid Velocity Pipe [m/s]				
	V_avga = 0.237789605	Average Fluid Velocity Annulus [m/s]				

Figure 4-12: Input spreadsheet for thermodynamic calculations of extracting phase

These inputs are then referenced to the output table pictured in the screen shot below from the BHE spreadsheet. The same theory as discussed in this chapter is used to populate the cells and give a final recommendation on number of boreholes to be installed. The number shown in the figure is 3, and is calculated for an average borehole length of 800 m.

Borehole Heat Transfer Spreadsheet OUTPUT			
Equation #	Calculated Values		Description
2	Radial Model		
	R_sk =	6.466E-03	Resistance of the Skin Zone [K/W]
	R_cm =	1.665E-03	Resistance of the Cement [K/W]
	R_cst =	2.429E-05	Resistance of the Casing Steel [K/W]
	R_fl =	6.233E-03	Resistance of the Fluid [K/W]
	R_pst =	3.475E-05	Resistance of the Pipe Steel [K/W]
	R_cld =	4.681E-05	Resistance from the convective effect on the Casing Inner Diameter [K/W]
	R_pod =	5.827E-05	Resistance from the convective effect on the Pipe Outer Diameter [K/W]
	R_pid =	6.501E-05	Resistance from the convective effect on the Pipe Inner Diameter [K/W]
	R_Tot =	1.459E-02	Total Thermal Resistance [K/W]
	ΔT =	18.75432226	Temperature Difference from T_form to T_fl [K]
	q_x =	128.508762	Instantaneous Heat Transfer [W/m]
1	d_BHE_radial =	2334.47117	Recommended length of BHE @ conditions input into Borehole Heat Transfer spreadsheet [m]
	# of boreholes =	3	
2	P_maximum =	6278.4	Maximum collapse pressure seen by pipe [kPa]
3	P_c (PVC) =	581.2	Maximum allowable collapse pressure of PVC [kPa]
	P_c (PE) =	615.2	Maximum allowable collapse pressure of PE [kPa]
	P_c (Steel) =	42601.6	Maximum allowable collapse pressure of Steel [kPa]

Figure 4-13: BHE thermodynamics spreadsheet output for extraction phase

4.6 BHE FEFLOW Modeling

Without comparison the results obtained in the BHE spreadsheet are simply speculative. To combat this problem a simple FEFLOW model was constructed in an attempt to simulate the analytical calculations performed in the thermodynamic tab of the BHE spreadsheet. The inputs to the FEFLOW model were kept the same as in the spreadsheet, as well as the apparent boundary conditions, and a quasi-steady state solution was calculated. This solution, although not the same as the spreadsheet results, gave a solution reasonably close to the spreadsheet. The comparison of the two methods will be shown in the next section of this chapter. The design of the FEFLOW model is discussed below and the outcome of this design is also shown.

Mesh Design

The first step in any FEM software, and arguably the most crucial in attaining accurate results, is the construction of a proper 3-D mesh. This mesh is used in the discretization of the governing equations of the thermodynamic model to calculate nodal values for the model. Each set of nodes belongs to an element and a collection of many elements makes up a mesh. Due to the fact that the governing equations are quite complex, they can only be approximated by the FEM model to a certain degree of accuracy. The accuracy of the approximation comes from the design of the model mesh. The idea of meshing is the greater number of mesh elements you include in your model the greater chance those elements have at collectively approximating your solution. It would then make sense to include as many elements and nodes as possible. However, in the case of an FEM calculation you have to consider the time it takes to compute. This time will depend on how fast your computer can make each calculation and how long you have in order to run the model program. A complicated model can include millions of elements each with their own nodes and can take place over hundreds of years in time steps of a fraction of a second. This leads to the computer performing an enormous amount of single calculations in order to approximate the model solution. The mesh design must then be thought of in the following way: how long should the approximation take to compute, and how accurate does it need to be.

In the case of the thermodynamic spreadsheet, the FEFLOW model was used to approximate a steady state temperature distribution at a defined point in time. Since the transient response of the model was not the goal of its processing, the mesh was able to be kept quite coarse; that is to say the number of elements inside the mesh was kept small. The main goal was to see if the FEM software, when given a similar set of inputs and boundary conditions, arrived at the same temperature distribution as the spreadsheet model. The design of the mesh consisted of the following super element dimensions.

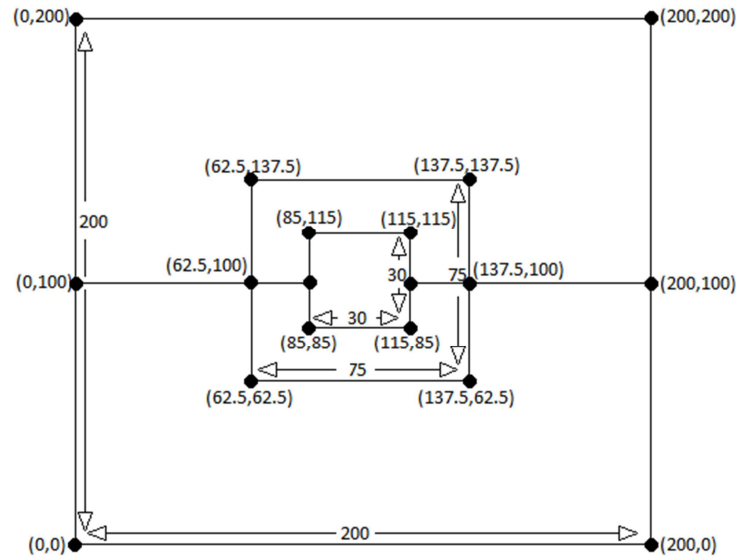


Figure 4-14: Super element dimensions in mesh design

After a design for the mesh geometry has been constructed, FEFLOW requires the user to specify a mesh density for each of the super elements (SE). In the case of this analysis a mesh density of 1 was used for the outside elements, 1.2 for the middle elements, and 1.5 for the center element. The mesh density numbers are a ratio used to tell FEFLOW how dense the mesh should be inside each of the SE. For example a mesh density of 1 applied to all the SE would distribute an even density across the whole 2D model. In contrast, the above defined mesh density will put 1.2 times as many mesh elements in the middle SE and 1.5 times as many mesh elements in the center SE as it will in the outer SE. Element density and minimum element number inputs are required before the program auto-constructs the triangular mesh.

Once a mesh is generated by the computer the user is responsible to check for errors in the generation. Errors will include long-thin triangles, missing spaces where a triangular element would not fit (called “holes” in the mesh), and SE boundary elements where the relative sizes of elements do not make sense. This process is very important and time must be taken to identify potential problems with the mesh. The user should regenerate the mesh, change the density values, and change the minimum number of elements to fix any potential problems. A good mesh should look rather uniform and neat. A screen shot of the mesh generated for this thesis is on the next page in figure 4.15.

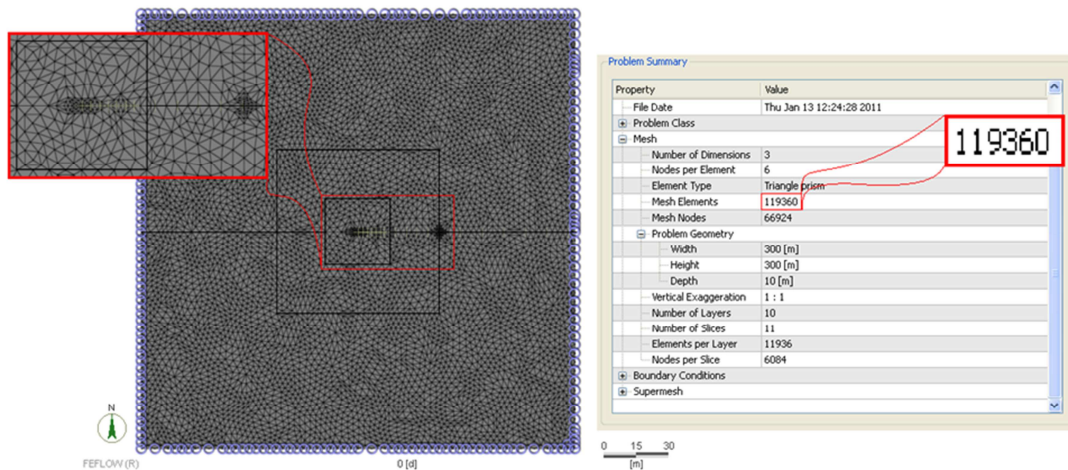


Figure 4-15: 2D mesh view

Notice in the diagram that the mesh has been generated with 119,360 elements. Although the mesh density looks to be quite dense, this is a simple model with a smaller amount of total elements than would be expected in a full simulation. Notice also how the mesh appears smaller in the center and especially small around the nodes. There are two areas of focus in the mesh, the BHE and a boundary condition. The BHE can be seen in the center of the generated mesh. The geometrical pattern which occurs at the BHE is due to the node design. Although in this report the node and mesh design are covered separately, they must be done concurrently in the design of the BHE model. The other area of concentrated elements represents a boundary in the mesh design. Here the two super mesh elements are connecting in such a way that the mesh has to be concentrated in order to avoid “holes”; this is done automatically by the computer.

Node Design

In the design of a BHE the heat transfer should extend from the wellbore as equally as possible; a perfectly circular gradient. Due to the differences in a computer generated mesh, slightly different nodal values will be assigned at equal radii from the BHE. This causes an uneven temperature plume which is an unnecessary deviation from the normal conditions. A cleverly designed node layout around the BHE can help guide the computer towards generating a more geometrical mesh. In the White Papers volume 5 (Diersch et al, 2010) they present some theory on defining the nodes in order to give an accurate mesh. The white papers formulate the “Direct estimation of nodal distance Δ ” (Diersch et al, 2010). The following figure has been borrowed from the White Pages in order to explain the distribution of nodes around the BHE.

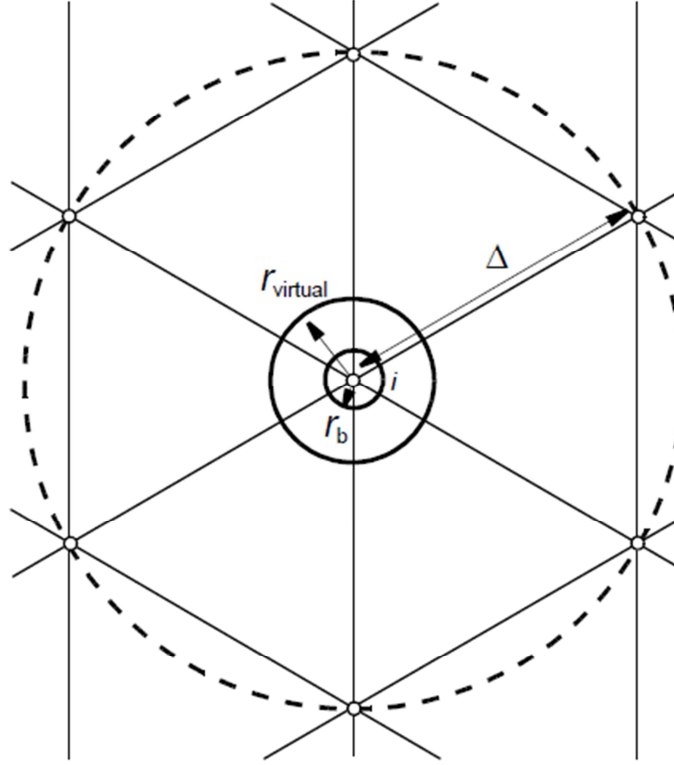


Figure 4-16: Nodal design of mesh (Diersch et al, 2010)

It can be seen that the suggested nodal design is 6 equally spaced nodes surrounding the BHE. With some simple algebra the Δ distance can be calculated using the convention named in the White Papers; this convention is shown below in equation 4.21 (Diersch et al, 2010):

$$\Delta = ar_b \quad a = \begin{cases} 4.81 & \text{for } n = 4 \\ 6.13 & \text{for } n = 6 \\ 6.66 & \text{for } n = 8 \end{cases} \quad (4.21)$$

Where: Δ = Nodal distance from center BHE
 a = correction factor for nodal distance
 r_b = drift radius of BHE

Once delta has been calculated the user can simply place nodes at the x and y component distance from the wellbore. For the TU Darmstadt BHE model the nodes were placed at a distance of 0.47 m from the center of the wellbore spaced out every 60 degrees around the center. This spacing of nodes resulted in the mesh pictured in figure 4.15. Figure 4.17 shows the trigonometry behind calculating the x and y coordinates for the 6 spaced out nodes.

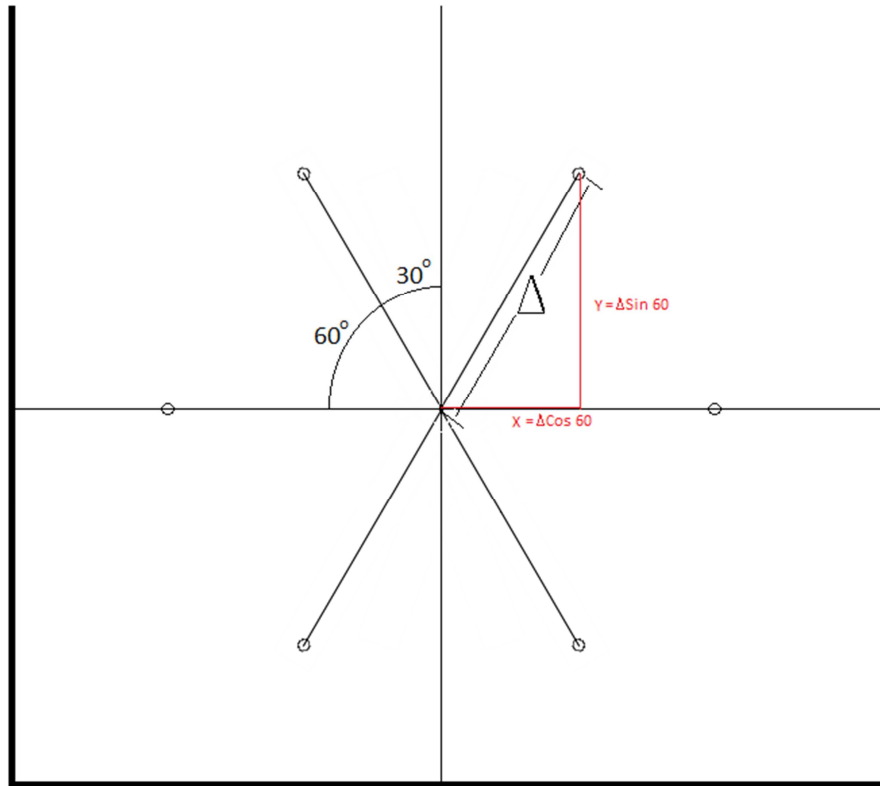


Figure 4-17: Spaced out nodes around the FEFLOW BHE

3D Design

After an appropriate mesh has been generated the user must build the 3D model. In the case of the TU Darmstadt BHE project the model was built to help justify the results of the spreadsheet. The spreadsheet is a one dimensional approximation of the heat transfer at a single depth. To model the one dimensional heat transfer calculation, a 10 m slice of borehole was split into ten equal layers of 1 m each. Then in the middle of the layers (slice 6 in the 3D model) a set of observation points were placed extending out into the formation. The borehole is only modeled in one 10 m section because we need only to approximate a one dimensional calculation. The approximation will act to verify the mathematics used in the spreadsheet model. If the spreadsheet model is able to accurately predict the temperature distribution at one depth, it should then work equally well at subsequent depths.

The FEFLOW programming will always calculate a 3D temperature distribution. In order to keep the model as one dimensional as possible the boundary conditions must be designed in a certain way. The first boundary condition exists at the outside edge of the 3D model. This is that the temperatures at the edge of the model are at 35 degrees Celsius. 35 degrees Celsius is the undisturbed reservoir temperature at a depth of 800 m. Next it is important to set the thermal properties of each of the elements. The assumption has been made that the reservoir rock will have a thermal conductivity of 2.8 W/mK and a volume specific heat capacity of 4.2 J/m³K. By selecting all of the elements in the model these values can be assigned to the entire reservoir.

The model then will consist of 10 layers at 1m each, an outer boundary condition of 35 degrees Celsius, a thermal conductivity of 2.8 W/mK, and a specific heat capacity of 4.2 J/m³K. The final step in the generation of the 3D model is to assign properties to the BHE. The FEFLOW input window for the BHE is seen in figure 4.18. Some of the variables are auto filled by the program and some are user inputs.

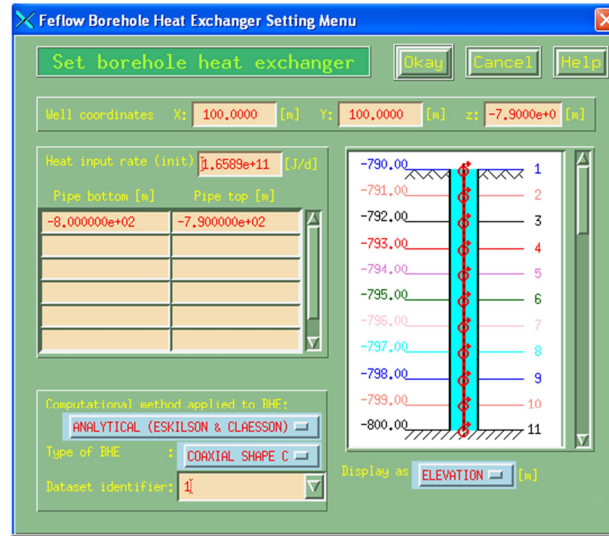


Figure 4-18: BHE input screen auto filled inputs

Figure 4.18 shows the inputs which are auto generated by the FEFLOW program. The well coordinates are not important for this model because they are only relevant to the datum established in the model (which is not specific to the TU Darmstadt well site). The heat input rate is governed by the by the inlet temperature. In the model built for this thesis the inlet temperature is known to be 90°C and so the heat input rate will be auto calculated once the inlet temperature has been set in the program. The last input of interest is the pipe bottom and pipe top fields. As can be seen the model exists at a depth of -800 m to a depth of -790 m. In the next window it can be seen the layer and slice distribution through the model. The temperature probes exist in the 6th slice and therefore lie at a depth of 795 m. However, due to the setting of the boundary conditions, uniform conditions should exist at depths between 790 m and 800 m so this discrepancy is not a concern.

Figure 4-19: User input parameters for the BHE

The final input parameters necessary for the model are the BHE user input parameters. Figure 4.19 shows the input window as is seen in FEFLOW classic program. Specific to the TU Darmstadt BHE project the borehole diameter is set to 0.1524 m, the pipe outer diameter at 0.0889 m, and the wall thickness of the pipe at 0.00734 m as per API spec regulations. The thermal conductivity of the steel is set to 60.5 W/mK, of the fluid is 0.65 W/mK and of the grout is 2.5 W/mK. The fluid value is an average conductivity of water at 90 degrees Celsius and the value for thermal conductivity of the grout is that of mortar cement. The other fluid parameters are specific to water at the given inlet conditions (90°C). The resistances in the BHE are calculated by the FEFLOW program so these need not be input. Finally after all values are input into FEFLOW, a 3D model can be generated that is ready to be run on the FEFLOW program. The results of the model are discussed in the next section compared with the spreadsheet results.

4.7 BHE Model Comparison

It has already been calculated that the suggested number of 800 m boreholes be three. A FEFLOW model was also constructed to calculate a steady state temperature distribution after charging the wellbore. The question still remains, can the values calculated in the spreadsheet be trusted as reasonable approximations considering the assumptions made?

The data from the FEFLOW model was input into the BHE spreadsheet under the following table. This data comprises a list of 18 temperature probes placed in the middle of our model at a depth of 800 m to calculate a temperature distribution from the center of the wellbore out to the end of the thermally effected radius.

Table 4-2: FEFLOW temperature distribution

Obs Point	Temperature [degC]	x coord [m]
1	88.6	0
19	74.6	0.462
2	64.6	2
3	59.7	4
4	56.9	6
5	54.8	8
6	53.0	10
7	51.5	12
8	48.8	17
9	46.9	22
10	45.3	27
11	43.9	32
12	42.9	37
13	41.0	47
14	39.6	57
15	38.3	67
16	37.2	77
17	36.2	87
18	35.3	97

Similar data was extracted from the spreadsheet and placed into the following table. The reference point for both models is the center of the wellbore ($x = 0$) and as is seen, there are only minor discrepancies with the calculated temperatures at relating depths. Another important point to notice is that the Excel spreadsheet has fewer temperature points than the FEFLOW model. However, during the comparison this difference will not matter as the spreadsheet results will be plotted on top of a line representing the FEFLOW results. If the points lie within or close to the line, they can be considered as valid approximations of the temperature distribution at that depth into the reservoir.

Table 4-3: Spreadsheet temperature distribution

Comparison Chart			
x coord [m]	Temperature [degC] FeFlow	Temperature [degC]	% differenc
0	88.6	89.9	1.49%
0.1761	74.6	75.9	1.68%
2	64.6	62.5	3.31%
6	56.9	55.5	2.61%
8	54.8	53.6	2.24%
10	53	52.2	1.61%
22	46.9	47.1	0.38%
32	43.9	44.7	1.71%
47	41	42.2	2.81%
67	38.3	39.9	4.01%
87	36.2	38.2	5.28%
97	35.3	37.5	5.91%
Maximum Error = 5.91%			

The two tables were plotted in Microsoft Excel and the result is seen in figure 4.20. The results show that the approximations of temperature distribution by the spreadsheet are quite close to the results obtained in the FEFLOW program. The comparison is also verified by calculating the percent differences in each of the values. The largest percent difference occurs at 97 m into the formation. The spreadsheet calculated a value of 37.5°C and the FEFLOW model a value of 35.3°C; the difference in approximations is 5.9%. Therefore, it can be stated that the spreadsheet will work to calculate a temperature distribution within approximately 6% error when compared to the FEFLOW model. This error should hold true at any depth and with any temperature difference as long as these same parameters are input into the FEFLOW model.

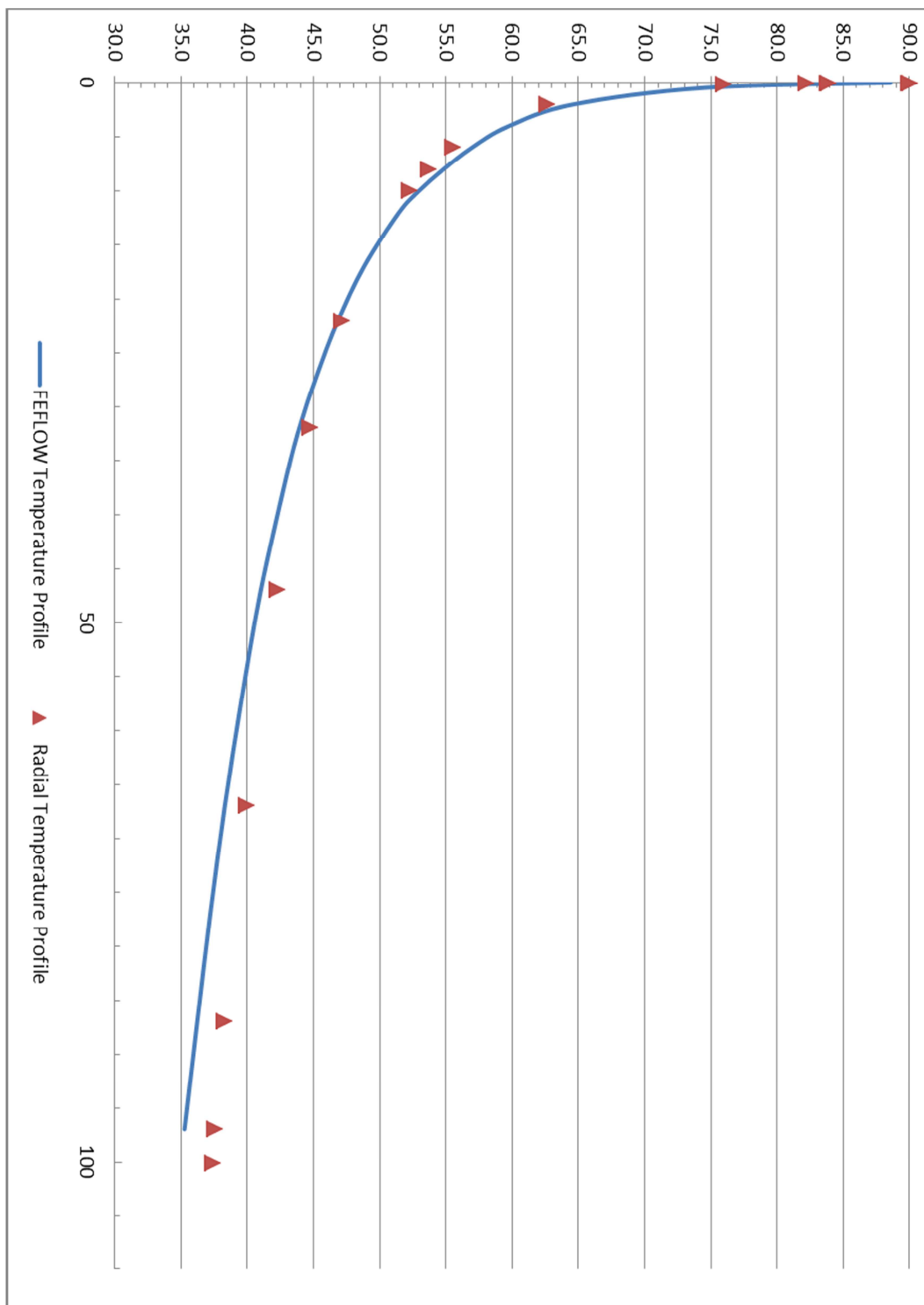


Figure 4-20: Chart of FEFLOW and spreadsheet data comparison

5 DRILLING PROGRAM

Date: January 25th, 2011
Subject: TU Darmstadt BHE Project
Revision #: 1

<u>SECTION</u>	<u>DESCRIPTION</u>
1	Scope
2	Well Information
3	Well site preparation and rig move
4	Emergency response plan
5	Area study and risk identification
6	Drilling operations

<u>FIGURE #</u>	<u>DESCRIPTION</u>
1	Stick Diagram

5.1 Scope

The TU Darmstadt drilling project is to be undertaken in order to install a borehole heat exchanger for the purpose of heating a newly renovated building on campus. The drilling program will cover aspects involved in drilling and casing the hole in preparation for the installation of a BHE. These aspects will include the conductor casing design, outer casing design, cementing/grouting program and basic operational procedures involved with drilling the borehole using a DTH hydraulic hammer drill.

Any and all scope changes, project revisions, and budget revisions should be recorded in the following table signed and dated by the responsible party prior to undertaking and after approval.

Table 5-1: Scope Change Summary Sheet

Summary of Changes		Impact of Changes			Approval	
Scope Change	Project Impact/Justification	Risk (1 to 5)	Time to Implement	Budget Change	Requested or Authorized	Date

5.2 Well Information

Well Name: _____
Well Type: Vertical Geothermal Borehole Heat Exchanger
Owner: TU Darmstadt Geoscience Department
Location: _____

Surface Coordinates:

Latitude: ____° ____' ____" N
Longitude ____° ____' ____" E

Prospective Reservoir:

Granodiorite Basement Rock (~ 60 m TVD)

Projected Total Depth:

Granodiorite Basement Rock (~800 m TVD)

Well Classification:

Geothermal Indirect use borehole heat exchanger

5.3 Well Site Preparation and Rig Move

Ensure proper construction considerations have been made prior to rig move. Issues to identify are listed below and should be considered prior to notifying drilling company.

Prior to rig mobilization the Drilling Foreman and Site Coordinator will review the rig move route and identify any special requirements. This review should occur within one week of the rig move and a pre-move plan should be constructed by the Site Coordinator in case of personnel reassignment. A copy of this plan should be sent to all involved parties as well as being attached to this program.

Prior to rig mobilization a pre-job safety meeting will be held with all involved parties including Site Coordinator and University officials. This meeting is called to discuss important safety issues like those listed below. The meeting is to be documented and a summary sent out to all involved parties as well as being attached to this program.

Prior to rig mobilization a Safe Work Permit is to be issued by TU Darmstadt to the Site Coordinator and Drilling Foreman which explains in detail the hazards and control procedures. Safe Work Permit will comply with the local regulatory body. Copies of the signed permit should be sent to all involved parties as well as being attached to this program.

The Drilling Foreman is responsible for overseeing all site operations and adhering to the guidelines and safe work practices endorsed by the local regulating body. The Drilling Forman shall be on site for all drilling operations outlined in this program. After the completion of the rig mobilization a summary shall be sent to the Site Coordinator and communicated with the involved parties representing TU Darmstadt. In the mobilization summary be sure to outline all concerns, recommendations, issues and operational notes to be followed up by TU Darmstadt and the Site Coordinator.

Important Issues to Identify and Control

- Weight Restrictions on roadways and within the Campus
- Contact university and government regulating bodies informing of proceeding operations
- Equipment travel permits: wide loads, traffic warning requirements, bridge restrictions
- Vehicle speed: On rig mobilization route and within campus boundaries
- Designated equipment mobilization routes
- Coordination of loads and placement on location
- Dangers of loading lose equipment
- Substance / Alcohol abuse and site safety considerations
- Incident reporting, personnel log books
- Post Move Assessment

Prior to Rig Move the following Notifications must be completed:

Site Coordinator:	Phone Number Here
Rig Coordinator:	Phone Number Here
Project Engineer:	Phone Number Here
University Liaison:	Phone Number Here

5.4 ERP: Emergency Response Plan

An emergency response plan should be adopted from TU Darmstadt or from the drilling company in case of a hazardous situation while drilling. This response plan will be briefed to the rig crew and all involved parties one week prior to the rig move and then again at the safety meeting before drilling operations commence.

5.5 Area Study and Risk Identification

Due to the limited information available for the Darmstadt area the study was restricted to geological evidence gathered from outcrops and knowledge of the fracture system in the area. Due to the fact that this group of wells will be the first in the area, caution should be taken when drilling the first well to ensure the predicted conditions exist. If discrepancies exist between the predicted underground and the actual underground, the site geologist should be notified immediately and the option to halt drilling operations should be considered. The following geological considerations should be made prior to drilling surface and main hole.

Conductor Hole

Soil layer of approximately 4-6 m TVD may need to be drilled out with auger type drill, or may employ a backhoe digging machine. A conductor casing will be set and cemented with concrete at the shoe before back-filling and compacting the ground. Make sure that the casing is vertical.

Surface Hole

Red Bed layer exists between 6-50 m TVD approximately. Layer consists of silt and sand stone stratified layers. Ground water flow in this region may cause problems with hole integrity. Tight hole conditions may exist further down into the layer

In the Red Bed layer between 6-50 m TVD expect to see 2-10 m zones of hard melaphyre rock sporadically placed throughout.

Surface hole should be drilled into weathered zone of granodiorite up to unconsolidated rock. At 50-70 m TVD should observe cutting samples for signs of weathering in order to pinpoint weathered boundary. Surface casing should be set 3-5 m TVD into unconsolidated granodiorite formation to ensure ground water hydraulic isolation.

Main Hole

Main hole set in granodiorite formation. Integrity issues should not be a problem. While drilling there may be minor loss of circulation zones as a fracture system does exist in the rock. Drill cores down to 80 m have shown signs of fractures with a few centimetres thickness and frequency of every 2-10 m. As drilling depth increases the fractures should become smaller in thickness and less frequent. There is no drilling history in this formation so caution should be used to check the validity of the above claims. Please report all loss of circulation zones.

There is no evidence of hydrocarbon bearing zones however due to the unknown nature of this drill the possibility of these zones should not be ruled out. Please have in place the available measures to deal with potential gas kicks or over pressured zones.

Cementing/Grouting

If for any reason during the cementing/grouting of each hole there are no returns to surface, drilling operations must not proceed before a CBL (cement bond log) is completed to determine the active cement top. Results should be communicated with the engineer/geologist in charge of operations and they will decide if remedial action is necessary.

Critical Success Factors

All incidents, hazards and near misses will be reported and documented. An incident follow up will proceed the incident, hazard or near miss with the formulation of a contingency plan to be put in place in order to avoid other such incidents.

Surface Casing is to be set 5 m or more within the consolidated formation to hydraulically seal the above ground water flow from the drilling operations and BHE operation within the main hole.

Surface cement returns to be expected on both grouting jobs. If returns are not seen then visual or logging methods must be undertaken in order to pinpoint the cement top. A failed cement job will lead to problems with BHE operation and will not be acceptable.

5.6 Drilling Operations

SURFACE HOLE: 0 m TVD – 60 m TVD (final depth of surface hole is not precise and should be decided when evidence of consolidated granodiorite formation exists, as per drilling operations.

1. Spud well with a fresh water drill mud as per program. Losses may occur in the surface hole but due to the nature of the drilling system loss of circulation material is not advised to be circulated. Increase flow rate in order to continue fluid circulation to surface if possible. There is a potential for ground water flow in this zone as well.
2. Equipment on site should include Mud Tank/Separation Tank, water pump, and necessary connection equipment and equipment for hazard mitigation.
3. Drill cutting samples should be taken every 1 m - 3 m in order to document the drilling process. Onsite geologist should be present during the drilling of the surface hole in order to document the existence of different layers. Key layers to identify are melaphyre layers and weathered granodiorite boundaries.
4. While drilling through the surface hole expect to experience borehole breakouts. These breakouts may indicate zones of ground water inflow and should be documented during the drilling process. Breakouts will be characterized by an excess in cuttings outflow or loss of fluid to formation.
5. PDC hammer bit or Tungsten Carbide bit should be used for the drilling operation.
 - a. 8" hole will need to be drilled. 6" Hammer with Casing Reamer extended to 8" hole will be used because of the limitation of the available drill technology. Largest hammer drill available is only 6 inches.
 - b. Each bit will be able to drill through the formation without a bit change or work over, however plan for two trips with a bit work over in-between (if necessary).
 - c. Drill to a depth of 60 m. Onsite geologist should be examining the cuttings in the last 10 m to identify signs of granodiorite weathering or Red Bed formation layer. The drilled hole must pass through the zone of weathered granodiorite into consolidated granodiorite. Ensure this by drilling 5 m – 9 m further than the last sign of weathering in granodiorite cuttings.
6. IF 60 m IS NOT ENOUGH DEPTH TO REACH CONSOLIDATED GRANODIORITE FURTHER DRILLING IS NECESSARY. PLEASE VERIFY SURFACE CASING SETTING DEPTH WITH GEOLOGIST BEFORE DRILLING CEASES.
7. Perform a wiper trip prior to reaching total depth to ensure proper hole cleaning. Increase string velocity as needed to ensure proper hole cleaning. Circulate a minimum of two bore hole volumes directly prior to surface casing run.

8. Ensure wellhead schematic is reviewed and space out has been verified prior to cutting casing and welding on casing bowl.
 - a. If mud returns to surface are not achieved, extra measures must be taken in order to support the main casing weight at surface. Confer with engineer/geologist in charge of operations for decision on what action to take.
9. Run casing in hole slowly to avoid pressure build up on formation.
10. Once the casing has reached TD, circulate and condition the drilling fluid in accordance with the Cementing Program guidelines supplied by the cementing company.
11. Cementing program is to be reviewed by the engineer/geologist in charge of drilling operations prior to the cementing job. The calculations of excesses and volumes should be double checked for validity at this time.
 - a. Surface Casing cement job is a single stage cementing procedure to be done with insulating cement (low thermal conductivity). Cement must also create an adequate seal to protect the surface casing from excess corrosion due to ground water contact and flow.
12. After proper cement set time, perform CBL to ensure proper cement sealing and identify cement top.

SURFACE CASING STRING:

- Float Shoe: 1 Joint – Thread Lock
- Casing: 1 joint – J-55, 25.29 kg/m – Thread Lock
- Float Collar: 1 Joint – Thread Lock
- Casing: To surface – J-55, 25.29 kg/m
- Centralizers: Space out every 3 joints. Mark positions in daily drilling reports

MAIN HOLE: 0 m TVD – 800 m TVD

1. BOP stack is not required for the drilling of the TU Darmstadt BHE project. Geology has confirmed that there is no potential for oil and gas in the drilled formation or over pressured zones. There exists no hydrocarbon window during the genesis of the granodiorite. As well the granodiorite contains no capture structure as it is vertically stratified with very low porosity. Over pressurization is not expected as the fracture system existing in the granodiorite vents to surface at several outcrops in the area. It is good practice to have a rotating head or stripper on the wellhead to divert the flow to the mud tank/pit.
2. Prior to drilling pressure test and function each of the existing string components

3. Pressure test surface casing: Surface casing must be tested to a pressure equal to 1.5 times the calculated Hydrostatic head at TVD and held for 15min with minimal bleed off. For example, if the surface casing is set at 60 m TVD then $1.5 \times P_{60m}$ means a pressure test of 880 kPa gauge pressure for 15 min with less than 10% bleed off. Report details of pressure test in daily drilling report.
4. Main hole will be drilled with a hydraulic down the hole hammer drill recommended with a tungsten carbide or PDC hammer bit. Suggested to run with PDC bit initially and if the bit performance is not adequate to change out bit for the tungsten carbide on next trip. The PDC bit cannot be worked over to improve performance. The tungsten carbide bit will have to be sharpened and worked over every approximately 100 m – 200 m of drilling.
5. Extensive borehole breakouts are not expected in this formation. Loss of circulation zones may occur but should not be substantial.
6. PDC hammer bit or Tungsten Carbide bit should be used for the drilling operation.
 - a. 6” bit with hammer assembly comprise DHA to drill specifications.
 - b. Drill to a TVD of 800 m, max measured depth of 900 m whichever comes first.
 - c. Perform a wiper trip every 300 m of drilled hole to ensure proper hole cleaning. Increase mud volume flow rate every wiper trip to ensure proper hole cleaning. Increase string velocity as needed to ensure proper hole cleaning. Circulate a minimum of two bore hole volumes directly prior to casing run.
7. Perform a final wiper trip prior to TD of the main hole. Hole conditions should be recorded at this time and high friction areas recorded in the drilling report. Also communicate high friction areas to site Engineer/Geologist to ensure casing clearance is maintained before running casing. If problem areas exist, well design should be reconsidered by engineering/geology officials.
8. Run casing in hole slowly to avoid pressure build up on formation.
9. Once the casing has reached TD, circulate and condition the drilling fluid in accordance with the Cementing Program guidelines supplied by the cementing company.
10. Cementing program is to be reviewed by the engineer/geologist in charge of drilling operations prior to the cementing job. The calculations of excesses and volumes should be double checked for validity at this time.
11. Casing cement job is a two stage cementing procedure to be done with a first stage of conductive cement and second stage of insulating cement (low thermal conductivity). Casing string must be run with the tools at set depths. Second stage cementing collar to be spaced out on casing string to sit at 200 m TVD. Record final setting depth of cementing collar.

MAIN CASING STRING:

- Float Shoe: 1 Joint – Thread Lock
- Casing: 1 Joint – J-55, .127 m, 17.11 kg/m – Thread Lock
- Float Collar: 1 Joint – Thread Lock
- Casing: To 200 m TVD – J-55, .127 m, 17.11 kg/m
- Cement Collar: 1 Joint – Thread Lock
- Casing: To Surface – J-55, .127 m, 17.11 kg/m
- Centralizers: Space out every 3 joints. Mark positions in daily drilling reports

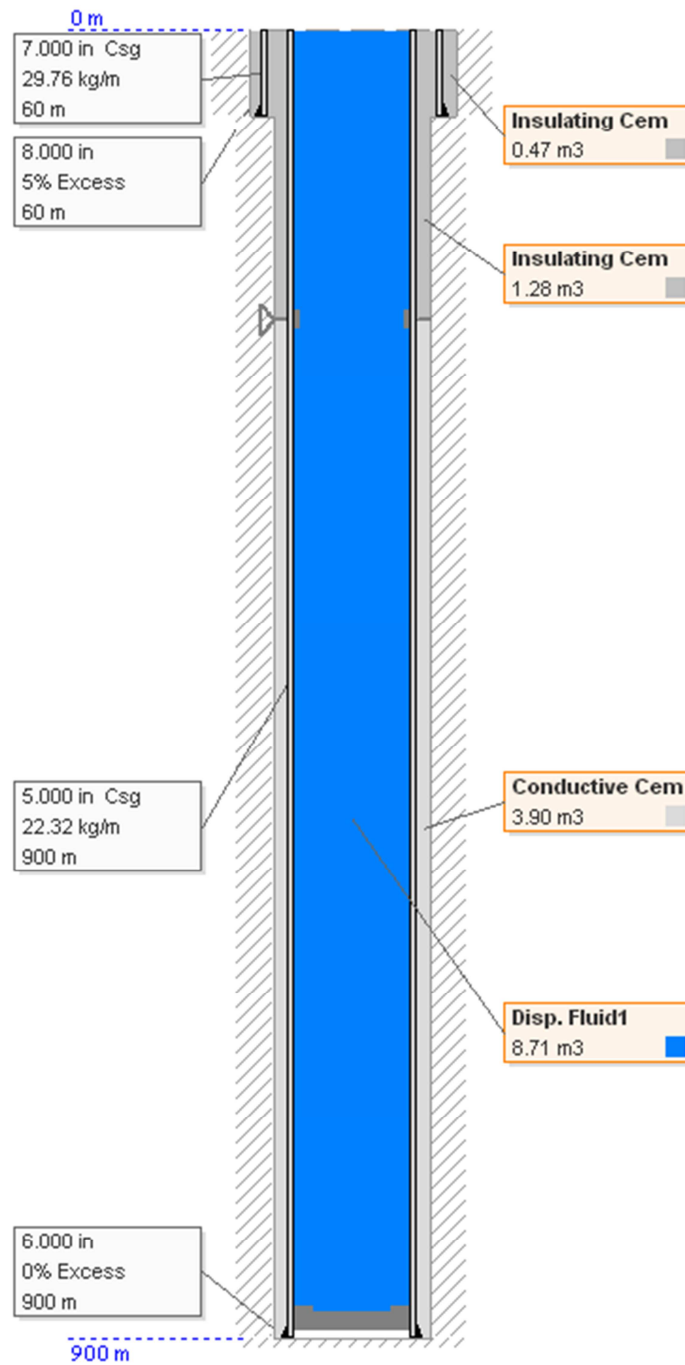


Figure 5-1:Drilling design sick diagram

6 COMPLETIONS PROGRAM

Date: January 25th, 2011
Subject: TU Darmstadt BHE Project
Revision #: 1

<u>SECTION</u>	<u>DESCRIPTION</u>
1	Scope
2	Well Information
3	Well site preparation and rig move
4	Emergency response plan
5	Area study and risk identification
6	Drilling operations

<u>FIGURE #</u>	<u>DESCRIPTION</u>
1	Stick Diagram

6.1 Scope

The TU Darmstadt drilling project is to be undertaken in order to install a borehole heat exchanger for the purpose of heating a newly renovated building on campus. The completions program will cover the aspects of BHE design which have not been covered in the drilling program. These aspects include, exchanger final dimensions, suggested operational flow rates, pipe material selection, completions string design, expected temperature distribution before and after BHE charging, expected initial heat extraction rate.

Any and all scope changes, project revisions, and budget revisions should be recorded in the following table signed and dated by the responsible party prior to undertaking and after approval.

Table 6-1: Record summary of scope changes

Summary of Changes		Impact of Changes			Approval	
Scope Change	Project Impact/Justification	Risk (1 to 5)	Time to Implement	Budget Change	Requested or Authorized	Date

6.2 Well Information

Well Name: _____
Well Type: Vertical Geothermal Borehole Heat Exchanger
Classification: Geothermal Direct Use Borehole Heat Exchanger
Owner: TU Darmstadt Geoscience Department
Location: _____

Surface Coordinates:

Latitude: ____° ____' ____" N
Longitude ____° ____' ____" E

Prospective Reservoir :

Granodiorite Basement Rock (~ 60 m TVD)

Projected Total Depth :

Granodiorite Basement Rock (~800 m TVD)

Well Classification :

Geothermal Borehole Heat Exchanger

Estimated Completion Days:

3 Days, tubing run and tied in to existing network

Estimated Wellbore Costs:

€ X.XX M Completed

6.3 Well site preparation and rig move

Completions operations should be undertaken immediately after drilling operations have ceased as the tubing can be run in hole with the drilling rig. However proper time should be left for the casing cement to dry and ensure the Cement Bond Log (CBL) has been performed before running in hole with tubing. If the drilling rig must be moved off of site before tubing installation, consider the following well site preparation and rig move instructions. If the drilling rig can remain on site until the tubing running procedures, ensure all drilling related equipment has been removed from site before completions equipment arrives on site; this means the mud tank, pump, and related equipment not required for completions operations.

If new Rig is to be mobilized to site:

Prior to rig mobilization the Completions Foreman and Site Coordinator will review the rig move route and identify any special requirements. This review should occur within one week of the rig move and a pre-move plan should be constructed by the Site Coordinator in case of personnel reassignment. A copy of this plan should be sent to all involved parties as well as being attached to this program.

Prior to rig mobilization a pre-job safety meeting will be held with all involved parties including Site Coordinator and University officials. This meeting is called to discuss important safety issues like those listed below. The meeting is to be documented and a summary sent out to all involved parties as well as being attached to this program.

Prior to rig mobilization a Safe Work Permit is to be issued by TU Darmstadt to the Site Coordinator and Drilling Foreman which explains in detail the hazards and control procedures. Safe Work Permit will comply with the local regulatory body. Copies of the signed permit should be sent to all involved parties as well as being attached to this program.

The Completions Foreman is responsible for overseeing all site operations and adhering to the guidelines and safe work practices endorsed by the local regulating body. The Completions Foreman shall be on site for all drilling operations outlined in this program. After the completion of the rig mobilization a summary shall be sent to the Site Coordinator and communicated with the involved parties representing TU Darmstadt. In the mobilization summary be sure to outline all concerns, recommendations, issues and operational notes to be followed up by TU Darmstadt and the Site Coordinator.

Important Issues to Identify and Control

- Weight Restrictions on roadways and within the Campus
- Contact to university and government regulating bodies informing of proceeding operations
- Equipment travel permits: such as wide loads, traffic warning requirements, bridge restrictions
- Vehicle speed: On rig mobilization route and within campus boundaries
- Designated equipment mobilization routes
- Coordination of loads and placement on location
- Dangers of loading loose equipment
- Substance / Alcohol abuse and site safety considerations
- Incident reporting, personnel log books
- Post Move Assessment

Prior to Rig Move the following Notifications must be completed:

Site Coordinator:	Phone Number Here
Rig Coordinator:	Phone Number Here
Project Engineer:	Phone Number Here
University Liason:	Phone Number Here

6.4 ERP: Emergency Response Plan

An emergency response plan should be adopted from TU Darmstadt or from the rig company in case of a hazardous situation while drilling. This response plan will be briefed to the completions crew and all involved parties one week prior to the rig move and then again at the safety meeting before drilling operations commence.

6.5 Area Study and Risk Identification

Tubing installation

Tubing is to be laid down on site prior to running in hole. Ensure proper containment structure to avoid injury.

Ensure proper well site cleaning and all hoses and cables are clearly marked to avoid trip hazards.

Be careful when running in hole with tubing at depth of cement collar as a restricted inner diameter will exist. Ensure before running in hole that casing is drifted to the maximum outer running diameter of the tubing.

Critical Success Factors

All incidents, hazards and near misses will be reported and documented. An incident follow up will be held after the incident, hazard or near miss with the formulation of a contingency plan to be put in place in order to avoid other such incidents.

Tubing setting depth to be off bottom hole by approximately 5m.

6.6 Completions Operations

MAIN Tubing String: 0 m TVD – 795 m TVD

If drilling rig is not being used:

1. Move in and rig up completions rig and related equipment.
2. Lay down tubing and prepare to run in hole
3. Properly stake and identify surface lines and cables
4. Tie in water lines to wellhead.
 - a. These may be needed to keep the hole filled with water in order to cut down on the string weight seen by the completions rig.
5. Run in hole with the following tubing string on 88.9 mm tubing to a depth of 795 m TVD.
 - a. 88.9 mm Wireline Re-entry Guide
 - b. 88.9 mm Tool landing nipple (preferably with nogo)
 - i. May be necessary for down hole temperature recording device
 - ii. Make record of dimensions and type of tool landing nipple chosen.
 - c. 88.9 mm J-55 13.69 kg/m, tubing to surface
 - i. Space out and land tubing string in wellhead tubing hanger
6. Assemble wellhead and rig out fill lines
7. Rig out completions rig and all equipment
8. Turn well over to TU Darmstadt operations managers

If drilling rig is to be used:

1. Rig out unrelated completions equipment and move off site
2. Rig in completions equipment and lay down tubing to be run in hole
3. Properly stake and identify surface lines and cables
4. Ensure water fill lines are still linked to rig and casing
 - a. There may be a need to keep the hole filled with water in order to cut down on the string weight seen by the completions rig.
5. Run in hole with the following tubing string on 88.9 mm tubing to a depth of 795 m TVD.
 - a. 88.9 mm Wireline re-entry guide
 - b. 88.9 mm Tool landing nipple (preferably with nogo)
 - i. May be necessary for down hole temperature recording device
 - ii. Make record of dimensions and type of tool landing nipple chosen
 - c. 88.9 mm J-55 13.69 kg/m, tubing to surface
6. Space out and land tubing string in wellhead tubing hanger
7. Assemble wellhead and rig out fill lines
8. Rig out drilling rig and all equipment
9. Turn well over to TU Darmstadt operations managers

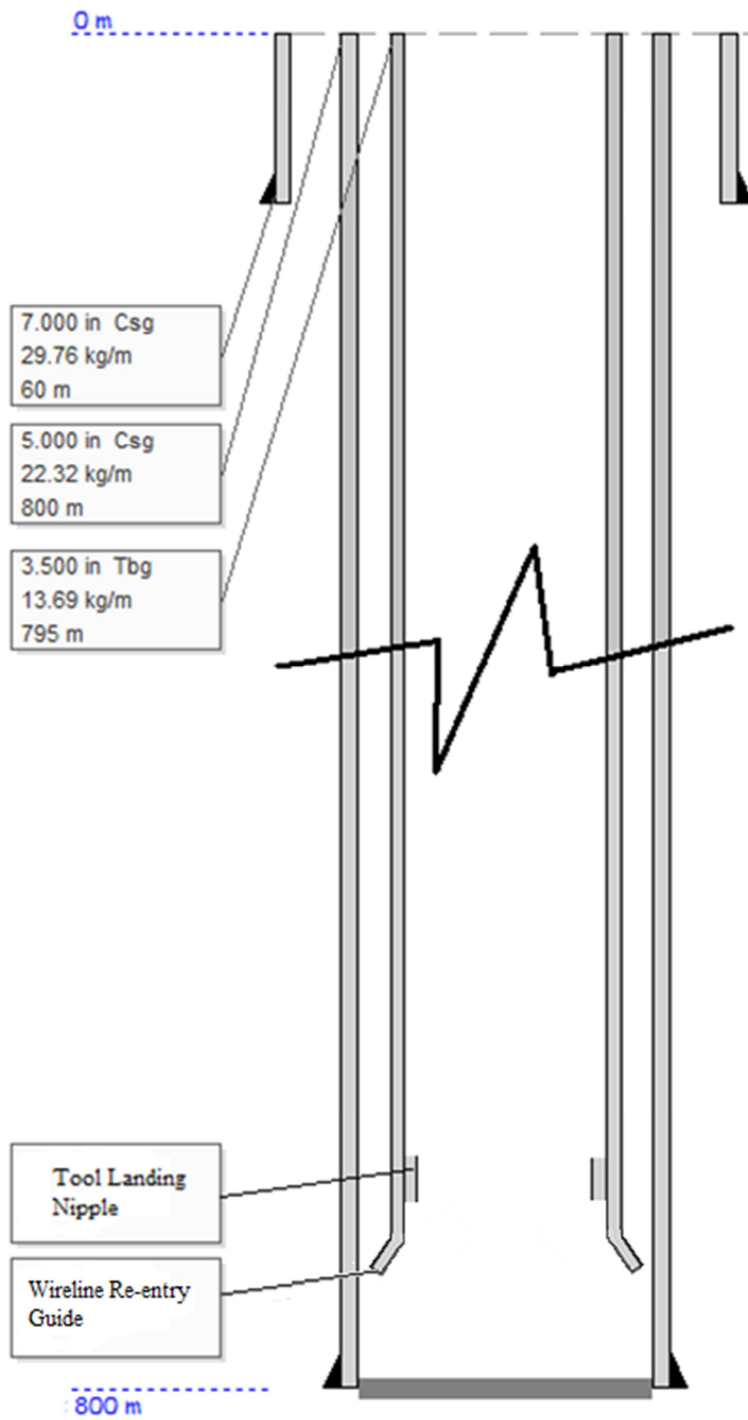


Figure 6-1: Completions stick diagram

7 CONCLUSIONS

The analysis contained in this thesis has given rise to a preliminary design of both borehole heat exchanger and drilling program. The programs should be used as a step towards the final completions and drilling design but are not to be considered as finished. The proper design of an expensive project such as the TU Darmstadt BHE project requires further FEM analysis because the area itself does not have analogue data to support the claims in this thesis. However, the thesis does combine the knowledge of BHE construction, thermodynamic calculations, drilling research and drilling theory into a single document.

The BHE construction was decided to consist of 3.5" (88.9 mm) steel tubing inside of 5" (127.0 mm) steel casing set to a depth of approximately 800 m. Steel was used in the design because of strength issues in the PVC/PE pipe. These issues put the collapse strength of the PVC/PE at approximately 600 kPa which was nearly 10 times smaller than the pressures seen by the tubing at bottom hole depth. Water was to be injected down the tubing and circulated up the annulus for heat transfer to be most efficient. This was because heat transfer occurs due to the thermal resistance of a medium and the temperature difference between this medium. Since the tubing best insulated the water, allowing it to reach the high bottom hole temperatures as cool as possible, it was chosen as the injection flow path for the BHE.

The thermodynamics were used to find an instantaneous one dimensional heat transfer distribution in the granodiorite thermal reservoir. This distribution calculation assumed steady state conditions calculated at the point in which the reservoir was fully charged to an acceptable thermally effected radius. Verification of the temperature distribution was done via FEFLOW and the results came to within a 6% error in temperature calculation. With acceptable accuracy the spreadsheet thermodynamics, based on Fourier's Law, were able to model the underground temperature distribution compared to the FEFLOW software. The calculation, when done at depths ranging from 40 m to 1000 m gave a theoretical temperature profile in the reservoir. The average skin zone value of this temperature distribution was used to calculate an average initial heat transfer rate of approximately 130 W/m of wellbore. Transient analysis is needed in order to calculate the regression of this value. However, based on this value it was decided that at least 3 wellbore heat exchangers were needed in order to supply the building with 300 kW of extraction heating.

The well was chosen to be drilled with down the hole hydraulic hammer drilling technology. This was chosen because of depth considerations and geological setting. Pneumatic air hammer drilling is not nearly as efficient as hydraulic hammer drilling at depths greater than around 300 m. Better cuttings transport, increased hole stability and decreased deviation are all reasons to choose the hydraulic hammer over the pneumatic hammer. The main advantage of rotary drilling is the ability to use heavy drill fluids. However the absence of any overpressure zones or hydrocarbon bearing formations warrants the use of pure water as a drilling fluid. The hydraulic hammer drill meets all of the operational requirements of the TU Darmstadt BHE project and can replace air hammer drilling in this application.

REFERENCES

- ASHME Shale Shaker Committee, 2004, '*Drilling Fluids Processing Handbook*'. Gulf Professional Publishing, Houston Texas.
- ASTM International, 2010, '*ASTM F480 – 06b1: Standard Specification for Thermoplastic Well Casing Pipe and Couplings Made in Standard Dimension Ratios (SDR), SCH 40 and SCH 80*'. Subcommittee F17.61.
- Bär, K, Arndt, D, Buß, A, & Sass, I, 2010, '*Rotliegendesteine in Hessen – Beste Voraussetzungen Für geothermische Nutzung*'. Festkolloquium Angewandte Geothermie, Technischen Universität Darmstadt, Darmstadt, Germany
- Bar-Cohen, Y. & Zucny, K. 2009. '*Drilling in Extreme Environments – Penetration and Sampling on Earth and other Planets*'. Wiley-VCH verlag GmbH & Co. KGaA. Weinheim, Germany.
- Beier, M. 2007. '*Urbane Beeinflussung des Grundwassers: Stoffemissionen und-immissionen am Beispiel Darmstadts*'. Dissertation, Technischen Universität Darmstadt. Darmstadt, Germany.
- Bengtson, H, 2010. '*Excel Spreadsheet Forced Convection Turb Pipe Flow: SI units*'. Bright Hub Engineering Forum, November 22 2010, <www.brighthub.com/engineering/mechanical/media/p/91067.aspx>
- Dayre, M. & Giraud, A. 1986. '*Mechanical Properties of granodiorite from laboratory tests*'. Institute de Recherches Interdisciplinaires de Geologie et Mechanique. Saint-Martin-d'Heres, France.
- Diersch, H.J.G. Bauer, D. Heidemann, W. Reuhaak, W. & Schatzl, P. '*Finite element formulation for borehole heat exchangers in modeling geothermal heating systems by FEFLOW*'. FEFLOW White Papers, Vol 5, Chapter 1.
- Dyckerhoff Drilling, 2008, '*Class G Grade HSR Cement MSDS*'. Viewed on November 21, 2010 <<http://www.dyckerhoff-bohrtechnik.de/online/en/Home/Products/WellCement.html>>

- Gu, Y. 2010. '*Design Calculations for Optimizing of an Existing Multifunction-Building with Borehole Heat Exchangers*'. Masters Thesis, Technische Universität Darmstadt. Darmstadt Germany.
- Harrison, Dr. H.G.. 2007. '*The ON-LINE Computational and Graphics Website for Petroleum Engineers & Geologists in: Drilling, Reservoir Engineering, Production, Geosciences & Economics*'. Cuttings Slip Velocity. E&P Information Management Consultant. Jan 2011. <<http://www.peteng.com/jmm/>>.
- Hawkes, C. 2008. '*GEOE 466 Introduction to Petrophysics*'. College of Geological Engineering, University of Saskatchewan. Saskatoon, Saskatchewan, Canada.
- Hellstrom, G, 1991, '*Ground Heat Storage, Thermal Analysis of Duct Storage Systems*', Department of Mathematical Physics, University of Lund, Sweden.
- Incropera, F.P. Dewitt, D.P. Bergman, T.L. & Adrienne, S. 2007. '*Fundamentals of Heat and Mass Transfer*'. Fifth Edition, John Wiley and Sons Inc, Hoboken NJ. Chapter 3.
- Melamed, Y. Kiselev, A. Gelfgat, M. Dreesen, D.S. Blacic, J. 1997. '*Hydraulic Hammer Drilling Technology: Developments and Capabilities*'. 8th Annual International Energy Week Conference. Houston, TX.
- Morita, Koji. Tago, Makoto. Ehara, Sachio. 2005. *Case studies on small-scale Power Generation with the Downhole Coaxial Heat Exchanger*. National Institute of Advanced Industrial Science and Technology, Onogawa, Japan. Akita University, Tegata, Japan. Kyushu University, Hakozaki, Japan. Proceedings World Geothermal Congress.
- Riechers, J. 2011. '*Wohin bohren wir? Masshaltigkeit konventioneller und innovativer hydraulischer GeoJetting Bohrtechnik*'. B.Sc. GZB – Internationales Geothermiezentrum. Hochschule Bochum, Germany.
- Roscoe Moss Company, 2008, '*Collapse Strength Calculations*'. Viewed 15 December 2010, < <http://www.roscoemoss.com/waterwell-calculations.html>>
- Wittig, Dilp. Ing Volker, Personal Communication, GZB Bochum, Germany. 2010.
- Valdimarsson, Pall 2010, PDF Lecture Document, "*17 – Thermoeconomics*", GEO607, University of Iceland, Slide 14.

APPENDIX A

The Temperature distribution calculated values under Applied Geosciences building of TU Darmstadt Botanical Gardens campus.

Temperature Field, Surface to bottom												
Depth	Formation Temperature	Skin Zone Temperature	Tempearture Probes [m into formation from wellbore]									
			2	6	8	10	22	32	47	67	87	100.3
40	12	71.8	51.2	40.2	37.3	35.1	27.2	23.5	19.7	16.1	13.5	12.4
45	12.15	71.9	51.3	40.3	37.4	35.2	27.4	23.6	19.8	16.3	13.7	12.6
50	12.3	71.9	51.3	40.4	37.5	35.3	27.5	23.8	19.9	16.4	13.8	12.7
55	12.45	72.0	51.4	40.5	37.6	35.4	27.6	23.9	20.1	16.6	14.0	12.9
60	12.6	72.0	51.5	40.6	37.7	35.5	27.7	24.0	20.2	16.7	14.1	13.0
65	12.75	72.0	51.6	40.7	37.9	35.6	27.9	24.1	20.3	16.8	14.3	13.2
70	12.9	72.1	51.6	40.8	38.0	35.8	28.0	24.3	20.5	17.0	14.4	13.3
75	13.05	72.1	51.7	40.9	38.1	35.9	28.1	24.4	20.6	17.1	14.6	13.5
80	13.2	72.1	51.8	41.0	38.2	36.0	28.2	24.5	20.8	17.3	14.7	13.6
85	13.35	72.2	51.9	41.1	38.3	36.1	28.3	24.7	20.9	17.4	14.9	13.8
90	13.5	72.2	51.9	41.2	38.4	36.2	28.5	24.8	21.0	17.6	15.0	13.9
95	13.65	72.2	52.0	41.3	38.5	36.3	28.6	24.9	21.2	17.7	15.1	14.1
100	13.8	72.3	52.1	41.4	38.6	36.4	28.7	25.0	21.3	17.8	15.3	14.2
105	13.95	72.3	52.2	41.5	38.7	36.5	28.8	25.2	21.4	18.0	15.4	14.4
110	14.1	72.3	52.2	41.6	38.8	36.6	28.9	25.3	21.6	18.1	15.6	14.5
115	14.25	72.4	52.3	41.7	38.9	36.7	29.1	25.4	21.7	18.3	15.7	14.7
120	14.4	72.4	52.4	41.8	39.0	36.8	29.2	25.6	21.8	18.4	15.9	14.8
125	14.55	72.4	52.5	41.8	39.1	36.9	29.3	25.7	22.0	18.6	16.0	15.0
130	14.7	72.5	52.5	41.9	39.2	37.0	29.4	25.8	22.1	18.7	16.2	15.1
135	14.85	72.5	52.6	42.0	39.3	37.1	29.5	25.9	22.2	18.8	16.3	15.3
140	15	72.5	52.7	42.1	39.4	37.2	29.7	26.1	22.4	19.0	16.5	15.4
145	15.15	72.6	52.8	42.2	39.5	37.3	29.8	26.2	22.5	19.1	16.6	15.6
150	15.3	72.6	52.8	42.3	39.6	37.4	29.9	26.3	22.7	19.3	16.8	15.7
155	15.45	72.7	52.9	42.4	39.7	37.5	30.0	26.5	22.8	19.4	16.9	15.9
160	15.6	72.7	53.0	42.5	39.8	37.7	30.1	26.6	22.9	19.5	17.1	16.0
165	15.75	72.7	53.1	42.6	39.9	37.8	30.3	26.7	23.1	19.7	17.2	16.2
170	15.9	72.8	53.1	42.7	40.0	37.9	30.4	26.8	23.2	19.8	17.4	16.3
175	16.05	72.8	53.2	42.8	40.1	38.0	30.5	27.0	23.3	20.0	17.5	16.5
180	16.2	72.8	53.3	42.9	40.2	38.1	30.6	27.1	23.5	20.1	17.7	16.6
185	16.35	72.9	53.4	43.0	40.3	38.2	30.8	27.2	23.6	20.3	17.8	16.8
190	16.5	72.9	53.4	43.1	40.4	38.3	30.9	27.4	23.7	20.4	17.9	16.9
195	16.65	72.9	53.5	43.2	40.5	38.4	31.0	27.5	23.9	20.5	18.1	17.1
200	16.8	73.0	53.6	43.3	40.6	38.5	31.1	27.6	24.0	20.7	18.2	17.2
205	16.95	73.0	53.7	43.4	40.7	38.6	31.2	27.7	24.1	20.8	18.4	17.4
210	17.1	73.0	53.7	43.5	40.8	38.7	31.4	27.9	24.3	21.0	18.5	17.5
215	17.25	73.1	53.8	43.6	40.9	38.8	31.5	28.0	24.4	21.1	18.7	17.7
220	17.4	73.1	53.9	43.7	41.0	38.9	31.6	28.1	24.5	21.3	18.8	17.8
225	17.55	73.1	54.0	43.8	41.1	39.0	31.7	28.2	24.7	21.4	19.0	18.0
230	17.7	73.2	54.0	43.9	41.2	39.1	31.8	28.4	24.8	21.5	19.1	18.1
235	17.85	73.2	54.1	44.0	41.3	39.2	32.0	28.5	25.0	21.7	19.3	18.3
240	18	73.3	54.2	44.1	41.4	39.3	32.1	28.6	25.1	21.8	19.4	18.4
245	18.15	73.3	54.3	44.2	41.5	39.5	32.2	28.8	25.2	22.0	19.6	18.6
250	18.3	73.3	54.3	44.2	41.6	39.6	32.3	28.9	25.4	22.1	19.7	18.7
255	18.45	73.4	54.4	44.3	41.7	39.7	32.4	29.0	25.5	22.3	19.9	18.9
260	18.6	73.4	54.5	44.4	41.8	39.8	32.6	29.1	25.6	22.4	20.0	19.0
265	18.75	73.4	54.6	44.5	41.9	39.9	32.7	29.3	25.8	22.5	20.2	19.2
270	18.9	73.5	54.6	44.6	42.0	40.0	32.8	29.4	25.9	22.7	20.3	19.3
275	19.05	73.5	54.7	44.7	42.1	40.1	32.9	29.5	26.0	22.8	20.4	19.5
280	19.2	73.5	54.8	44.8	42.2	40.2	33.1	29.7	26.2	23.0	20.6	19.6
285	19.35	73.6	54.9	44.9	42.3	40.3	33.2	29.8	26.3	23.1	20.7	19.8
290	19.5	73.6	54.9	45.0	42.4	40.4	33.3	29.9	26.4	23.2	20.9	19.9
295	19.65	73.6	55.0	45.1	42.5	40.5	33.4	30.0	26.6	23.4	21.0	20.1
300	19.8	73.7	55.1	45.2	42.6	40.6	33.5	30.2	26.7	23.5	21.2	20.2
305	19.95	73.7	55.2	45.3	42.7	40.7	33.7	30.3	26.9	23.7	21.3	20.4
310	20.1	73.7	55.2	45.4	42.8	40.8	33.8	30.4	27.0	23.8	21.5	20.5
315	20.25	73.8	55.3	45.5	42.9	40.9	33.9	30.6	27.1	24.0	21.6	20.7
320	20.4	73.8	55.4	45.6	43.0	41.0	34.0	30.7	27.3	24.1	21.8	20.8

325	20.55	73.9	55.4	45.7	43.1	41.1	34.1	30.8	27.4	24.2	21.9	21.0	20.7
330	20.7	73.9	55.5	45.8	43.2	41.3	34.3	30.9	27.5	24.4	22.1	21.1	20.8
335	20.85	73.9	55.6	45.9	43.3	41.4	34.4	31.1	27.7	24.5	22.2	21.3	21.0
340	21	74.0	55.7	46.0	43.4	41.5	34.5	31.2	27.8	24.7	22.4	21.4	21.1
345	21.15	74.0	55.7	46.1	43.5	41.6	34.6	31.3	27.9	24.8	22.5	21.6	21.3
350	21.3	74.0	55.8	46.2	43.6	41.7	34.7	31.5	28.1	25.0	22.7	21.7	21.4
355	21.45	74.1	55.9	46.3	43.7	41.8	34.9	31.6	28.2	25.1	22.8	21.9	21.6
360	21.6	74.1	56.0	46.4	43.8	41.9	35.0	31.7	28.3	25.2	23.0	22.0	21.7
365	21.75	74.1	56.0	46.5	43.9	42.0	35.1	31.8	28.5	25.4	23.1	22.2	21.9
370	21.9	74.2	56.1	46.6	44.0	42.1	35.2	32.0	28.6	25.5	23.2	22.3	22.0
375	22.05	74.2	56.2	46.6	44.1	42.2	35.3	32.1	28.7	25.7	23.4	22.5	22.2
380	22.2	74.2	56.3	46.7	44.2	42.3	35.5	32.2	28.9	25.8	23.5	22.6	22.3
385	22.35	74.3	56.3	46.8	44.3	42.4	35.6	32.3	29.0	26.0	23.7	22.7	22.5
390	22.5	74.3	56.4	46.9	44.5	42.5	35.7	32.5	29.2	26.1	23.8	22.9	22.6
395	22.65	74.3	56.5	47.0	44.6	42.6	35.8	32.6	29.3	26.2	24.0	23.0	22.8
400	22.8	74.4	56.6	47.1	44.7	42.7	36.0	32.7	29.4	26.4	24.1	23.2	22.9
405	22.95	74.4	56.6	47.2	44.8	42.8	36.1	32.9	29.6	26.5	24.3	23.3	23.1
410	23.1	74.4	56.7	47.3	44.9	42.9	36.2	33.0	29.7	26.7	24.4	23.5	23.2
415	23.25	74.5	56.8	47.4	45.0	43.1	36.3	33.1	29.8	26.8	24.6	23.6	23.4
420	23.4	74.5	56.9	47.5	45.1	43.2	36.4	33.2	30.0	26.9	24.7	23.8	23.5
425	23.55	74.6	56.9	47.6	45.2	43.3	36.6	33.4	30.1	27.1	24.9	23.9	23.7
430	23.7	74.6	57.0	47.7	45.3	43.4	36.7	33.5	30.2	27.2	25.0	24.1	23.8
435	23.85	74.6	57.1	47.8	45.4	43.5	36.8	33.6	30.4	27.4	25.2	24.2	24.0
440	24	74.7	57.2	47.9	45.5	43.6	36.9	33.8	30.5	27.5	25.3	24.4	24.1
445	24.15	74.7	57.2	48.0	45.6	43.7	37.0	33.9	30.6	27.7	25.5	24.5	24.3
450	24.3	74.7	57.3	48.1	45.7	43.8	37.2	34.0	30.8	27.8	25.6	24.7	24.4
455	24.45	74.8	57.4	48.2	45.8	43.9	37.3	34.1	30.9	27.9	25.8	24.8	24.6
460	24.6	74.8	57.5	48.3	45.9	44.0	37.4	34.3	31.1	28.1	25.9	25.0	24.7
465	24.75	74.8	57.5	48.4	46.0	44.1	37.5	34.4	31.2	28.2	26.0	25.1	24.9
470	24.9	74.9	57.6	48.5	46.1	44.2	37.6	34.5	31.3	28.4	26.2	25.3	25.0
475	25.05	74.9	57.7	48.6	46.2	44.3	37.8	34.7	31.5	28.5	26.3	25.4	25.2
480	25.2	74.9	57.8	48.7	46.3	44.4	37.9	34.8	31.6	28.7	26.5	25.6	25.3
485	25.35	75.0	57.8	48.8	46.4	44.5	38.0	34.9	31.7	28.8	26.6	25.7	25.5
490	25.5	75.0	57.9	48.9	46.5	44.6	38.1	35.0	31.9	28.9	26.8	25.9	25.6
495	25.65	75.0	58.0	49.0	46.6	44.7	38.3	35.2	32.0	29.1	26.9	26.0	25.8
500	25.8	75.1	58.1	49.0	46.7	44.9	38.4	35.3	32.1	29.2	27.1	26.2	25.9
505	25.95	75.1	58.1	49.1	46.8	45.0	38.5	35.4	32.3	29.4	27.2	26.3	26.1
510	26.1	75.2	58.2	49.2	46.9	45.1	38.6	35.6	32.4	29.5	27.4	26.5	26.2
515	26.25	75.2	58.3	49.3	47.0	45.2	38.7	35.7	32.5	29.7	27.5	26.6	26.4
520	26.4	75.2	58.4	49.4	47.1	45.3	38.9	35.8	32.7	29.8	27.7	26.8	26.5
525	26.55	75.3	58.4	49.5	47.2	45.4	39.0	35.9	32.8	29.9	27.8	26.9	26.7
530	26.7	75.3	58.5	49.6	47.3	45.5	39.1	36.1	33.0	30.1	28.0	27.1	26.8
535	26.85	75.3	58.6	49.7	47.4	45.6	39.2	36.2	33.1	30.2	28.1	27.2	27.0
540	27	75.4	58.7	49.8	47.5	45.7	39.3	36.3	33.2	30.4	28.3	27.4	27.1
545	27.15	75.4	58.7	49.9	47.6	45.8	39.5	36.4	33.4	30.5	28.4	27.5	27.3
550	27.3	75.4	58.8	50.0	47.7	45.9	39.6	36.6	33.5	30.6	28.6	27.7	27.4
555	27.45	75.5	58.9	50.1	47.8	46.0	39.7	36.7	33.6	30.8	28.7	27.8	27.6
560	27.6	75.5	59.0	50.2	47.9	46.1	39.8	36.8	33.8	30.9	28.8	28.0	27.7
565	27.75	75.5	59.0	50.3	48.0	46.2	39.9	37.0	33.9	31.1	29.0	28.1	27.9
570	27.9	75.6	59.1	50.4	48.1	46.3	40.1	37.1	34.0	31.2	29.1	28.3	28.0
575	28.05	75.6	59.2	50.5	48.2	46.4	40.2	37.2	34.2	31.4	29.3	28.4	28.2
580	28.2	75.6	59.3	50.6	48.3	46.5	40.3	37.3	34.3	31.5	29.4	28.6	28.3
585	28.35	75.7	59.3	50.7	48.4	46.6	40.4	37.5	34.4	31.6	29.6	28.7	28.5
590	28.5	75.7	59.4	50.8	48.5	46.8	40.6	37.6	34.6	31.8	29.7	28.9	28.6
595	28.65	75.8	59.5	50.9	48.6	46.9	40.7	37.7	34.7	31.9	29.9	29.0	28.8
600	28.8	75.8	59.6	51.0	48.7	47.0	40.8	37.9	34.8	32.1	30.0	29.2	28.9
605	28.95	75.8	59.6	51.1	48.8	47.1	40.9	38.0	35.0	32.2	30.2	29.3	29.1
610	29.1	75.9	59.7	51.2	48.9	47.2	41.0	38.1	35.1	32.4	30.3	29.5	29.2
615	29.25	75.9	59.8	51.3	49.0	47.3	41.2	38.2	35.3	32.5	30.5	29.6	29.4
620	29.4	75.9	59.9	51.4	49.1	47.4	41.3	38.4	35.4	32.6	30.6	29.8	29.5
625	29.55	76.0	59.9	51.4	49.2	47.5	41.4	38.5	35.5	32.8	30.8	29.9	29.7
630	29.7	76.0	60.0	51.5	49.3	47.6	41.5	38.6	35.7	32.9	30.9	30.1	29.8
635	29.85	76.0	60.1	51.6	49.4	47.7	41.6	38.8	35.8	33.1	31.1	30.2	30.0
640	30	76.1	60.2	51.7	49.5	47.8	41.8	38.9	35.9	33.2	31.2	30.4	30.1
645	30.15	76.1	60.2	51.8	49.6	47.9	41.9	39.0	36.1	33.4	31.4	30.5	30.3
650	30.3	76.1	60.3	51.9	49.7	48.0	42.0	39.1	36.2	33.5	31.5	30.7	30.4
655	30.45	76.2	60.4	52.0	49.8	48.1	42.1	39.3	36.3	33.6	31.6	30.8	30.6
660	30.6	76.2	60.5	52.1	49.9	48.2	42.2	39.4	36.5	33.8	31.8	31.0	30.7

665	30.75	76.2	60.5	52.2	50.0	48.3	42.4	39.5	36.6	33.9	31.9	31.1	30.9
670	30.9	76.3	60.6	52.3	50.1	48.4	42.5	39.7	36.7	34.1	32.1	31.3	31.0
675	31.05	76.3	60.7	52.4	50.2	48.6	42.6	39.8	36.9	34.2	32.2	31.4	31.2
680	31.2	76.3	60.8	52.5	50.3	48.7	42.7	39.9	37.0	34.3	32.4	31.6	31.3
685	31.35	76.4	60.8	52.6	50.4	48.8	42.8	40.0	37.2	34.5	32.5	31.7	31.5
690	31.5	76.4	60.9	52.7	50.5	48.9	43.0	40.2	37.3	34.6	32.7	31.9	31.6
695	31.65	76.5	61.0	52.8	50.6	49.0	43.1	40.3	37.4	34.8	32.8	32.0	31.8
700	31.8	76.5	61.1	52.9	50.7	49.1	43.2	40.4	37.6	34.9	33.0	32.2	31.9
705	31.95	76.5	61.1	53.0	50.8	49.2	43.3	40.5	37.7	35.1	33.1	32.3	32.1
710	32.1	76.6	61.2	53.1	50.9	49.3	43.5	40.7	37.8	35.2	33.3	32.5	32.2
715	32.25	76.6	61.3	53.2	51.0	49.4	43.6	40.8	38.0	35.3	33.4	32.6	32.4
720	32.4	76.6	61.4	53.3	51.2	49.5	43.7	40.9	38.1	35.5	33.6	32.8	32.5
725	32.55	76.7	61.4	53.4	51.3	49.6	43.8	41.1	38.2	35.6	33.7	32.9	32.7
730	32.7	76.7	61.5	53.5	51.4	49.7	43.9	41.2	38.4	35.8	33.9	33.1	32.8
735	32.85	76.7	61.6	53.6	51.5	49.8	44.1	41.3	38.5	35.9	34.0	33.2	33.0
740	33	76.8	61.7	53.7	51.6	49.9	44.2	41.4	38.6	36.1	34.2	33.4	33.1
745	33.15	76.8	61.7	53.8	51.7	50.0	44.3	41.6	38.8	36.2	34.3	33.5	33.3
750	33.3	76.8	61.8	53.8	51.8	50.1	44.4	41.7	38.9	36.3	34.4	33.7	33.4
755	33.45	76.9	61.9	53.9	51.9	50.2	44.5	41.8	39.0	36.5	34.6	33.8	33.6
760	33.6	76.9	62.0	54.0	52.0	50.4	44.7	42.0	39.2	36.6	34.7	34.0	33.7
765	33.75	76.9	62.0	54.1	52.1	50.5	44.8	42.1	39.3	36.8	34.9	34.1	33.9
770	33.9	77.0	62.1	54.2	52.2	50.6	44.9	42.2	39.5	36.9	35.0	34.3	34.0
775	34.05	77.0	62.2	54.3	52.3	50.7	45.0	42.3	39.6	37.1	35.2	34.4	34.2
780	34.2	77.1	62.3	54.4	52.4	50.8	45.1	42.5	39.7	37.2	35.3	34.6	34.3
785	34.35	77.1	62.3	54.5	52.5	50.9	45.3	42.6	39.9	37.3	35.5	34.7	34.5
790	34.5	77.1	62.4	54.6	52.6	51.0	45.4	42.7	40.0	37.5	35.6	34.9	34.6
795	34.65	77.2	62.5	54.7	52.7	51.1	45.5	42.9	40.1	37.6	35.8	35.0	34.8
800	34.8	77.2	62.6	54.8	52.8	51.2	45.6	43.0	40.3	37.8	35.9	35.2	34.9
805	34.95	77.2	62.6	54.9	52.9	51.3	45.8	43.1	40.4	37.9	36.1	35.3	35.1
810	35.1	77.3	62.7	55.0	53.0	51.4	45.9	43.2	40.5	38.0	36.2	35.4	35.2
815	35.25	77.3	62.8	55.1	53.1	51.5	46.0	43.4	40.7	38.2	36.4	35.6	35.4
820	35.4	77.3	62.9	55.2	53.2	51.6	46.1	43.5	40.8	38.3	36.5	35.7	35.5
825	35.55	77.4	62.9	55.3	53.3	51.7	46.2	43.6	40.9	38.5	36.7	35.9	35.7
830	35.7	77.4	63.0	55.4	53.4	51.8	46.4	43.8	41.1	38.6	36.8	36.0	35.8
835	35.85	77.4	63.1	55.5	53.5	51.9	46.5	43.9	41.2	38.8	37.0	36.2	36.0
840	36	77.5	63.2	55.6	53.6	52.0	46.6	44.0	41.4	38.9	37.1	36.3	36.1
845	36.15	77.5	63.2	55.7	53.7	52.2	46.7	44.1	41.5	39.0	37.2	36.5	36.3
850	36.3	77.5	63.3	55.8	53.8	52.3	46.8	44.3	41.6	39.2	37.4	36.6	36.4
855	36.45	77.6	63.4	55.9	53.9	52.4	47.0	44.4	41.8	39.3	37.5	36.8	36.6
860	36.6	77.6	63.5	56.0	54.0	52.5	47.1	44.5	41.9	39.5	37.7	36.9	36.7
865	36.75	77.6	63.5	56.1	54.1	52.6	47.2	44.6	42.0	39.6	37.8	37.1	36.9
870	36.9	77.7	63.6	56.2	54.2	52.7	47.3	44.8	42.2	39.8	38.0	37.2	37.0
875	37.05	77.7	63.7	56.2	54.3	52.8	47.4	44.9	42.3	39.9	38.1	37.4	37.2
880	37.2	77.8	63.8	56.3	54.4	52.9	47.6	45.0	42.4	40.0	38.3	37.5	37.3
885	37.35	77.8	63.8	56.4	54.5	53.0	47.7	45.2	42.6	40.2	38.4	37.7	37.5
890	37.5	77.8	63.9	56.5	54.6	53.1	47.8	45.3	42.7	40.3	38.6	37.8	37.6
895	37.65	77.9	64.0	56.6	54.7	53.2	47.9	45.4	42.8	40.5	38.7	38.0	37.8
900	37.8	77.9	64.1	56.7	54.8	53.3	48.0	45.5	43.0	40.6	38.9	38.1	37.9
905	37.95	77.9	64.1	56.8	54.9	53.4	48.2	45.7	43.1	40.8	39.0	38.3	38.1
910	38.1	78.0	64.2	56.9	55.0	53.5	48.3	45.8	43.2	40.9	39.2	38.4	38.2
915	38.25	78.0	64.3	57.0	55.1	53.6	48.4	45.9	43.4	41.0	39.3	38.6	38.4
920	38.4	78.0	64.4	57.1	55.2	53.7	48.5	46.1	43.5	41.2	39.5	38.7	38.5
925	38.55	78.1	64.4	57.2	55.3	53.8	48.7	46.2	43.7	41.3	39.6	38.9	38.7
930	38.7	78.1	64.5	57.3	55.4	53.9	48.8	46.3	43.8	41.5	39.7	39.0	38.8
935	38.85	78.1	64.6	57.4	55.5	54.1	48.9	46.4	43.9	41.6	39.9	39.2	39.0
940	39	78.2	64.7	57.5	55.6	54.2	49.0	46.6	44.1	41.7	40.0	39.3	39.1
945	39.15	78.2	64.7	57.6	55.7	54.3	49.1	46.7	44.2	41.9	40.2	39.5	39.3
950	39.3	78.2	64.8	57.7	55.8	54.4	49.3	46.8	44.3	42.0	40.3	39.6	39.4
955	39.45	78.3	64.9	57.8	55.9	54.5	49.4	47.0	44.5	42.2	40.5	39.8	39.6
960	39.6	78.3	65.0	57.9	56.0	54.6	49.5	47.1	44.6	42.3	40.6	39.9	39.7
965	39.75	78.4	65.0	58.0	56.1	54.7	49.6	47.2	44.7	42.5	40.8	40.1	39.9
970	39.9	78.4	65.1	58.1	56.2	54.8	49.7	47.3	44.9	42.6	40.9	40.2	40.0
975	40.05	78.4	65.2	58.2	56.3	54.9	49.9	47.5	45.0	42.7	41.1	40.4	40.2
980	40.2	78.5	65.3	58.3	56.4	55.0	50.0	47.6	45.1	42.9	41.2	40.5	40.3
985	40.35	78.5	65.3	58.4	56.5	55.1	50.1	47.7	45.3	43.0	41.4	40.7	40.5
990	40.5	78.5	65.4	58.5	56.6	55.2	50.2	47.9	45.4	43.2	41.5	40.8	40.6
995	40.65	78.6	65.5	58.6	56.7	55.3	50.3	48.0	45.6	43.3	41.7	41.0	40.8
1000	40.8	78.6	65.6	58.6	56.8	55.4	50.5	48.1	45.7	43.5	41.8	41.1	40.9

